DYNAMICS OF PYRIDINE ADSORPTION ON HYDROTREATING CATALYSTS

By

CHAROEN KONGKATONG

Bachelor of Science

Chulalongkorn University

Bangkok, Thailand

1985

Submitted to the Faculty of the
Graduate College of the
Oklahoma State University
in partial fullfillment of
the requirements for
the Degree of
MASTER OF SCIENCE
July, 1988

DYNAMICS OF PYRIDINE ADSORPTION

ON HYDROTREATING CATALYSTS

Thesis Approved:

Mayis Seapan

Thesis Adviser

Robert S. Robinson Jr.

Dan L. Fox

Norman N. Durham

Dean of the Graduate College

ABSTRACT

The adsorption of pyridine on two Ni-Mo/alumina hydrotreating catalysts (HDN-60 and Shell 324) was investigated. Equilibrium and dynamic adsorption data were collected at 100, 200, 250, 300, 400, and 450 C in the pyridine partial pressure range of 533-800 N/m^2 (4-6 mm Hg). The equilibrium results described two kinds of adsorption: physical adsorption at temperatures below 250 C and chemisorption which was predominant at temperatures above 250 C. The initial rate of adsorption at low temperatures was larger than that at high temperatures and the time to reach equilibrium at low temperatures was shorter than that at high temperatures. Pyridine adsorption at the temperatures studied demonstrated a 30-60 % irreversibility. A reversible adsorption model demonstrated different types of adsorption from the dynamic study. At temperatures below 250 C, there were three types of adsorption and at higher temperatures, four or five types of adsorption occurred in the process. Temperature programmed adsorption of pyridine on catalyst showed a strong adsorption at temperatures higher than 420 C. This high temperature adsorption may be attributed to coke formation.

ACKNOWLEDGEMENTS

I wish to express my sincere appreciation to my major advisor, Dr. Mayis Seapan, for his guidance, encouragement, interest and valuable suggestions. I would also like to thank Dr. Gary L. Foutch and Dr. Robert L. Robinson, Jr. as members of my examining committee.

Special thanks are due to Oklahoma State University, School of Chemical Engineering, and the University Center for Energy Research (UCER) for the financial support I received during the course of this work.

I would like to thank all my friends, both in Oklahoma and in Thailand, for their help in completing this project.

I would like to acknowledge my lovely friend, Pavinee Wongcharoenrat, for giving me the encouragement to succeed in this project.

Finally, I would like to express my gratitude to my parents, Chuchai and Kittima Kongkatong, my aunts, and other family members for their support, encouragement, and understanding.

TABLE OF CONTENTS

LIST OF TABLES

LIST OF FIGURES

Figure Page

CHAPTER I

INTRODUCTION

In oil refining, catalysts are used in such processes as hydrotreating, hydrocracking, isomerization and hydroreforming, to selectively improve the yields of desired chemical reactions. Organic nitrogen compounds, which are usually present in most oil fractions, are responsible for deactivation and/or poisoning of these catalysts. Moreover, nitrogen-containing compounds are sources of air pollution when the fuels containing them are burned. As such, removal of nitrogen compounds is an essential part of the processing of oil fractions in the presence of catalysts.

Hydrodenitrogenation (HDN) is a common method for nitrogen removal from petroleum liquids. For heterocyclic nitrogen compounds, HDN usually proceeds by saturation of the heterocyclic ring followed by ring fracture at a carbon-nitrogen bond and subsequent conversion of the nitrogen to ammonia. However, some of the basic intermediates irreversibly adsorb on the acidic sites of catalyst poisoning the catalyst.

Typical heterocyclic nitrogen compounds found in petroleum and coal derived liquids are pyrrole, indole, carbazole, pyridine, quinoline, and acridine. Since many of

the nitrogen compounds which occur in petroleum are pyridine derivatives, pyridine is usually selected to study the interaction between the nitrogen compounds and catalysts. Furthermore, pyridine has a simple structure and only a few intermediates are formed when it is hydrogenated.

In a previous study, Kittrell (1986) studied the adsorption of pyridine on a hydrotreating catalyst at 450 C in a pyridine partial pressure of 284-2130 N/m^2 (2.13-15.98 mm Hg) and showed two different types of adsorption; an irreversible adsorption attributed to coke formation and a reversible adsorption. However, he reported only equilibrium pyridine adsorption at a high temperature (450 C).

The purpose of this study was to extend Kittrell's work and to investigate the adsorption of pyridine on two different hydrotreating catalysts at different temperatures. The specific objectives of this study were as follows:

1. to measure the transient and equilibrium adsorption of pyridine on the hydrotreating catalysts;

2. to study the effect of temperatures on pyridine adsorption;

3. to study the surface heterogeneity of the catalysts using adsorption dynamic measurements.

CHAPTER II

LITERATURE REVIEW

Characterization of a catalyst in terms of its acidity, number and type of active sites has been studied to determine the ability of catalyst in chemical transformation under specified conditions. The acidic sites of a catalyst can be classified as Bronsted and Lewis types. A Bronsted site is defined as any site on the catalyst surface which tends to lose protons. In contrast, a Lewis acid site is the one which is able to accept electrons from a molecule or ion, for instance, from an adsorbent in a catalytic reaction (Tanabe, 1970).

The infrared spectra of adsorbed pyridine and ammonia on catalytic surfaces have been used extensively to explain the distinction between Lewis and Bronsted acid sites. Mapes and Eischens (1956) studied the infrared spectra of ammonia adsorbed on a silica-alumina catalyst and observed two types of adsorption. They suggested that the presence of Lewis acid sites was indicated by the spectra of adsorbed NH_3 whereas the presence of protons on the surface or Bronsted acid sites was identified by the spectra of NH_4^+.

Parry (1963) reported that the infrared spectra of pyridine adsorbed on acidic solids are in the range of a

1400-1700 cm^{-1}. He suggested that the bands at 1455-1459 cm^{-1} can be attributed to Lewis acidity and the band at 1540 cm^{-1} shows the presence of Bronsted acidity.

The differences in catalyst preparation and pretreatment techniques affect the catalyst structure resulting in different acidic properties. Pines and Haag (1959) studied the intrinsic acidity and catalytic activity of alumina as a catalyst support. They found that the catalytic behavior of alumina depended on its method of preparation. The alumina which was prepared by the hydrolysis of aluminum isoperoxide showed strongly acidic properties; however, the alumina which was prepared by precipitation of sodium or potassium aluminate showed weak catalytic effect. They also suggested that the catalytic activity of alumina could mostly be attributed to the presence of Lewis acid sites but Bronsted acid sites on alumina, if present at all, were of very low acid strength. Moreover, the temperature of calcination in the range between 600 and 700 C provided the highest catalytic activity of alumina. The low activity of catalyst at low temperatures was due to the presence of too much water, and that at high temperatures was a result of the changes in the catalyst structure.

There have been some studies concerning the surface structure and activity of catalysts by the adsorption of nitrogen compounds on catalysts. Mills, et al., (1950) studied the adsorption of nitrogen compounds on cracking catalysts. They suggested that basic organic nitrogen

compounds were retained on the catalyst surface by both chemical and physical forces. In addition, the amount of quinoline chemisorbed was lower than that of pyridine at higher temperatures, however, the gain in weight at lower temperatures by both quinoline and pyridine was almost identical. The catalyst adsorbed by quinoline appeared to have a pale green color at 425 C and lower. In contrast, the color of catalyst turned black at temperatures above 425 C which was attributed to a slow decomposition of quinoline on the surface.

Richardson and Benson (1957) estimated the surface acidity of a silica-alumina cracking catalyst by the amount of permanently adsorbed basic gas. They found that the adsorbed gas comprised of two fractions; one desorbed rapidly while the other, which was considered as a measure of the surface acidity, desorbed much more slowly. The amount of acidic sites did not exceed a few tenths of milliequivalent per gram of catalyst and covered no more than a few percent of the total surface. Their estimate based on a surface area of 400 m^2/g and 10 A^2 per pyridine molecule was 0.1 milliequivalent/g (0.1 m mol/g).

Sheets and Hansen (1772) investigated the promoted adsorption of pyridine on oil-covered nickel and the effects of coadsorbed catalyst poisons. There was no chemisorption of pyridine detected on unpoisoned films; however, after exposure of freshly evaporated nickels to carbon monoxide, oxygen, and carbon disulfide, pyridine was determined to be

coordinately adsorbed. These results suggested a second mechanism in which the poison acted not only to inhibit the adsorption of a reactant but also to induce irreversible chemisorption of the species. Thus, most of the surface sites were blocked not by the poison, but by the reactant.

Morrow, et al., (1976) studied the infrared spectra of the adsorbed pyridine on platinum and nickel. They suggested that pyridine dissociatively chemisorbed on silica-supported platinum forming a σ bond at the "2" position and a coordinate bond with the nitrogen lone pair electrons. However, a different strongly adsorbed pyridine was formed on silica-supported nickel as a simple nitrogen-coordinated pyridine lied perpendicular to the surface.

Takahashi, et al., (1976) investigated the behavior of pyridine on a silica-alumina catalyst by a thermal desorption method. Their results showed only one peak in the desorption curve and the small amount of pyridine was strongly adsorbed at temperatures above 300 C without any decomposition. Hence, the stronger acid sites of the silica-alumina were distributed in different acid strengths.

Fransen, et al., (1976) studied the adsorption of pyridine on a reduced Mo-alumina catalyst. They concluded that both Lewis and Bronsted acid sites were present on a reduced catalyst and most of the adsorbed pyridine was associated with the molybdenum part of the catalyst. They also suggested that only molybdenum oxide played a role in hydrogenation.

Schwarz, et al., (1978) combined an infrared spectroscopy technique with temperature programmed desorption (TPD) to study the adsorption of pyridine on silica-alumina catalysts. They suggested that the desorption kinetic for each silica-alumina catalyst was first-order in pyridine coverage. The activation energies for desorption of pyridine on a 90 silica/10 alumina by weight from Lewis and Bronsted sites were only 5.3 and 7.2 kcal/mol, respectively.

Morterra, et al., (1978) studied the pyridine chemisorption on a η-alumina dehydrated at temperatures between 25-700 C using infrared spectroscopy and microgravimetry. They found that the total pyridine uptake increased with increasing dehydration temperature. As such, the surface unsaturation produced upon dehydration was primarily responsible for the adsorption of pyridine. In addition, at temperatures above 400 C, they observed other reaction mechanisms. The color of alumina catalyst became brown, suggesting coke deposition and new bands appeared in the infrared spectrum at 1634, 1553, 1368 and 1294 cm^{-1}.

Segawa and Hall (1982) conducted a study on the adsorption of pyridine on a molybdena-alumina catalyst. For the oxidized catalyst, the Lewis acid sites were associated with the alumina surface while the Bronsted sites depended strongly upon the presence of molybdate species. For the reduced catalyst, however, Lewis acid sites appeared on both the molybdena and alumina portions. Furthermore, after the catalyst was evacuated, the amount of irreversibly adsorbed

pyridine left on the catalyst was about one-half of the equilibrium value. Upon the evacuation of the pyridine adsorbed catalyst at about 300 C, Lewis-bound pyridine was removed satisfactorily, however, above this temperature, all of the Bronsted-bound pyridine desorbed abruptly and only a small amount of more strongly Lewis-bound pyridine was held on the alumina catalyst. Hall, et al., (1984) observed the site selective adsorption of nitrogen compounds on sulfided Mo/alumina. They found that most of the pyridine adsorption occurred on the alumina surface.

Suarez, et al., (1985) studied the acidic properties of a molybdena-alumina catalyst by adsorbed pyridine. They found that there were two types of Lewis sites, having different acid strength, on the alumina surface.

Deeba and Hall (1985) studied the catalyst acidity by pyridine chemisorption on a series of silica-alumina cracking catalysts and on alumina. Their experimental results indicated that the initial uptake was very fast and adsorption equilibrium was reached in a few minutes. They also showed that the activation energy for desorption was equivalent to the heat of adsorption and that both decreased continuously with increasing coverage.

Entz (1984) used a thermogravimetric analyzer (TGA) to study the adsorption of pyridine and its hydrogenation derivatives on a Ni-Mo/alumina catalyst and to investigate the effect that nitrogen compounds had on the adsorption of hydrogen on the catalyst. Adsorption of ammonia on the

catalyst decreased hydrogen adsorption by 29 % while n-pentylamine decreased hydrogen adsorption by 47 %. The irreversibly adsorbed compounds resulting from pyridine and piperidine hydrogenation reduced the amount of hydrogen adsorption by 41 and 44 %, respectively.

Kittrell (1986) studied the equilibrium and transient adsorption of pyridine on a Ni-Mo/alumina hydrotreating catalyst. He found that the equilibrium adsorption isotherms for pyridine demonstrated idealized Langmuir characteristics and the equilibrium pyridine adsorption decreased linearly with temperature. Pyridine adsorption at 450 C showed a 33 % irreversibility which was suggested to be due to coke formation. He also showed the possibility of characterization of different adsorption sites by transient adsorption measurements using a TGA.

In summary, the acidic characteristics of hydro-treatment and hydrocracking catalysts are important to their activity. Two types of acidic sites are known to exist on catalytic surfaces: Bronsted and Lewis acid sites. The infrared spectra of adsorbed organic nitrogen compounds have been used extensively to distinguish the proportion of Bronsted and Lewis acid sites on catalysts. Chemisorption of a nitrogen base on a catalyst surface causes a modest reduction in the total number of active sites and strongly modifies the acid strength distribution. The activities of different catalysts are determined to be proportional to their ability to adsorb basic nitrogen

compounds. The effects of catalyst preparation and the changes in catalyst structure also demonstrate the difference in the acidic properties.

During the adsorption of pyridine on a Mo/alumina catalyst in oxide state, most of the pyridine adsorb on the molybdenum part of the catalyst, however, when the catalyst is sulfided, a majority of the pyridine adsorbs on the alumina surface rather than the molybdenum surface. Furthermore, one significant phenomenon is coke formation on the catalyst surface at temperatures above 400 C during nitrogen base poisoning of a catalyst.

There has been little study conducted on the effect of temperature on the transient and equilibrium adsorption of nitrogen compounds. In addition, little has been reported on the gravimetric techniques to study different types of adsorbed pyridine on a catalyst surface. Using weight-time relation may be advantageous in investigation of different types of adsorption, for example, in differentiating between non-activated and activated adsorption.

The purpose of this work is to study the adsorption of pyridine on hydrotreating catalysts. The transient adsorption phenomenon and its relationship with non-activated and activated adsorption will be studied. Furthermore, equilibrium adsorption will be investigated as a function of temperature. The possibility of reversible and irreversible adsorption and coke formation at high temperatures will also be investigated.

CHAPTER III

EXPERIMENTAL EQUIPMENT AND PROCEDURE

Equipment

Adsorption measurements of pyridine on catalysts were made gravimetrically with a Cahn System 113 Thermal Gravimetric Analyzer (TGA). The major part of the system 113 is the Cahn 2000 recording electrobalance which measures weight changes of a catalyst pellet suspended in a temperature controlled gas stream. The microbalance is capable of measuring the weight of sample up to 2.5 milligrams and observe the weight change as small as 0.1 microgram. The basic concept of microbalance is to convert the weight change into an electrical signal which can be recorded on a strip chart recorder.

The Cahn system 113 also contains a Micricon process controller. The basic devices in the Micricon consist of a proportional-integral-derivative (PID) controller and a programmer. The controller is able to raise the temperature in the furnace at a rate between 0 and 5 C/minute up to a maximum temperature of 1150 C. The programmer serves as a setpoint source external to the controller. In other words, the programmer can change the setpoint temperature in the

furnace as time progresses. The temperature is measured with a chromel-alumel thermocouple and the reading is shown on the screen of the Micricon. The thermocouple not only provides temperature information but also gives the signal to the controller which adjusts the input of power to the electric furnace.

The Cahn system 113 also includes a time derivative computer and a strip chart recorder system which contains an automatic range expander and percent sample weight accessories. The function of automatic range expander is to keep the output signal between two fixed limits and the percent sample weight accessory conducts the output results recorded as a percentage of the weight gain or loss.

Other auxiliary equipments used in this project include a porosimeter, a constant temperature water bath, a gas chromatograph, a Laser Raman Microscope, a Fourier Transform Infra-Red Microscope and a Scanning Electron Microscope. A Quantachrome SP-10B Scanning Porosimeter was used to determine the surface area and pore volume of the catalysts. The constant temperature bath was used to evaporate pyridine and prepare a pyridine/helium mixture with a desired concentration. The gas chromatograph was used to measure the concentration of pyridine in the helium gas. Laser Raman and Fourier Transform Infra-red Microscopes were used to characterize which compounds adsorbed on the catalyst after the adsorption of pyridine. A Scanning Electron Microscope was used to observe the

structure of catalyst before and after the adsorption of pyridine and/or coke formation on the catalyst surface.

A schematic diagram of the experimental system is shown in Figure 1. A Precision Differential Thermometer and Thermoregulator was provided to maintain a constant temperature water bath. Two 200 ml filter flasks contained 200 ml of liquid pyridine were arranged in series in the constant temperature bath. Ultra-high purity helium (99.999%) was passed through an Oxisorb adsorber (Scientific Gas product) in order to remove water and oxygen and flowed through gas dispersion tubes and into the constant temperature pyridine. Helium with pyridine vapors then flowed out of the second saturator and through a heated stainless steel tube (1/4 in. O.D.), which was maintained above the boiling point of pyridine (115 C), to the TGA. In later experiments, instead of two 200 ml flasks, only one 200 ml gas washing bottle equipped with a 30 mm fritted glass disc was used. Analysis of the pyridine partial pressure with the gas chromatograph showed almost identical concentrations of pyridine in helium in both systems. After entering the TGA, helium/pyridine vapor and helium blanket gas flowed down over a suspended catalyst pellet and then exited through another heated line to the gas chromatograph. A Varian (Model 3700) GC, equipped with a flame ionization detector (FID) and a Hewlett Packard 3390A integrator was used to determine the partial pressure of pyridine in the helium stream. The column was a 3.175 mm x 1.52 m stainless

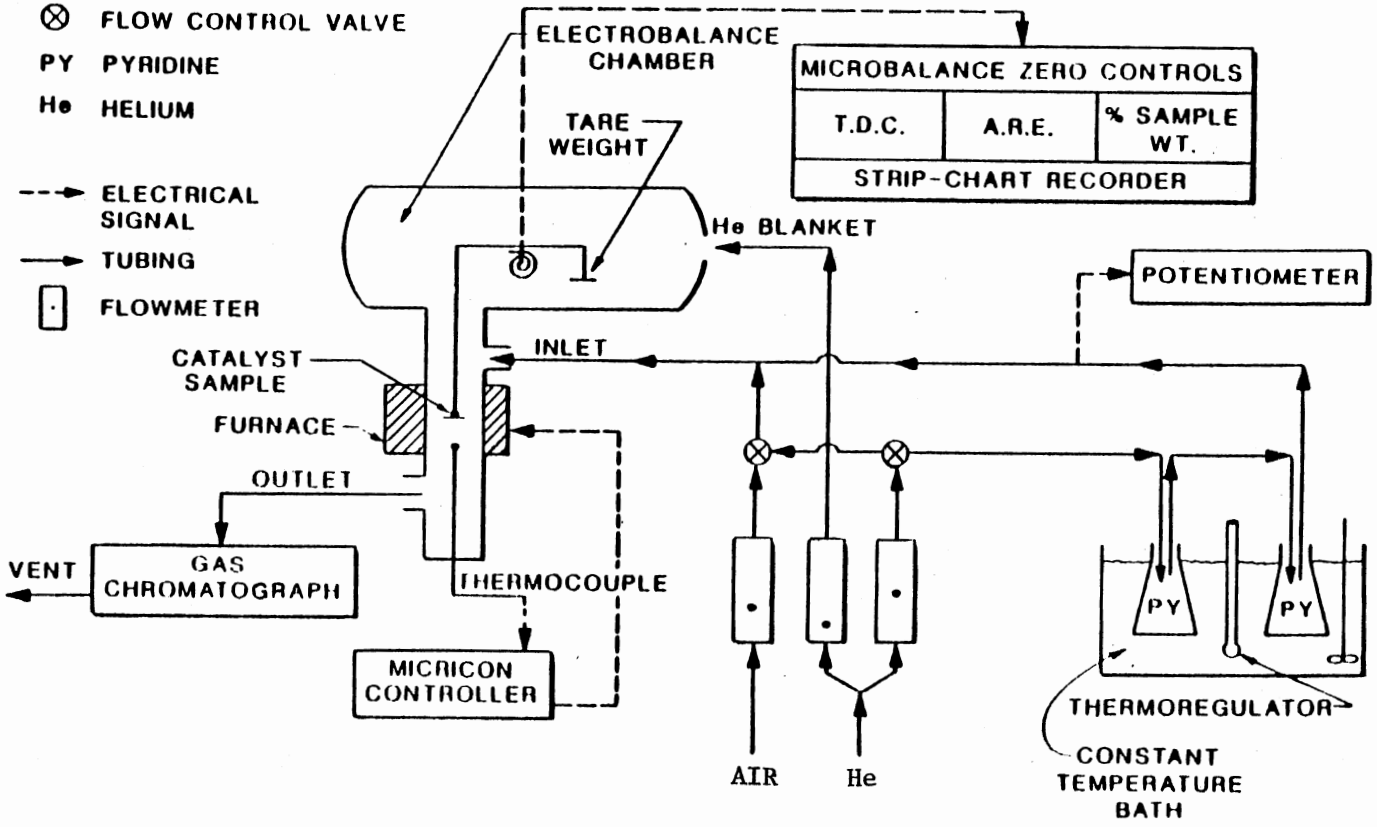

Figure 1. Schematic Flow Diagram of Experimental System

steel tubing packed with 10% Carbowax 20 M on 80/100 mesh chromosorb W-HP. The temperature scheme consisted of operating both the injector and the detector at 160 C, and the column at 150 C.

Experimental Procedure

Commercial Shell 324 and HDN-60 Ni-Mo/alumina catalysts were used in this study. The properties of these catalysts are given in Table I. A single catalyst pellet with a mass of 6-18 mg was held in a small nichrome wire basket hung by a fine nichrome wire inside the TGA hangdown tube. For the calcination, dry air (zero-grade) with a rate of 60 cm^3/min was passed over the catalyst sample while the temperature was gradually raised to 500 C in 6 h. The catalyst sample was held at 500 C for 24 h. During the first 12 h period, air was used to calcine the catalyst sample until the weight of catalyst was stabilized. After that, the catalyst was further calcined at 500 C in ultra-high purity (UHP) helium flowing at a rate of 60 cm^3/min for 12 h.

After calcination, the temperature was decreased from 500 C to the experimental temperature under a flow of UHP helium at a rate of 0.42 C/min. The adsorption experiments were conducted at the temperatures of 100, 200, 250, 300, 400, and 450 C. When the equilibrium weight was achieved at these temperatures, the flow of helium at a rate of 60 cm^3/min was directed through the containers of liquid pyridine. The mixture of helium and pyridine vapor flowed

TABLE I

PROPERTIES OF SHELL 324 AND HDN-60 CATALYSTS

Catalyst	Shell 324	HDN-60
Shape	Cylindrical	Trilobe
Nominal diameter, mm	1.6*	1.23*
Chemical Properties, wt%		
Nickel	2.67*	3*
Molybdenum	13.05*	22*
Physical Properties		
Surface Area, m^2/g cat.	202**	197**
Total Pore Volume, cm^3/g cat.	0.52**	0.41**

* Vendor's data
** Measured by mercury penetration in this work

through a heated line to enter into the TGA. A stream of UHP helium with a rate of 40 cm^3/min was used as a blanket gas to protect the electrobalance from contact with pyridine. These two streams got mixed in the TGA hangdown tube before contacting the catalyst. The flow was maintained until the change in the adsorption weight of catalyst was less than 0.001 mg/h, corresponding to approximately 50 μ g/(g cat. h), for 2 h. The total pressure of helium and pyridine mixture in the TGA system was 1 atm (760 mm Hg).

In a few experiments pyridine was desorbed from the catalyst to determine the reversible and irreversible adsorbed portions of the pyridine. Desorption of pyridine from catalyst samples was conducted by passing helium at a rate of 60 cm^3/min over the sample at the same temperature used in the adsorption experiment. Desorption experiment was continued until a weight change of less than 0.001 mg/h was achieved.

In one case the catalyst was subjected to a temperature programmed adsorption. The temperature programmed adsorption experiment was similar to the adsorption of pyridine on a catalyst surface at constant temperature. After the equilibrium adsorption of pyridine was achieved at the initial temperature, the temperature was increased linearly at a rate of 1.67 C/min in the presence of pyridine partial pressure until 450 C. The temperature was then kept constant at this value and the weight change was monitored.

In one experiment, the adsorption and desorption were repeated to observe the reproducibility of the phenomena. After establishment of equilibrium and desorption experiments, the adsorption and desorption experiments were repeated and conducted until a weight change of less than 0.001 mg/g was achieved in each case. In other words, the operating procedure of repeated adsorption/desorption experiments was similar to the adsorption and desorption experiments at constant temperature.

During these experiments, to avoid any contamination of the system with adsorbing gas from the previous run, the system was cleaned. Before each experimental run, the TGA was evacuated to 0.1 millitorr for 2 hours in order to remove any contamination which may have remained inside the system.

CHAPTER IV

EXPERIMENTAL RESULTS

The experimental results, which are presented in this chapter, consist of the transient and equilibrium adsorption data of pyridine on both Shell 324 and HDN-60 catalysts, adsorption reversibility and irreversibility data, temperature programmed adsorption (TPA) data under a pyridine partial pressure. Adsorption reversibility experimentations were made to measure the portion of pyridine that was irreversibly adsorbed on the catalyst. Finally, TPA under pyridine partial pressure demonstrated an interesting behavior in that coke may form on the catalyst surface at high temperatures.

The experiments were carried out at temperatures between 100 and 450 C, and a pyridine partial pressure range between 533-800 N/m^2 (4-6 mm Hg). A total of 25 experimental runs was attempted. A summary of the conditions of these runs is shown in Table II and the equilibrium adsorption data for Shell 324 and HDN-60 catalysts are listed in Table III. The data of Runs 1-8 are not reported here because these runs were aborted during calcination due to system contamination. Adsorption of pyridine in Runs 9, 11, 15, and 20 did not reach

TABLE II

SUMMARY OF ALL EXPERIMENT RUNS

Run no.	Catalyst Type	Temperature (C)	Pyridine Partial Pressure (N/m^2)	Comments and Observations
.1	Shell 324	500	-	only calcination.
2	Shell 324	500	-	only calcination.
3	Shell 324	450	-	ignored because of some contamination problem in the TGA system.
4	Shell 324	450	-	ignored because of some contamination problem in the TGA system.
5	Shell 324	500	-	only calcination.
6	Shell 324	500	-	only calcination.
7	HDN-60	500	-	only calcination.
8	HDN-60	500	-	only calcination.

TABLE II (Continued)

Run no.	Catalyst Type	Temperature (C)	Pyridine Partial Pressure (N/m^2)	Comments and Observation
9	Shell 324	300	604	catalyst fell down from the basket.
10	HDN-60	200	685	equilibrium was achieved.
11	HDN-60	450	716	electrical problem in the TGA system after 70 h.
12	HDN-60	300	647	equilibrium was achieved.
13	HDN-60	200	639	equilibrium was achieved.
14	HDN-60	500	-	catalyst fell down from the basket during calcination.
15	HDN-60	450	657	catalyst fell down from the basket after 90 h.
16	Shell 324	450	527	equilibrium was achieved.

TABLE II (Continued)

Run no.	Catalyst Type	Temperature (C)	Pyridine Partial Pressure (N/m^2)	Comments and Observations
17	Shell 324	400	568	equilibrium was achieved and the catalyst sample was analyzed by Scanning Electron Microscope.
18	Shell 324	300	709	equilibrium was achieved and the catalyst sample was analyzed by Scanning Electron Microscope.
19	Shell 324	200	653	equilibrium was achieved at 200 C and then temperature was increased to 300 C in 1 h (1.67 C/min).
20	Shell 324	450	611	electrical problem in the TGA system.
21	Shell 324	250	653	equilibrium was achieved at 250 C and then temperature was increased to 450 C in 2 h (1.67 C/min).

TABLE II (Continued)

Run no.	Catalyst Type	Temperature (C)	Pyridine Partial Pressure (N/m^2)	Comments and Observations
22	Shell 324	100	732	equilibrium was achieved.
23	Shell 324	500	-	electrical problems in the TGA system during calcination.
24	Shell 324	250	571	equilibrium was achieved.
25	Shell 324	100	721	equilibrium was achieved and readsorption was studied after desorption.

TABLE III

PYRIDINE ADSORPTION EQUILIBRIUM DATA

Run no.	Catalyst Type	Temp. C	Pyridine Partial Pressure N/m^2 (mm Hg)	Catalyst Weight mg	Time to reach Equi-librium h	Adsorbed Amount μ mol/g cat.
10	HDN-60	200	685 (5.14)	7.4765	7	232.13
12	HDN-60	300	647 (4.85)	7.6050	92	569.24
13	HDN-60	200	639 (4.79)	6.7402	7	250.34
16	Shell 324	450	527 (3.95)	13.1501	220	212.68
17	Shell 324	400	568 (4.26)	14.4375	210	749.54
18	Shell 324	300	709 (5.32)	17.3844	300	499.86

TABLE III (Continued)

Run no.	Catalyst Type	Temp. C	Pyridine Partial Pressure N/m^2 (mm Hg)	Catalyst Weight mg	Time to reach Equi-librium h	Adsorbed Amount μ mol/g cat.
19	Shell 324	200	653	11.6205	58	399.77
		300	(4.82)		96	447.38
21	Shell 324	250	653	13.7278	27	229.23
		450	(4.91)		147	1081.3
22	Shell 324	100	732 (5.49)	12.865	10	470.38
24	Shell 324	250	571 (4.28)	13.7180	20	231.97
25	Shell 324	100	721	12.7255	28	410.02
		100	(5.43)	12.8578	27	418.23

equilibrium. The catalyst fell down from the basket in Runs 9 and 15 and the TGA system was shut down automatically by electrical problems in Runs 11 and 20. Therefore, only the adsorption dynamic data of these runs can be used. Figure 2 shows the corresponding equilibrium adsorption on Shell 324 and HDN-60 catalysts at different temperatures.

The transient adsorption data of pyridine on Shell 324 catalyst in the intervals of 2 min, 10 min, and 1 h are shown in Table A-I in Appendix A and are plotted in Figures 3-5. In addition, Table A-II in Appendix A and Figures 6-8 show the transient adsorption data in different time intervals for pyridine adsorption on HDN-60 catalyst. In addition to the raw transient adsorption data, Tables A-I and A-II also show the experimental conditions of each run. Based on the Antoine correlation (Reid, et al., 1977), the saturated pressure of pyridine at 25 C is 20.5 mm Hg. However, gas chromatographic analysis showed that the partial pressure of pyridine in the outlet helium stream was lower than the saturated pressure by 5-6 times. The reason is that the helium-pyridine mixture was diluted with helium blanket gas in the system. The total pressure in the TGA system was 1 atm (760 mm Hg).

Adsorption reversibility experiments were conducted in five runs and the results are shown in Table IV. Furthermore, in Run 25, after establishment of equilibrium adsorption and desorption at 100 C, the adsorption and desorption were repeated to observe the reproducibility of

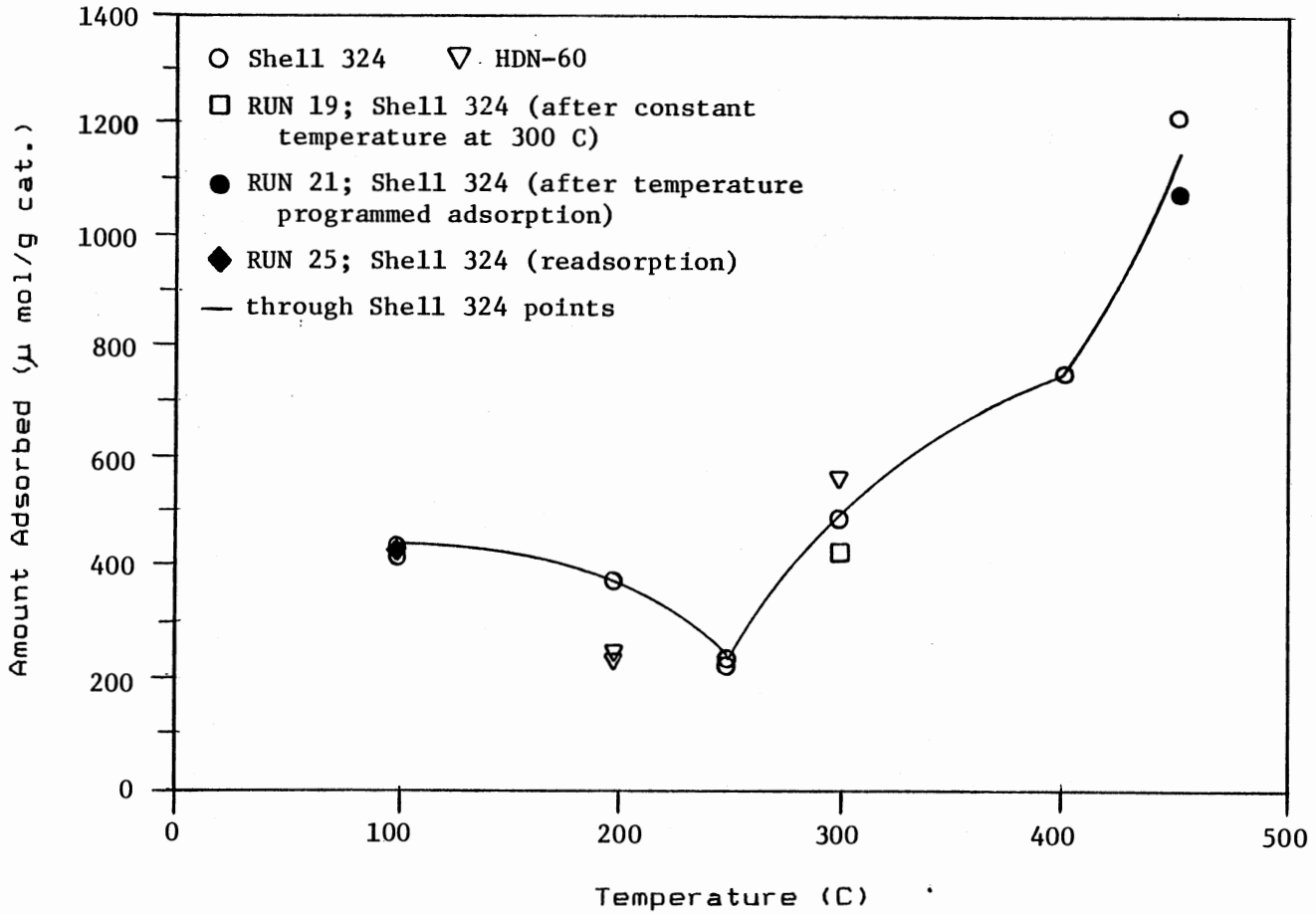

Figure 2. Equilibrium Pyridine Adsorption

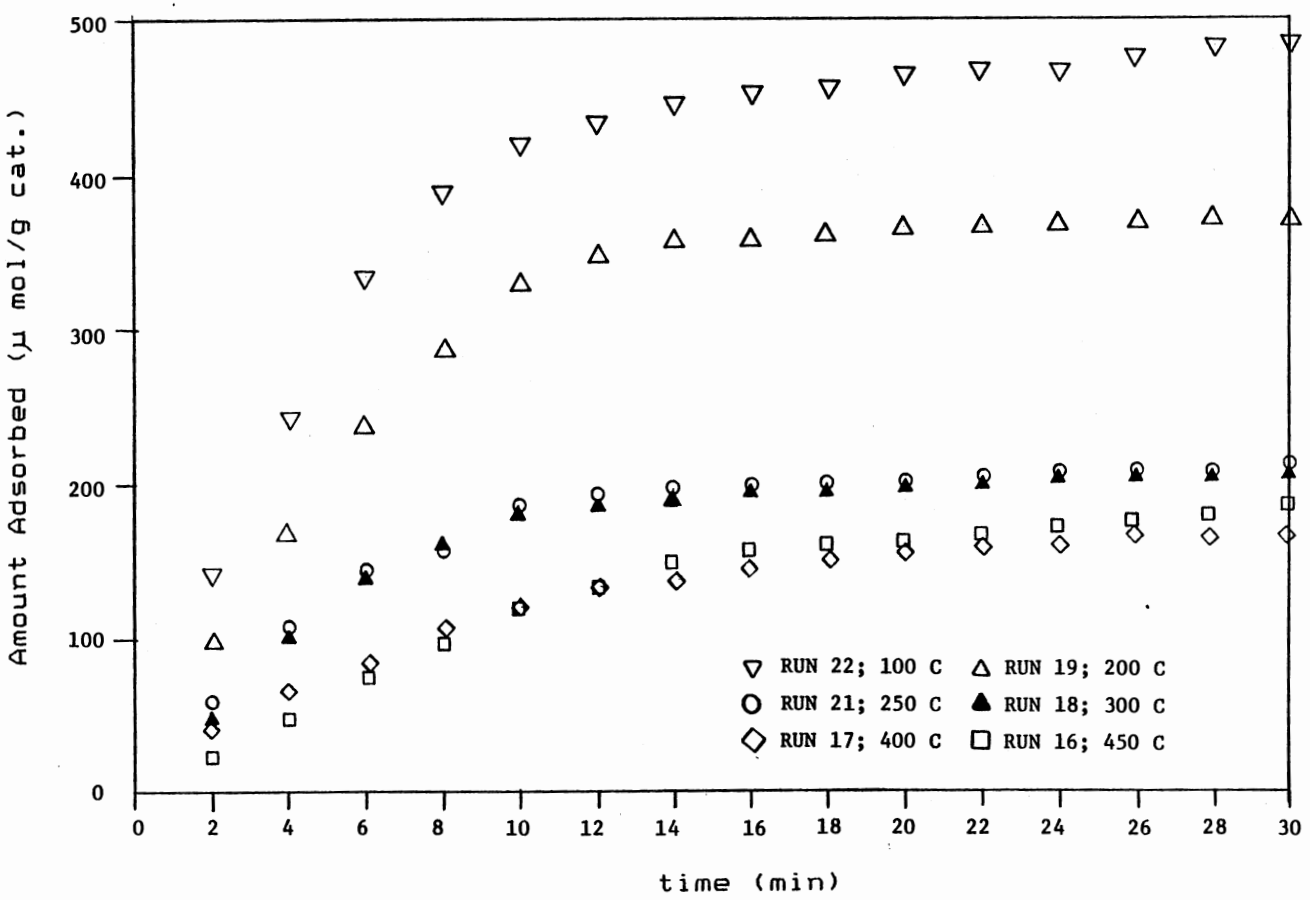

Figure 3. Transient Pyridine Adsorption on Shell 324 Catalyst (0-30 min period).

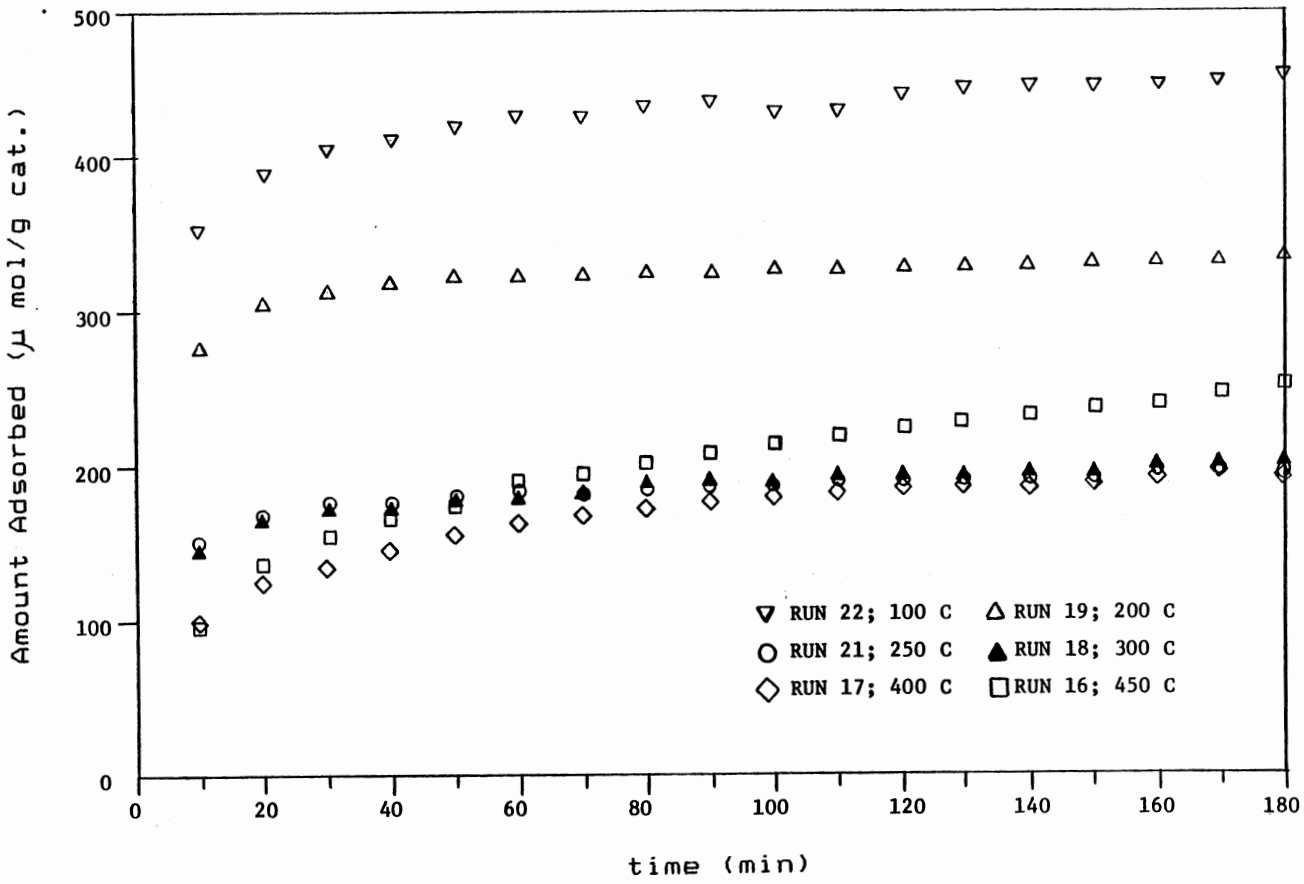

Figure 4. Transient Pyridine Adsorption on Shell 324 Catalyst (0-180 min period).

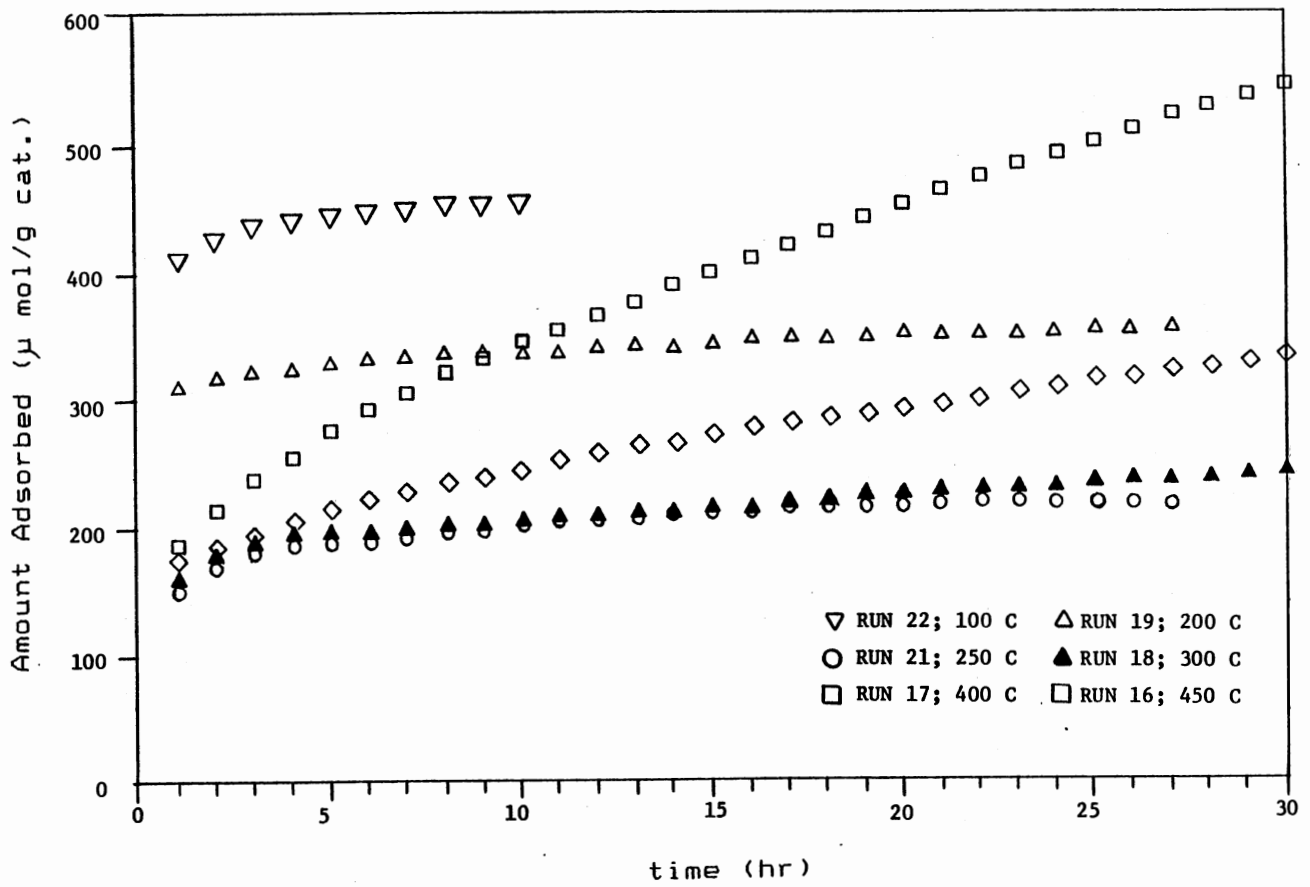

Figure 5. Transient Pyridine Adsorption on Shell 324 Catalyst (0-1800 min period).

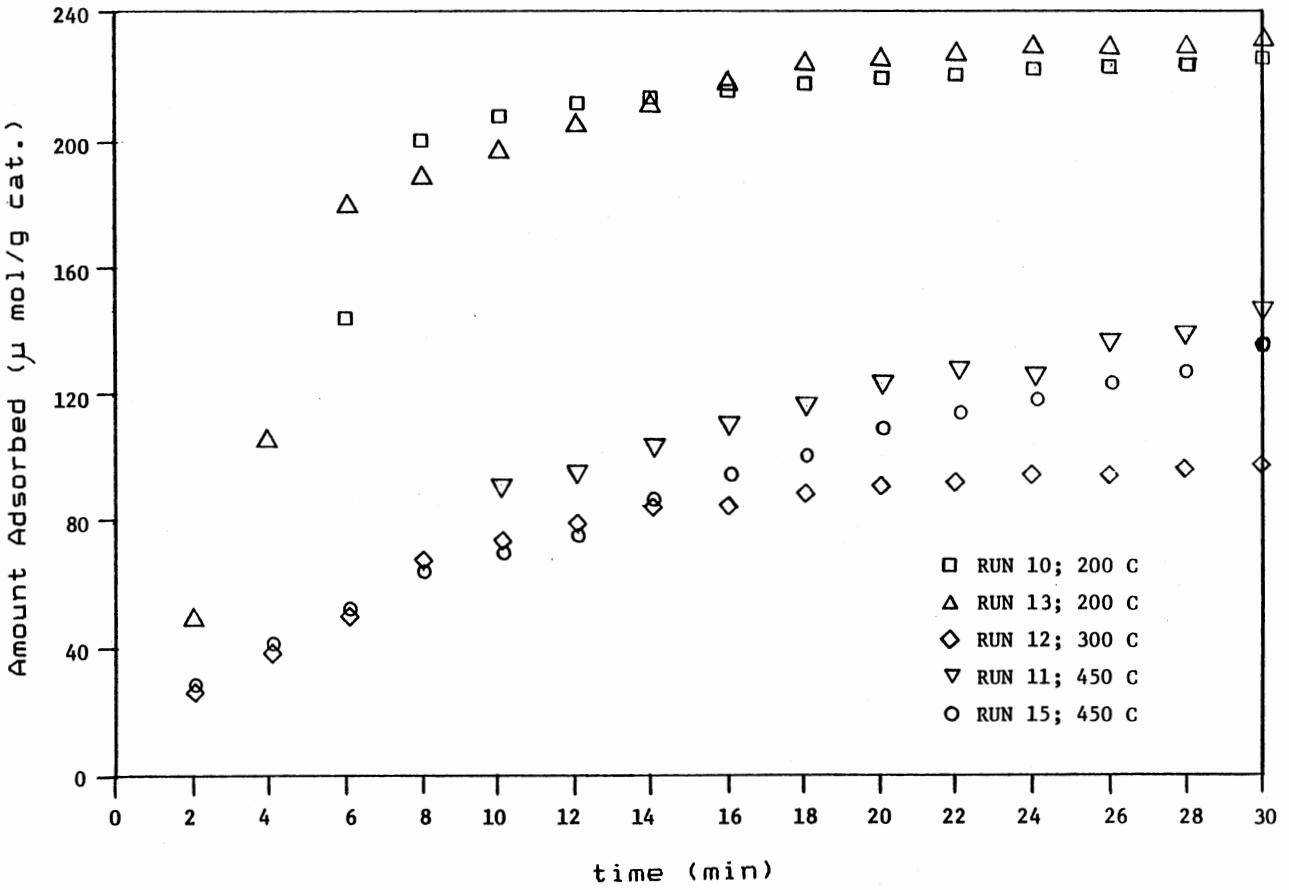

Figure 6. Transient Pyridine Adsorption on HDN-60 Catalyst (0-30 min period).

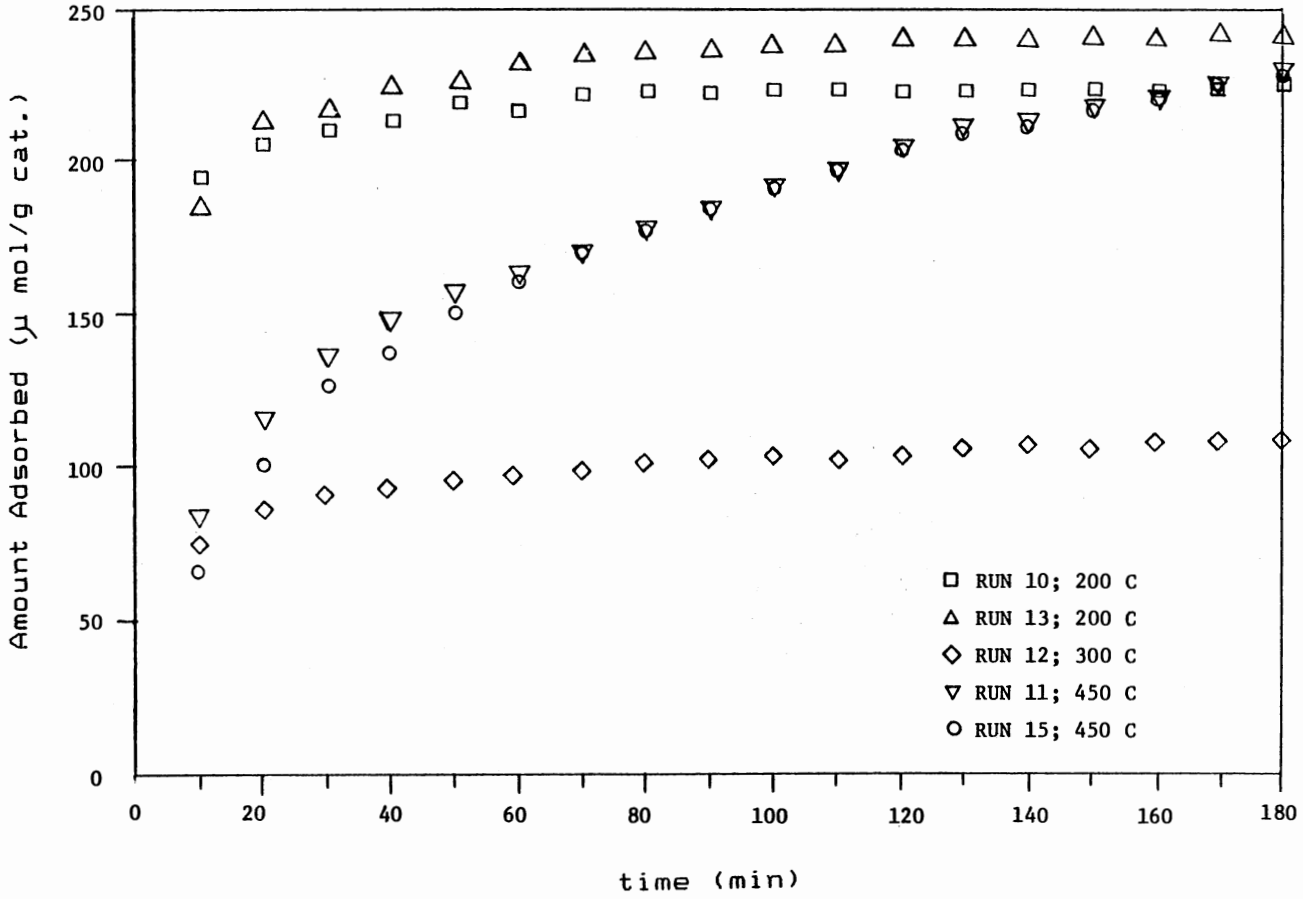

Figure 7. Transient Pyridine Adsorption on HDN-60 Catalyst (0-180 min period).

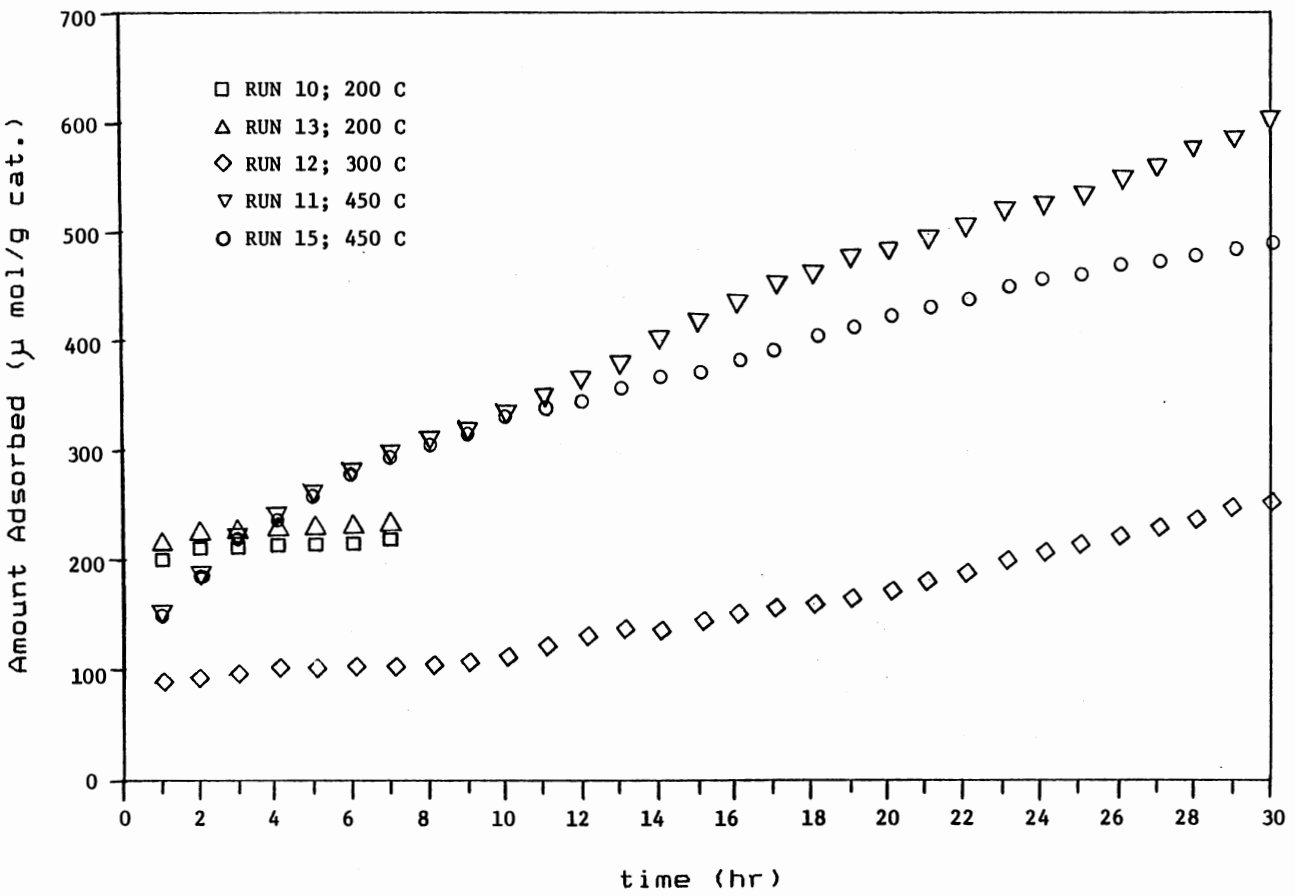

Figure 8. Transient Pyridine Adsorption on HDN-60 Catalyst (0-1800 min period).

TABLE IV

PYRIDINE IRREVERSIBLE ADSORPTION DATA

Run	Temp. (C)	Cat. Wt. (mg) initial	Cat. Wt. (mg) after ads.	Cat. Wt. (mg) after des.	Irreversibility#
10*	200	7.4765	7.6151	7.5528	55 %
12*	300	7.6050	7.9470	7.7115	31 %
13*	200	6.7402	6.8735	6.7954	41 %
24**	250	13.7180	13.9694	13.8262	43 %
25**	100	12.7255	13.1377	12.8578	34 %
		12.8578	13.146	12.897***	41 %

* HDN-60 catalyst.
** Shell 324 catalyst.
*** Desorption after equilibrium readsorption of Run 25 was achieved.
\# Irreversibility = $\frac{\text{(wt. after des. - initial wt.)}}{\text{wt. after ads. - initial wt.}} \times 100$

the phenomena. The catalyst readsorbed pyridine vapor and a new equilibrium was established at 418.2 μ mol/g cat (33.04 mg/g cat) compared with 410.05 μ mol/g cat (32.392 mg/g cat) of the first equilibrium adsorption. After a new equilibrium was achieved, desorption was conducted which showed a value of 163.25 μ mol/g cat (12.897 mg/g cat) irreversibility adsorbed pyridine on the catalyst compared with 162.75 μ mol/g cat (12.858 mg/g cat) of the first desorption. This indicated that multiple adsorption and desorption did not have a permanent effect on the catalyst.

Additional runs were made in temperature programmed adsorption mode, where the temperature was increased at the rate of 1.67 C/min under pyridine partial pressure. One can expect a decrease of weight on catalyst during this temperature increase. However, in Run 19, after establishment of equilibrium adsorption at 200 C, when temperature was increased to 300 C and maintained constant at this temperature, the catalyst readsorbed pyridine vapor and the equilibrium was completed at 449.91 μ mol/g cat (35.343 mg/g cat) compared with 399.14 μ mol/g cat (31.532 mg/g cat) at 200 C. In Run 21, after the equilibrium adsorption was established at 250 C, the temperature was increased to 450 C at a rate of 1.67 C/min in the pyridine atmosphere. As the temperature increased, the pyridine started to desorb from the catalyst. However, after 420 C, pyridine started to readsorb on the catalyst. The temperature was then maintained at 450 C to achieve a new

equilibrium adsorption which showed a value of 1080 μ mol/g cat (85.34 mg/g cat) compared to 229.28 μ mol/g cat (18.109 mg/g cat) at 250 C. Tables A-III and A-IV in Appendix A shows the raw adsorption data during this period and Figures 9 and 10 are the graphic presentation of this weight change.

One may expect the experimental results to be affected by several sources of error. Pyridine can adsorb on the nichrome wire basket and increase the weight. Buoyancy effect due to differences in density at temperatures and pyridine partial pressures can decrease the weight reading. Finally, the random error in reading the measuring weight can cause errors in the measurements. Therefore, an error analysis is conducted and discussed in Appendix C.

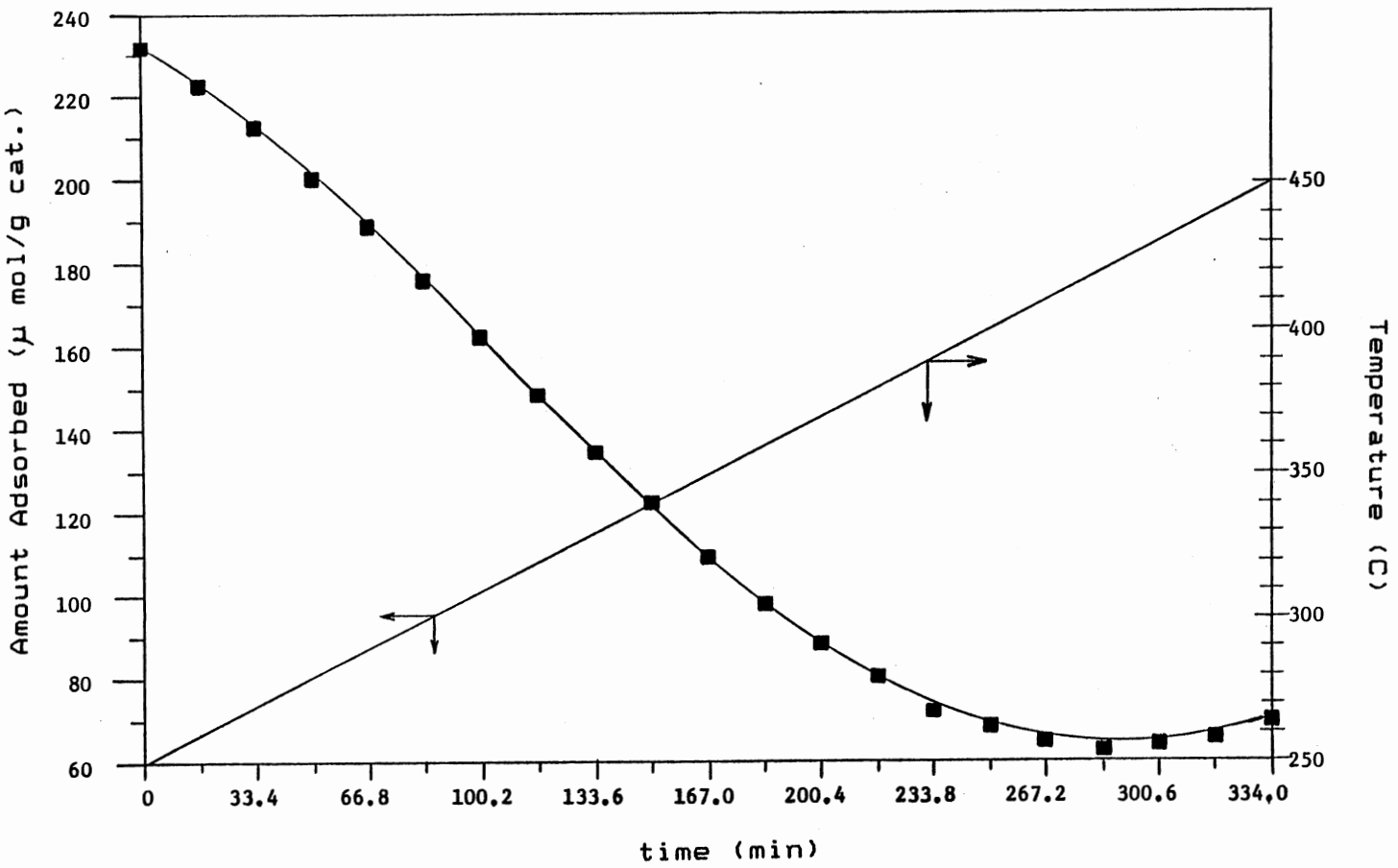

Figure 9. Temperature Programmed Adsorption under Pyridine Partial Pressure-Run 21

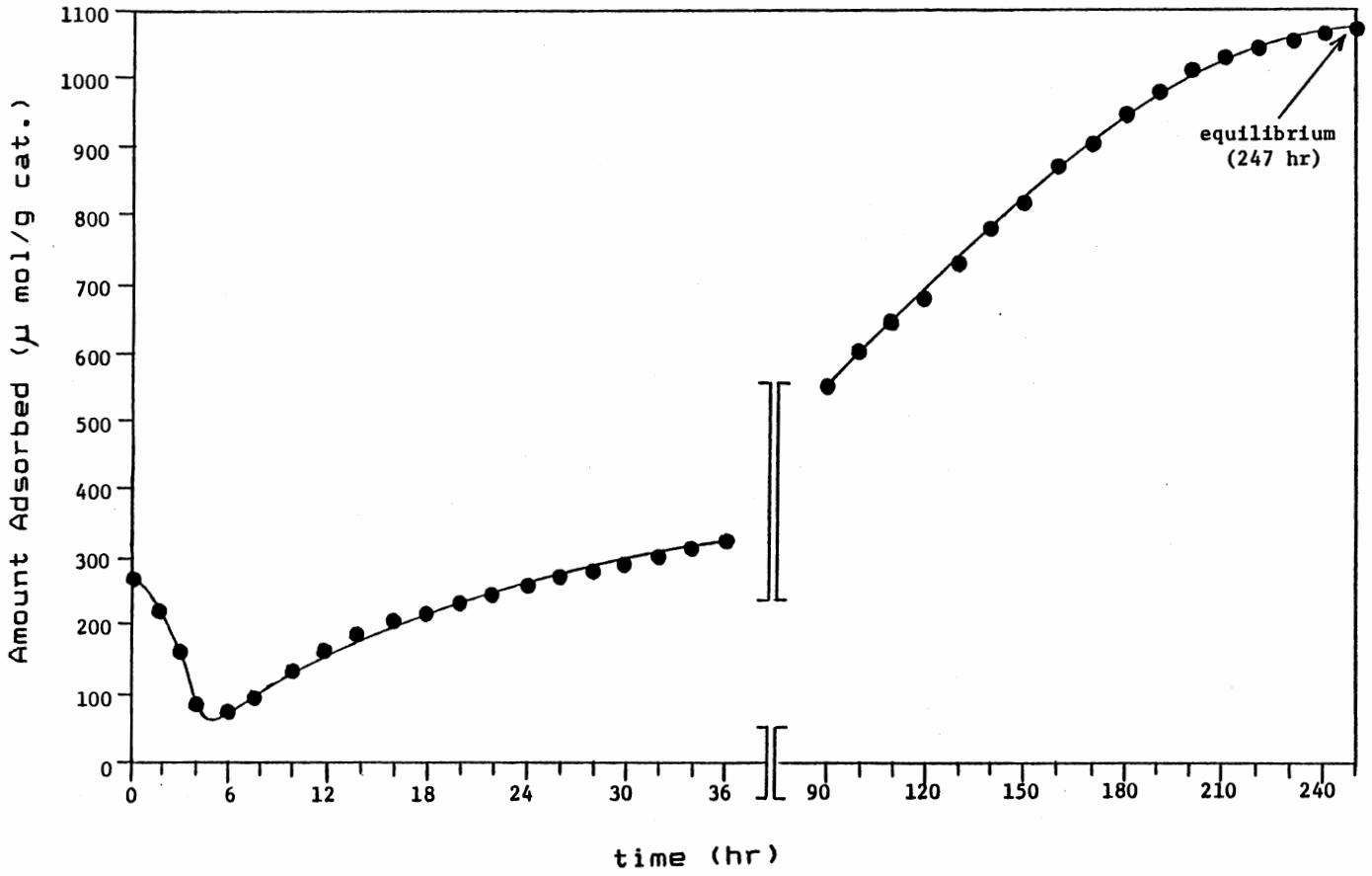

Figure 10. Transient Pyridine Adsorption at 450 C-Run 21
(after Temperature Programmed Adsorption)

CHAPTER V

DISCUSSION

Analysis of the adsorption data in this work may be divided into two sections of equilibrium and dynamics.

Equilibrium Adsorption

Basically, there are two types of gas adsorption on solid surface: physical adsorption and chemisorption. Physical adsorption is characterized by a decrease in the amount of adsorbed species as the temperature increases. In contrast, chemisorption (both non-activated and activated) is favored by an increase in the temperature (Smith, 1985).

The equilibrium adsorption data of pyridine on both Shell 324 and HDN-60 catalysts, which are shown in Figure 2, indicate the relation between temperature and the amount of adsorbed pyridine. Considering the general characteristics of adsorption, two different types of pyridine adsorption on Ni-Mo/alumina are observed: physical adsorption and chemisorption. The adsorption of pyridine on Ni-Mo/alumina in the range of temperature below 250 C is attributed predominantly to physical adsorption, since the equilibrium adsorption decreases with increased temperature. The adsorption in the temperature ranges above 250 C is

predominantly by chemisorption, since the equilibrium adsorption increases with increased temperature. In general, adsorption is not limited to a monolayer on the surface. Multilayer adsorption may occur on the catalyst surface at any temperature, but it primarily exists at low temperatures. However, Table III shows that the maximum fractional surface coverage of pyridine is only 28 % of total surface coverage by a monolayer at the lowest temperature and 74 % at the highest temperature. This is corresponding to 1.539 and 1.509 m mol/g cat (121.6 and 119.2 mg/g cat) for Shell 324 and HDN-60 catalysts respectively. The basis for calculation of the monolayer coverage is described in the Appendix B.

The equilibrium adsorption data at different temperatures can be used to calculate the heat of adsorption. The heat of adsorption at the initial stages of adsorption can be determined by the relationship between the initial rate of adsorption and temperature. The adsorption and desorption may be expressed as:

$$P + S \underset{k_2}{\overset{k_1}{\rightleftharpoons}} PS$$

where;

P represents the molecules of pyridine in the gas phase,

S represents the catalyst active sites, and

PS represents the adsorbed pyridine on a catalyst site.

The adsorption rate, r_a will be:

$$r_a = k_1 P_p C_s = A P_p \exp(-E_a/RT) C_s \quad (1)$$

The desorption rate, r_d will be:

$$r_d = k_2 C_{ps} = D C_{ps} \exp(-E_d/RT) \quad (2)$$

where, C_{ps} = the concentration of active sites occupied by pyridine in equivalent mol/g cat.

C_s = the concentration of unoccupied active sites in equivalent mol/g cat.

k_1 = adsorption rate constant, $(N/m^2 \text{ time})^{-1}$

k_2 = desorption rate constant, time^{-1}

E_a = activation energy of adsorption, J/mole

E_d = activation energy of desorption, J/mole

A, D = preexponential constants

T = temperature (K)

R = 8.314 J/(mol K)

P_p = pyridine partial pressure in N/m^2

At equilibrium, the rate of adsorption equals to the rate of desorption, so that

$$(AP_p)\exp(-E_a/RT)C_{s(eq)} = [DC_{ps(eq)}]\exp(-E_d/RT) \quad (3)$$

A balance on the active sites on the catalyst surface gives

$$C_{so} = C_s + C_{ps} \quad (4)$$

Substituting equation (4) into equation (3) gives:

$$(AP_p)\exp(-E_a/RT)[C_{so}-C_{(ps)eq}] = [DC_{(ps)eq}]\exp(-E_d/RT) \quad (5)$$

Rearranging equation (5) yields:

$$\frac{C_{(ps)eq}}{C_{so} - C_{(ps)eq}} = (AP_p/D)\exp[-(E_a-E_d)/RT] \quad (6)$$

$$\ln\left[\frac{C_{(ps)eq}}{C_{so} - C_{(ps)eq}}\right] = \ln(B) - \left(\frac{Q}{RT}\right) \quad (7)$$

where, $B = AP_p/D$

Q = heat of adsorption = $E_a - E_d$ in J/mol

If the surface is homogeneous and the heat of adsorption is constant, a plot of $\ln [C_{(ps)eq}/(C_{so} - C_{(ps)eq})]$ versus 1/T will produce a straight line with a slope of -Q/R. Thus, one can calculate the heat of adsorption from this slope. Figure 11 shows the relation between $\ln[C_{(ps)eq}/(C_{so} - C_{(ps)eq})]$ and 1/T for pyridine adsorption on Shell 324 catalyst as measured in this work. It clearly indicates that the surface is not homogeneous and at least two different types of adsorption occur on the catalyst. If these points are represented by three straight lines, using a least square regression, the heat of adsorption in the temperature range between 250 and 400 C is 1.9×10^{-3} J/mol and that between 400 and 450 C is 6.4×10^{-3} J/mol. However, the heat of adsorption in the temperature range between 100 and 250 C is -4.1×10^{-4} J/mol.

One point to explain is the negative value of heat of

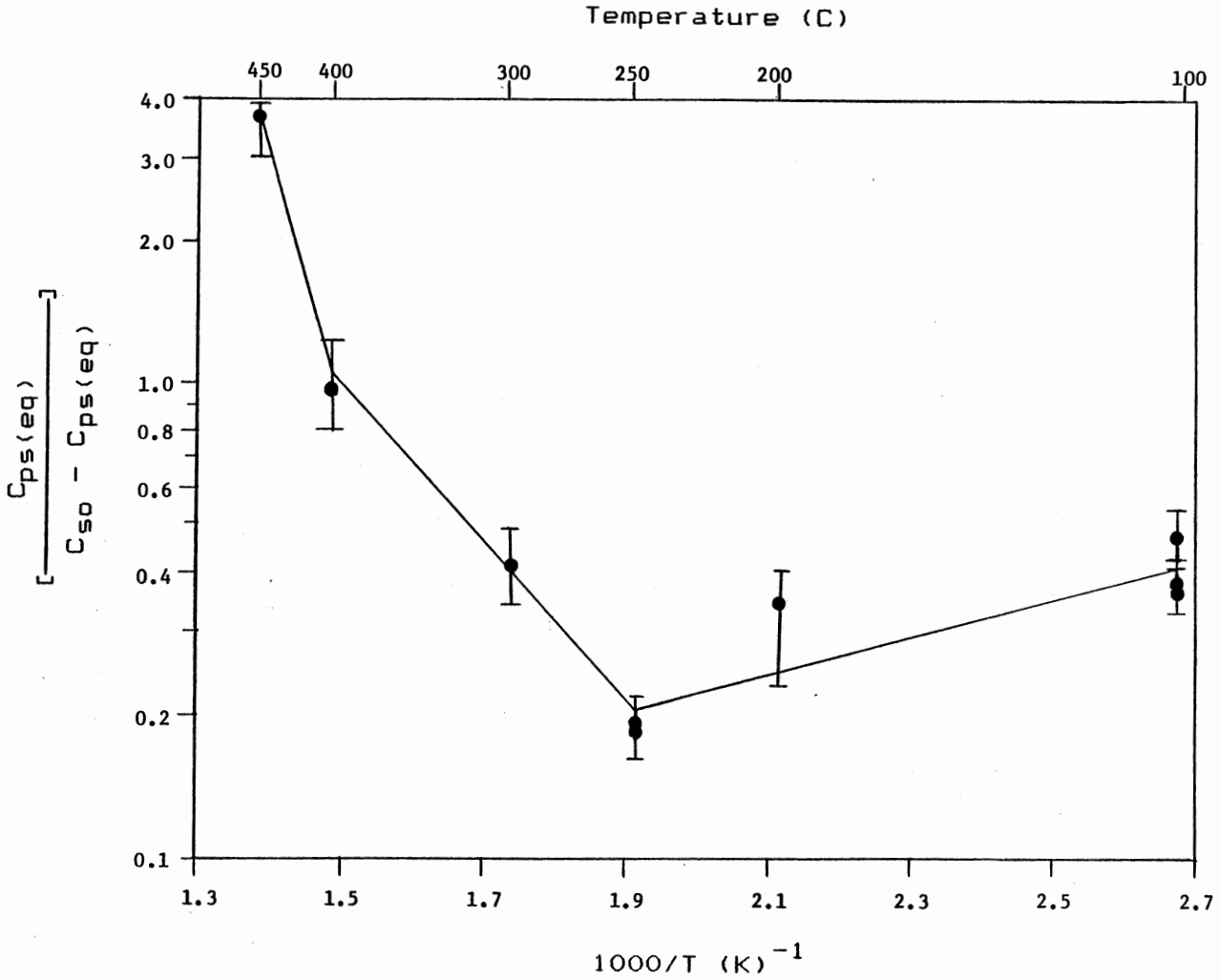

Figure 11. Equilibrium Adsorption Weight Dependence on Temperature

adsorption at equilibrium in the lower temperature range where the adsorption is expected to be physical adsorption. The activation energy, E_a, of physical adsorption is usually very small and may be assumed zero. Thus, physical adsorption is exceedingly rapid at any temperature, and takes place as fast as the adsorbate reaches the surface (Hayward and Trapnell, 1964). Therefore, it may be shown that the activation energy of desorption at low temperatures is approximately equal to the heat of adsorption. The negative sign of heat of adsorption at low temperatures may be regared as an endothermic process. Similar observations have also been made by Deeba and Hall (1985) who studied the chemisorption of pyridine on a silica-alumina catalyst in the temperature range between 150-400 C. They also found that the initial uptake was very fast and the equilibrium was reached within a few minutes. The amount of pyridine adsorption at low temperatures is more than the amount at high temperatures. In addition, Kittrell (1986) studied the equilibrium and transient pyridine adsorption on a Ni-Mo/ alumina hydrotreating catalyst. He found that the equilibrium pyridine adsorption decreased linearly with increasing temperature.

Dynamic Adsorption

Assuming that the rate of desorption is negligible at the early stages of adsorption, equation (1) becomes:

$$r_a = (AP_p)\exp(-E_a/RT)[C_{so} - C_{ps}] \quad (8)$$

Defining θ as the fractional coverage of the catalyst surface, this equation becomes:

$$r_a = (AP_p)\exp(-E_a/RT)[1 - \theta].C_{so} \quad (9)$$

At the initial stage of adsorption, θ is approximately zero, therefore,

$$r_a = (AP_p)\exp(-E_a/RT).C_{so} \quad (10)$$

$$\ln (r_a) = \ln (AP_pC_{so}) - E_a/RT \quad (11)$$

A plot of initial rates of adsorption versus 1/T should give a straight line with a slope of $-E_a/R$. The initial rates of adsorption are determined by the amount adsorbed at the first two minutes of each temperature in Figure 3 and Table A-I. This plot is shown in Figure 12 and yields a negative value of activation energy, -5.26×10^{-4} J/mol. The explanation of a negative sign of activation energy is unknown.

However, it is hard to conceive that a molecule like pyridine can be adsorbed only one way on a complex catalyst surface. Kittrell (1986) found two different types of adsorption at 450 C and suggested that one type of adsorption was possibility due to coke formation and the other was a reversible pyridine adsorption. Physical adsorption and different types of chemisorption can occur simultaneously. Smith (1985) suggests that for a given gas

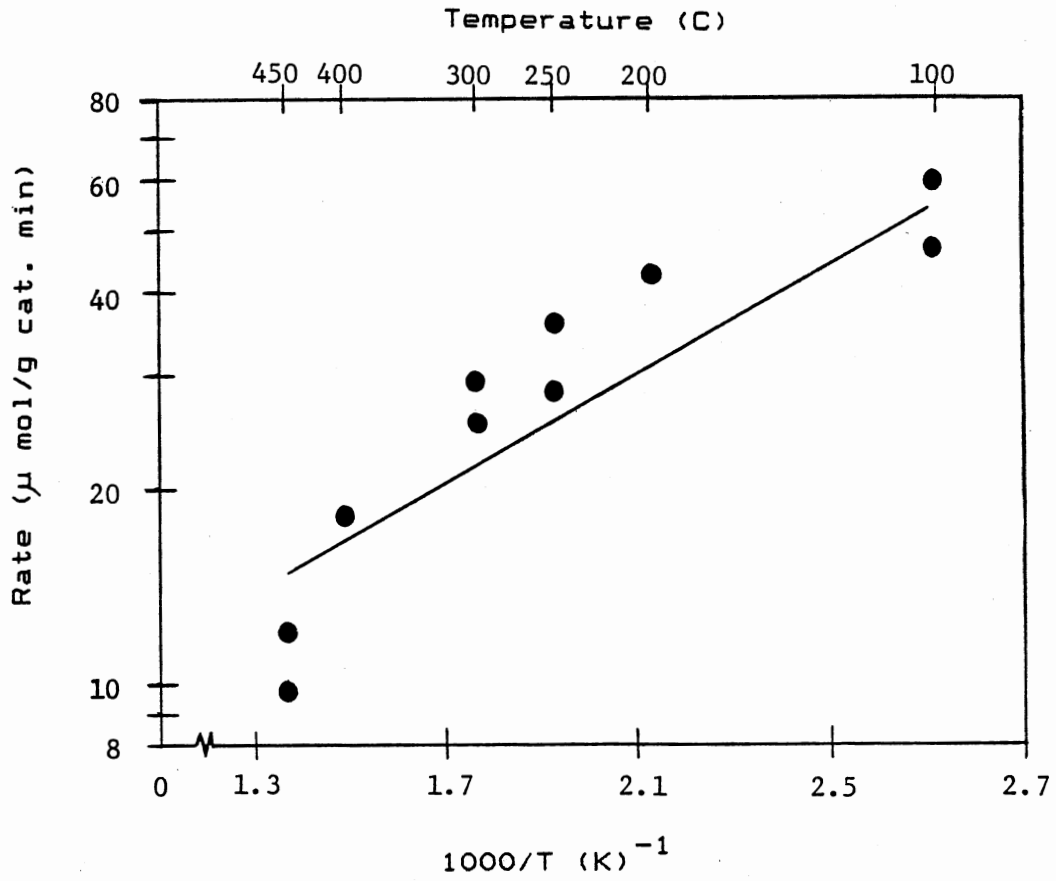

Figure 12. Initial Pyridine Adsorption Rate Dependence on Temperature

and solid the initial chemisorption is frequently non-activated, while the later stages of adsorption are activated chemisorption. Chemisorption is substantiated by the following observations: 1) reversibility experiments indicated that 41 %, to 55 % of the adsorbed pyridine at 200 C and 31 % of that at 300 C were held irreversibly on the HDN-60 catalyst. Similarly, 43 % of pyridine adsorbed at 250 C and 41 % of that at 100 C were irreversibly held on Shell 324 catalyst surface. 2) the color of catalyst was changed from light green-yellow at the beginning of the experiments to gray-black below 250 C and black at temperatures 300, 400, and 450 C at the end of the experiments, indicating some chemical bond transformation.

Figure 3 also demonstrates that the initial rate of adsorption at low temperatures is higher than that at high temperatures. Figures 4 and 5, which show the transient adsorption during 3 and 30 h periods, indicate that the amount of pyridine adsorption at temperatures above 250 C continues to increase for a long period of time while the amount adsorbed at temperatures below 250 C reaches a steady-state value in a shorted time period.

Similarly, for HDN-60 catalyst, Figure 6 shows that the initial rate at low temperatures is higher than that at high temperatures. Figures 7 and 8 show the amount adsorbed at high temperatures tends to increase over time while the amount adsorbed at 200 C reaches an equilibrium value in a shorter time. These suggest that at temperatures higher

than 250 C there may be additional types of adsorption contributing to the catalyst weight.

A simple model, similar to that of Kittrell (1986), including both adsorption and desorption stages, is developed and used to analyze the experimental data.

From equations (1) and (2), the total rate of adsorption, r, can be expressed as:

$$r = \frac{dC_{ps}}{dt} = k_1 P_p C_s - k_2 C_{ps} \qquad (12)$$

Substitution of the active site balance from equation (4), into equation (12) gives:

$$\frac{dC_{ps}}{dt} = k_1 P_p (C_{so} - C_{ps}) - k_2 C_{ps} \qquad (13)$$

$$\frac{dC_{ps}}{dt} = k_1 P_p C_{so} - (k_1 P_p + k_2) C_{ps} \qquad (14)$$

Before integrating this equation, define two variables, q_1 and q_2, as follows:

$$q_1 = k_1 P_p C_{so} \qquad (15)$$

$$q_2 = k_1 P_p + k_2 \qquad (16)$$

Substitution into equation (8) gives:

$$\frac{dC_{ps}}{dt} = q_1 - q_2 C_{ps} \qquad (17)$$

Integration of the above equation gives:

$$\ln (q_1 - q_2 C_{ps}) = - q_2 t + \ln C \qquad (18)$$

Where C is the constant of integration. The boundary condition for this integration is:

$$@\ t = 0,\ C_{ps} = 0 \qquad (19)$$

which gives:

$$\ln [q_1 - q_2 C_{ps}] = - q_2 t + \ln q_1 \qquad (20)$$

$$\ln \left[\frac{q_1 - q_2 C_{ps}}{q_1}\right] = - q_2 t \qquad (21)$$

Now replace q_1 and q_2 with the appropriate terms:

$$\ln \left[\frac{k_1 P C_{so} - (k_1 P + k_2) C_{ps}}{k_1 P_p C_{so}}\right] = - q_2 t \qquad (22)$$

When t approaches infinity or at equilibrium, equation (5) results in:

$$k_1 P_p (C_{so} - C_{(ps)eq}) = k_2 C_{(ps)eq}$$

$$C_{(ps)eq} = \frac{k_1 P_p C_{so}}{k_1 P_p + k_2} \qquad (23)$$

where; $k_1 = (AP_p)\exp(-E_a/RT)$

$k_2 = (D)\exp(-E_d/RT)$

Dividing all the terms inside the log term of equation (22) by $(k_1 P_p + k_2)$ gives:

$$\ln\left[\frac{C_{(ps)eq} - C_{ps}}{C_{(ps)eq}}\right] = -q_2 t$$

$$\ln\left[\frac{C_{(ps)eq}}{C_{(ps)eq} - C_{ps}}\right] = q_2 t \qquad (24)$$

The model of equation (24) demonstrates the reversible adsorption of a catalyst. A plot of $\ln [C_{(ps)eq}/(C_{(ps)eq} - C_{ps})]$ versus time should produce a straight line with slope of q_2 if only one adsorption mechanism occurs.

For Shell 324 catalyst, however, in the range of temperature between 100 and 250 C, Figures 13-18 demonstrate three straight lines instead of only one straight line. These Figures indicate that there are three different types of adsorption occurring on the catalyst surface. As the temperature increases, additional adsorption mechanisms appear to become effective. Figure 19 shows four different types of adsorption at 300 C, where as Figures 20 and 21 show five mechanisms for adsorption at 400 and 450 C, respectively. As shown in Table A-I and Figure 3, the initial rate of adsorption and initial adsorbed amount at low temperatures are higher than those at high temperatures. Therefore, the first mechanism, which occurs rapidly at low temperatures, may be attributed to a non-activated or physical adsorption whereas the following mechanisms may be considered as slow activated adsorptions. The speculations of different type of adsorption occurring on the catalyst surface are the adsorption on a Lewis site, a Bronsted site,

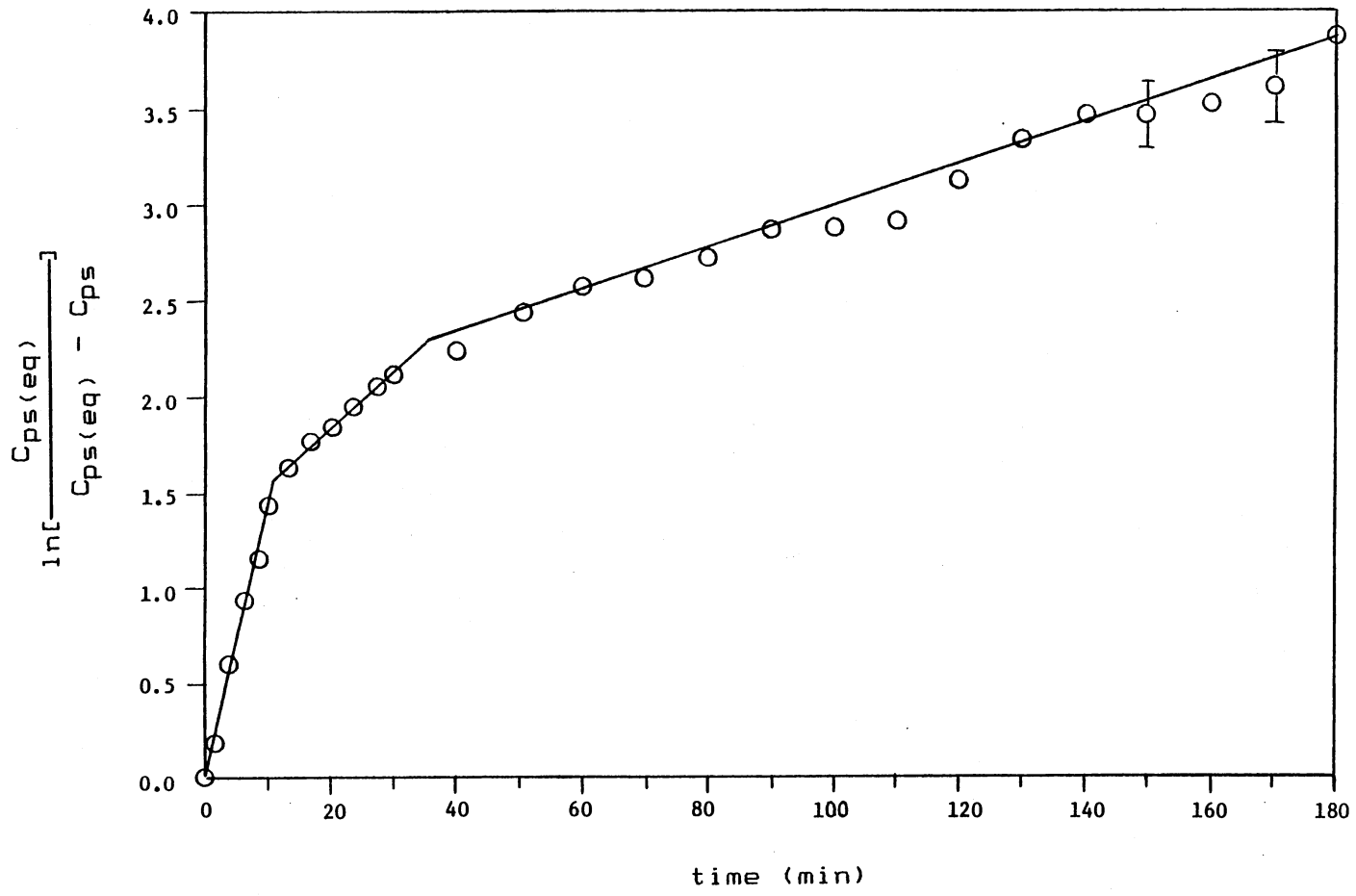

Figure 13. Reversible Adsorption Model Plot of Run 22, 100 C (Shell 324)

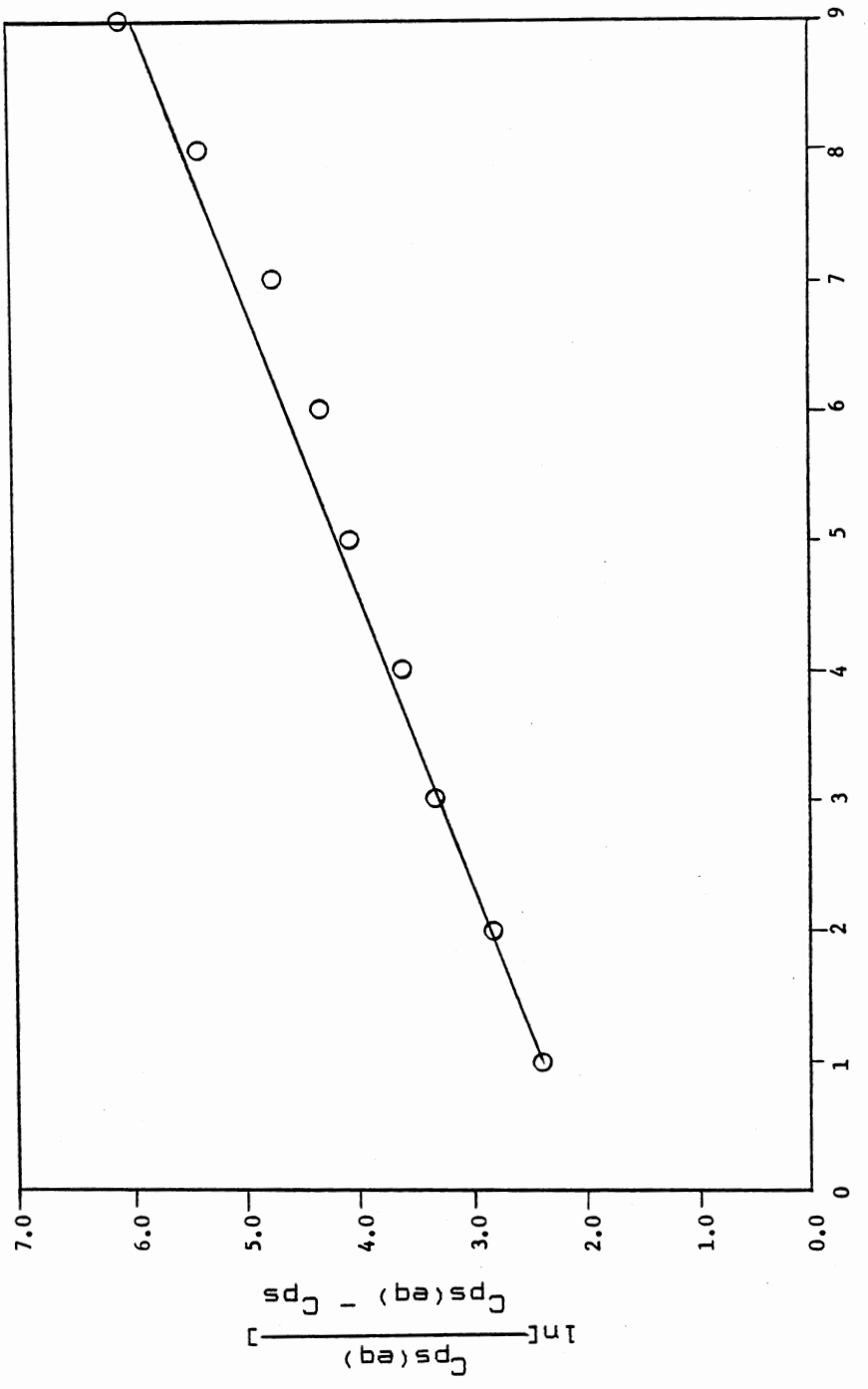

Figure 13. (Continued)

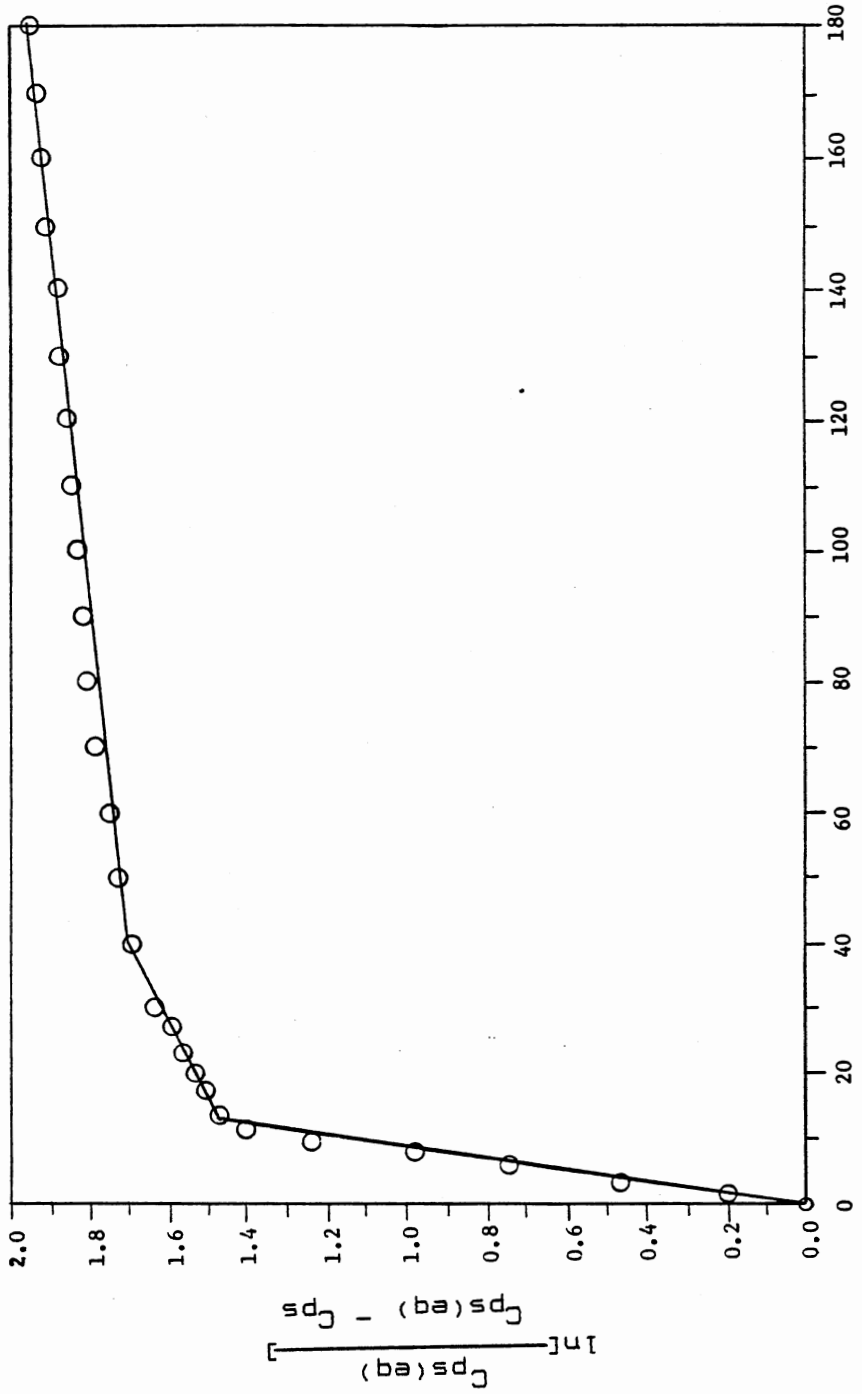

Figure 14. Reversible Adsorption Model Plot of Run 25, 100 C (Shell 324)

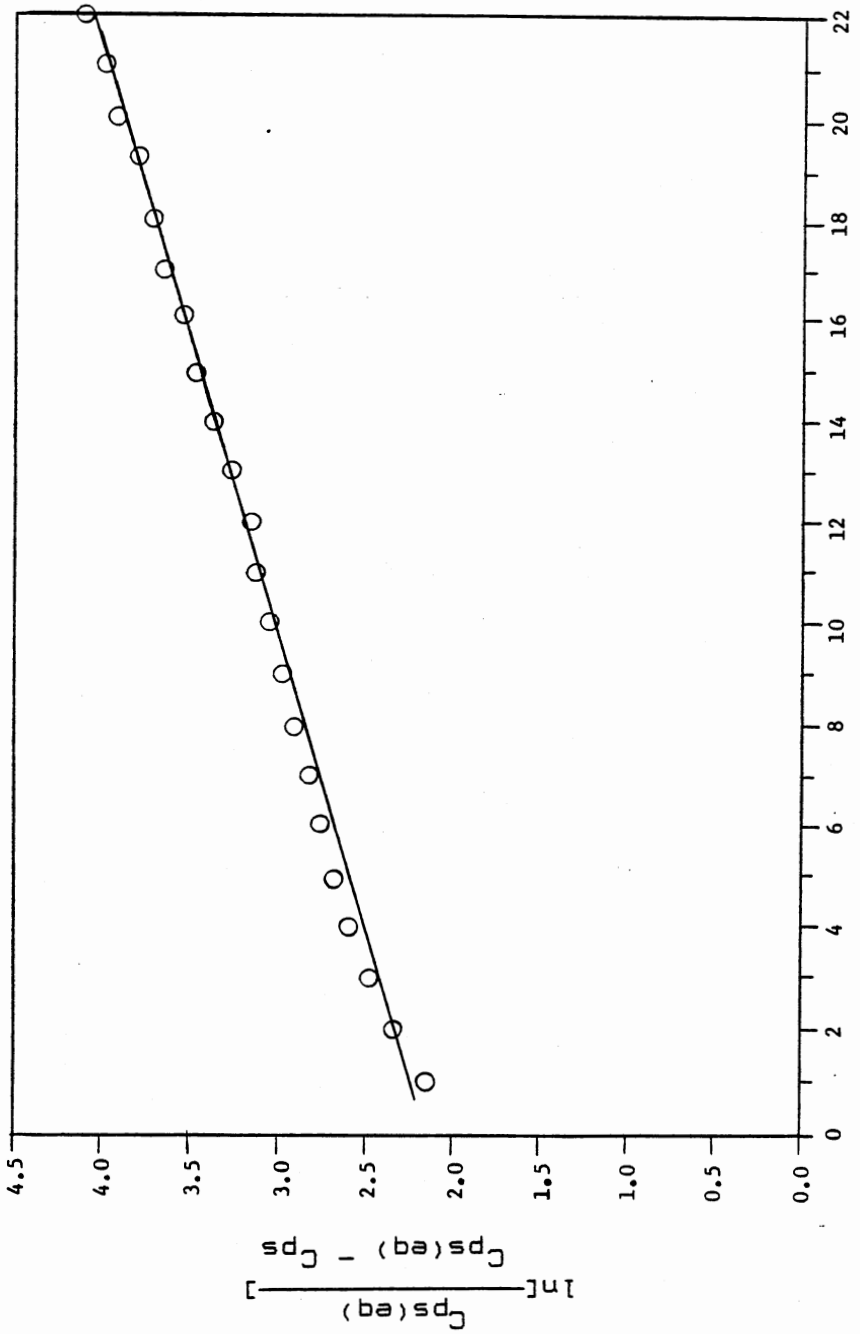

Figure 14. (Continued)

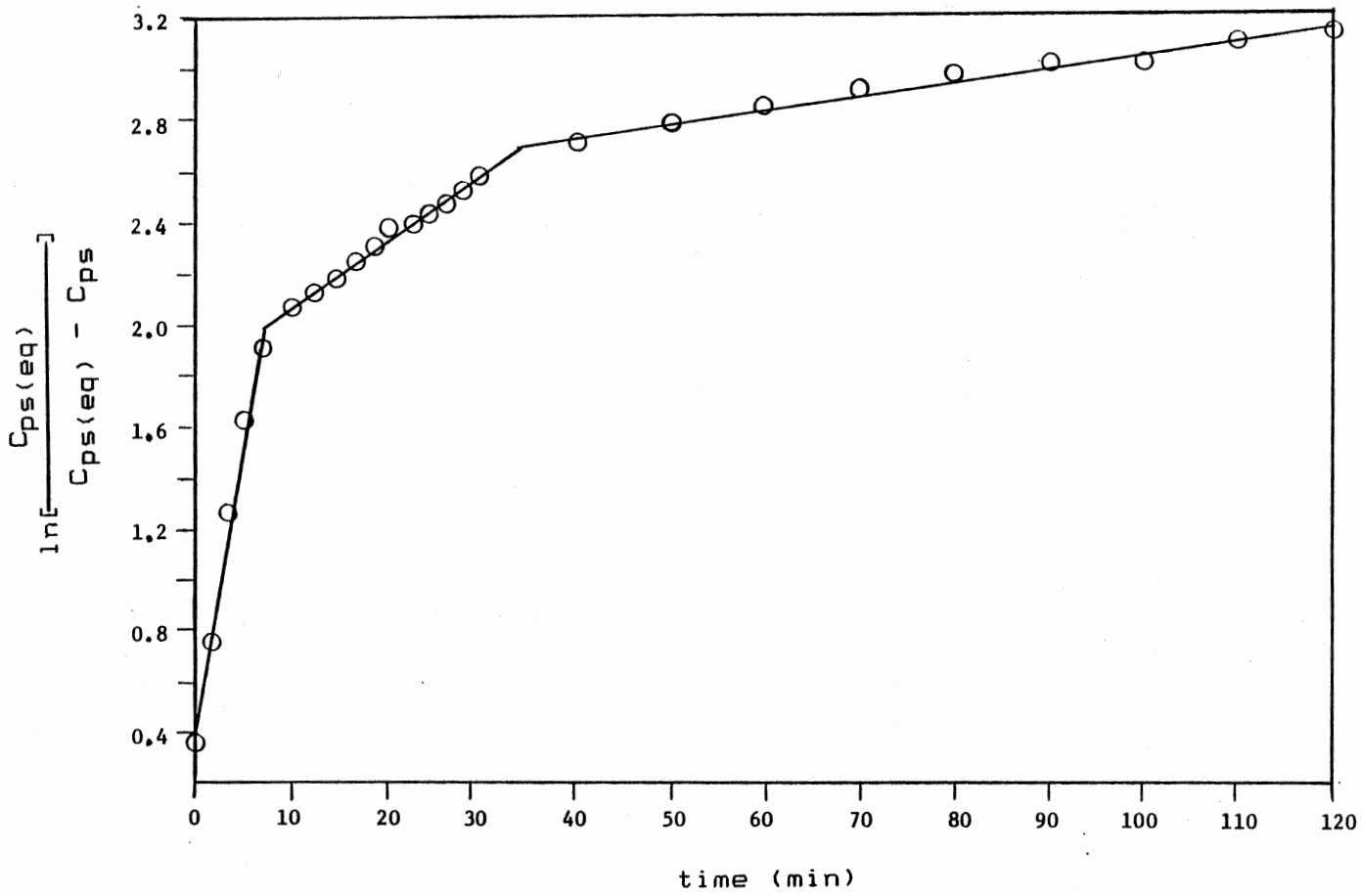

Figure 15. Reversible Adsorption Model Plot of Run 25, 100 C after Desorption (Shell 324)

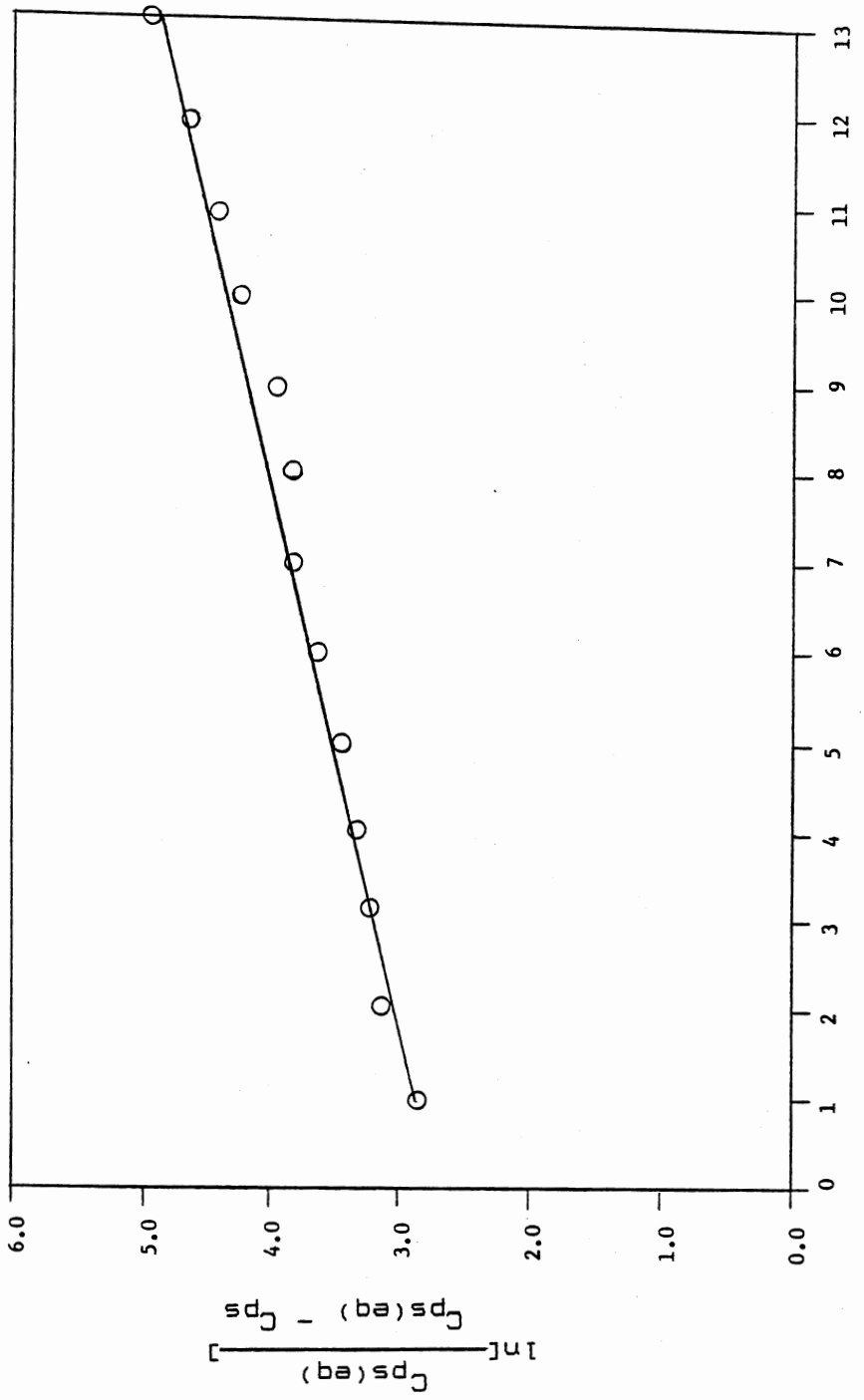

Figure 15. (Continued)

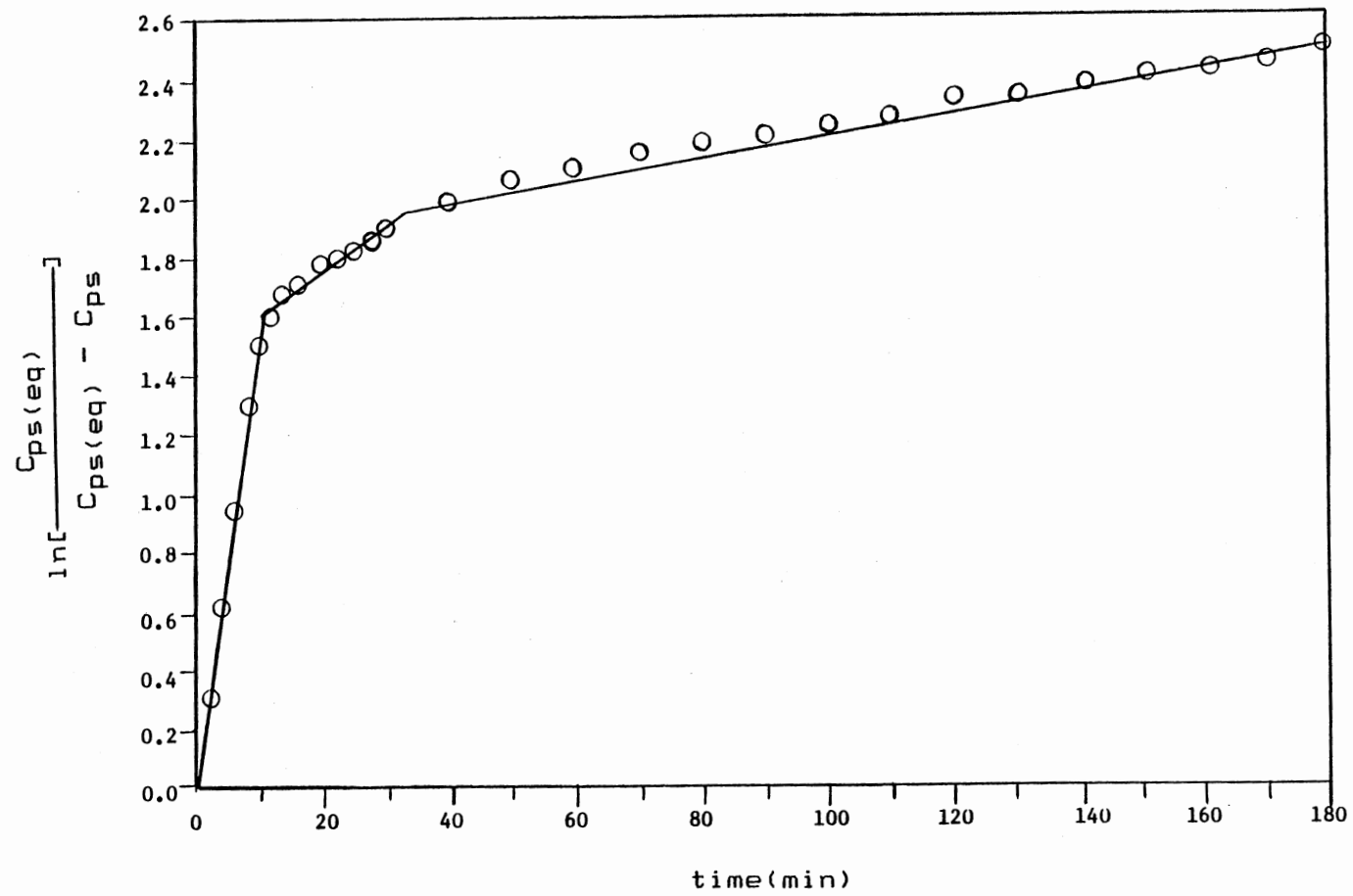

Figure 16. Reversible Adsorption Model Plot of Run 19, 200 C (Shell 324)

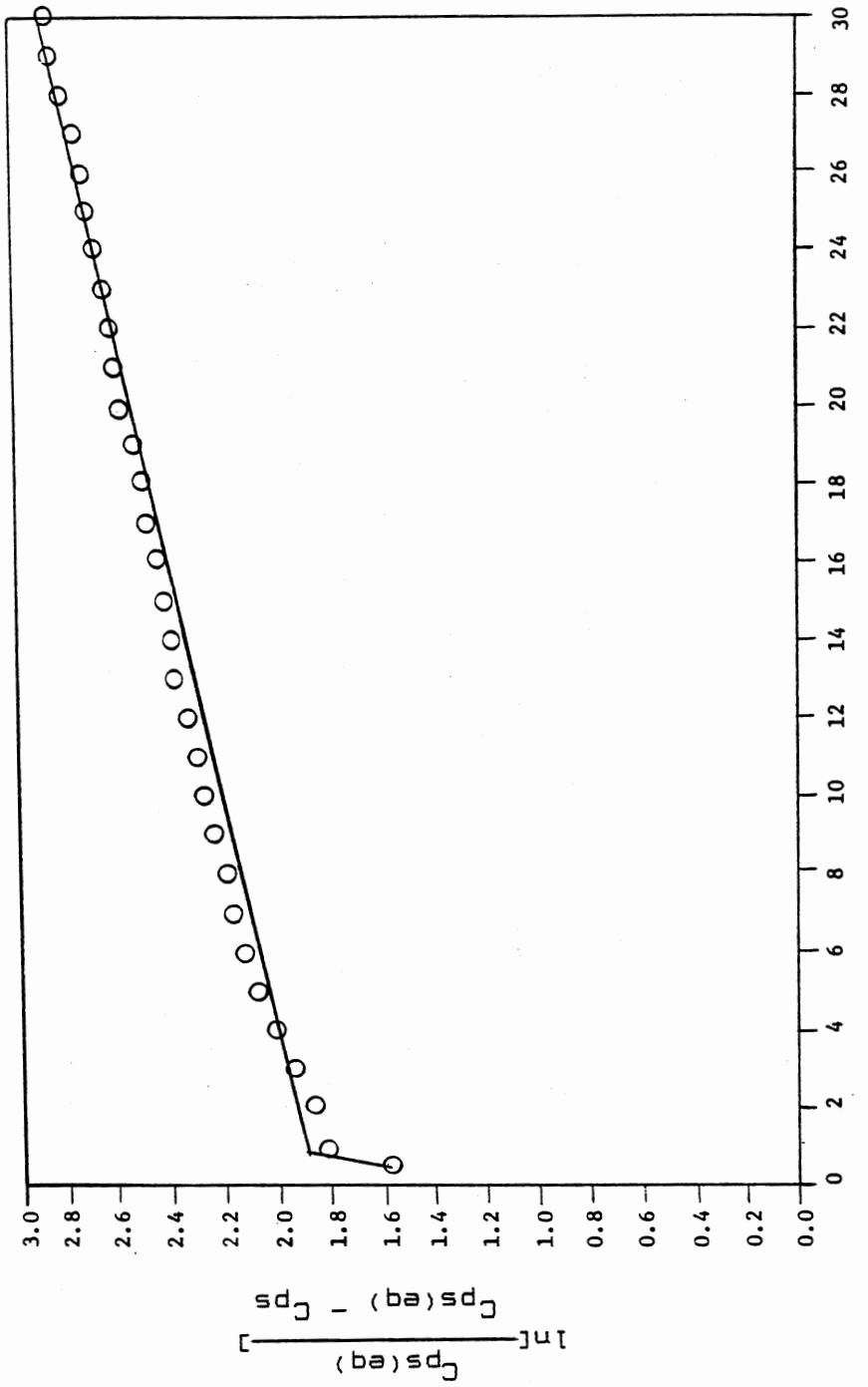

Figure 16. (Continued)

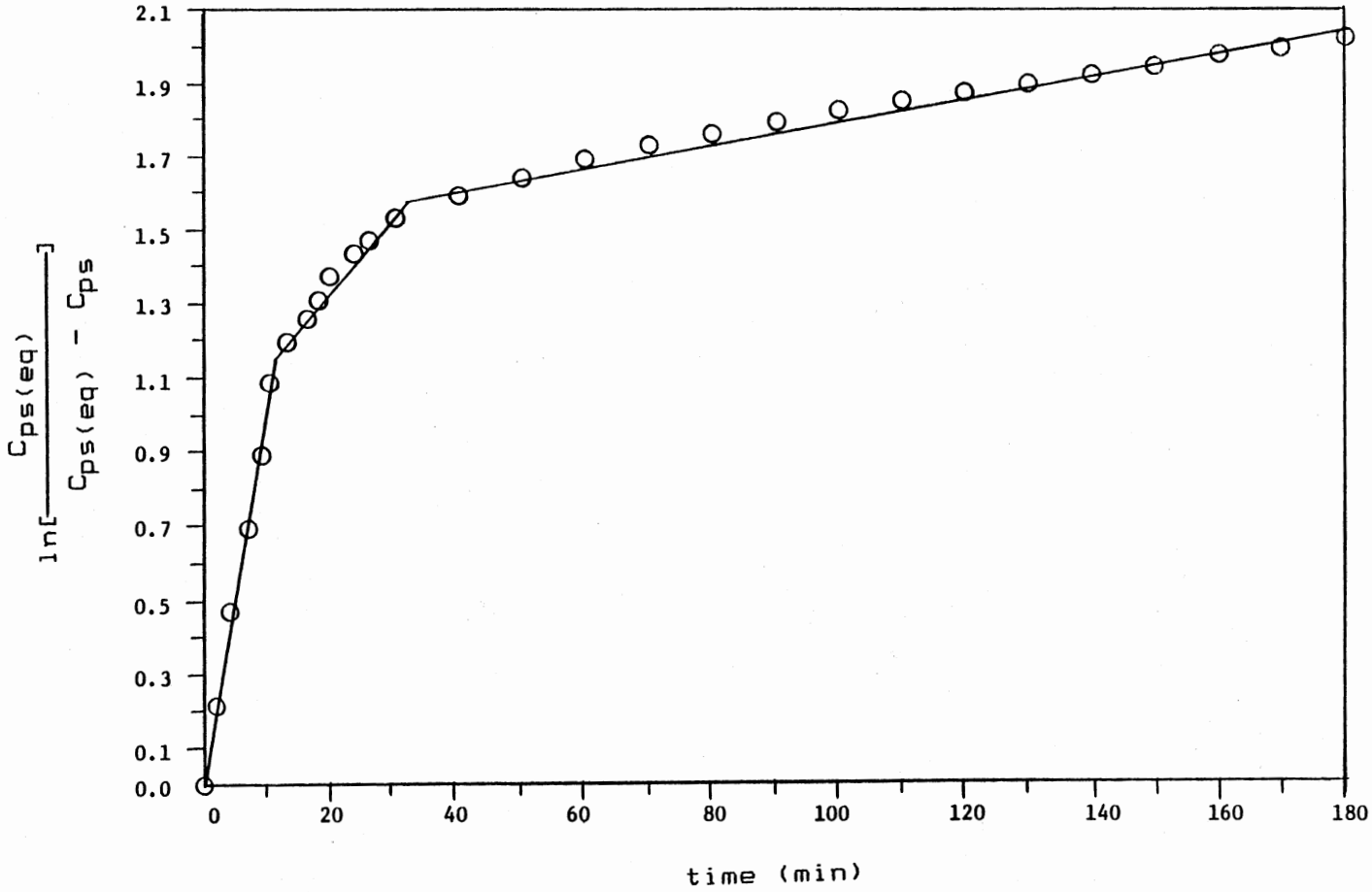

Figure 17. Reversible Adsorption Model Plot of Run 21, 250 C (Shell 324)

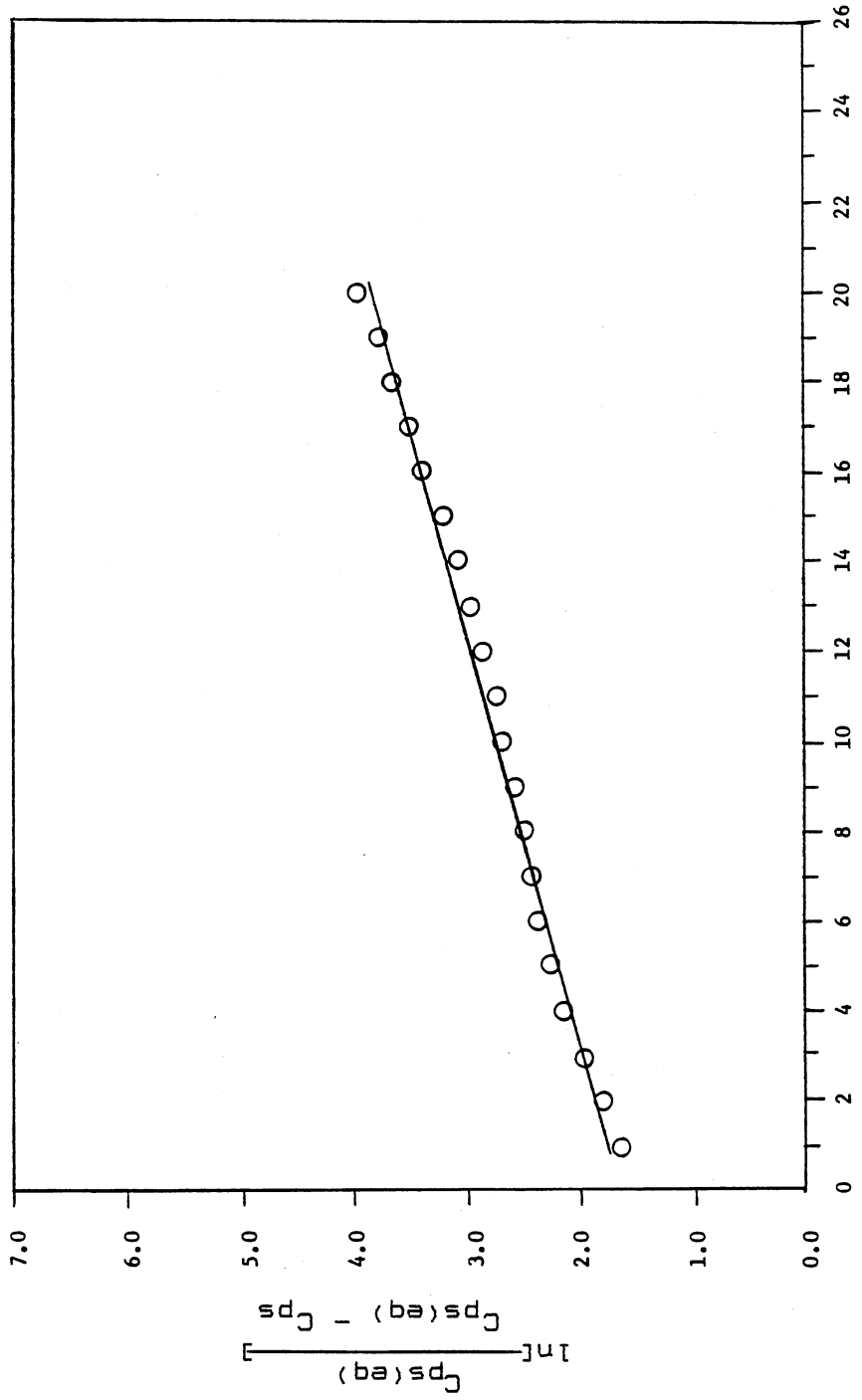

Figure 17. (Continued)

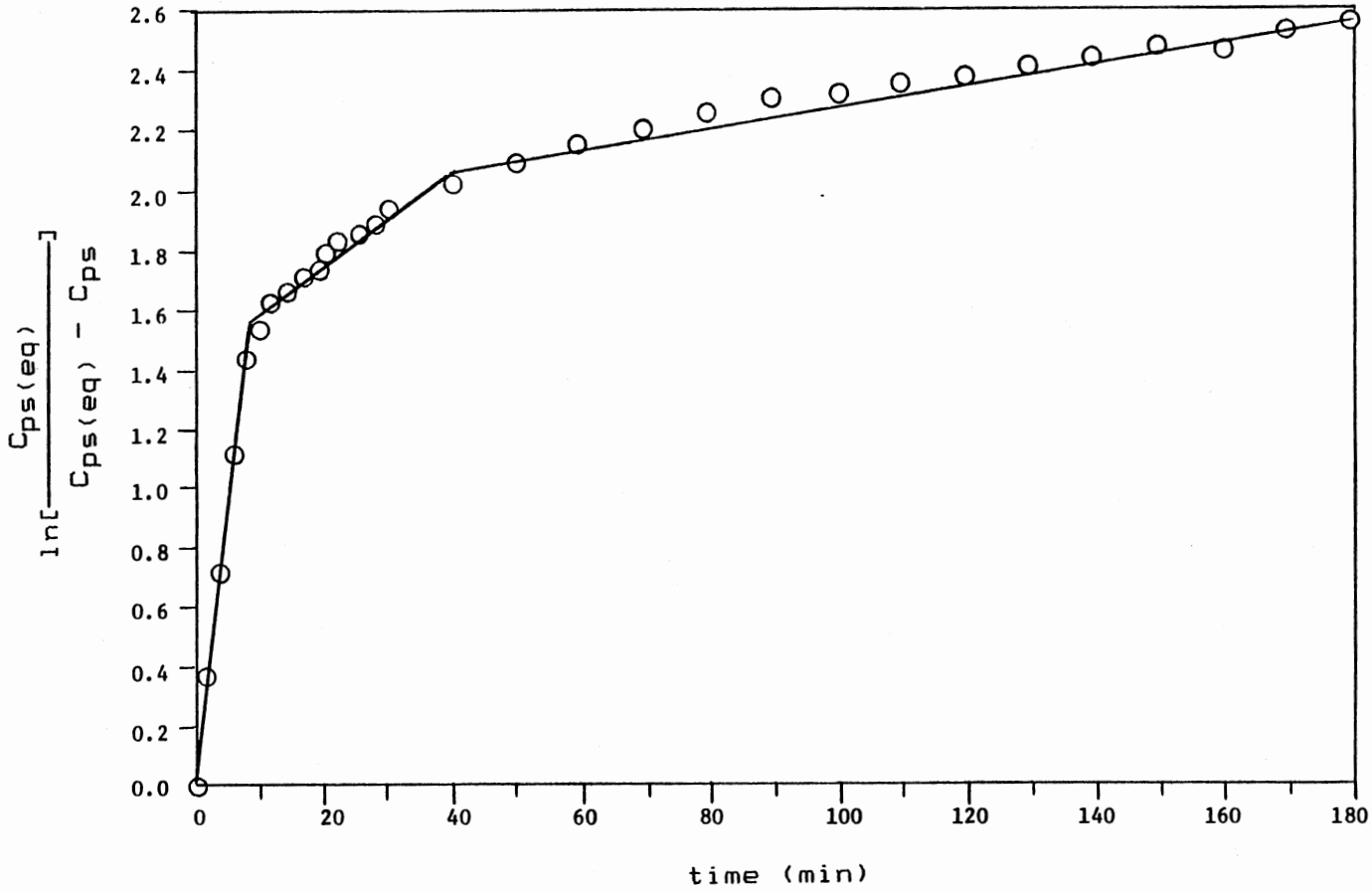

Figure 18. Reversible Adsorption Model Plot of Run 24, 250 C (Shell 324)

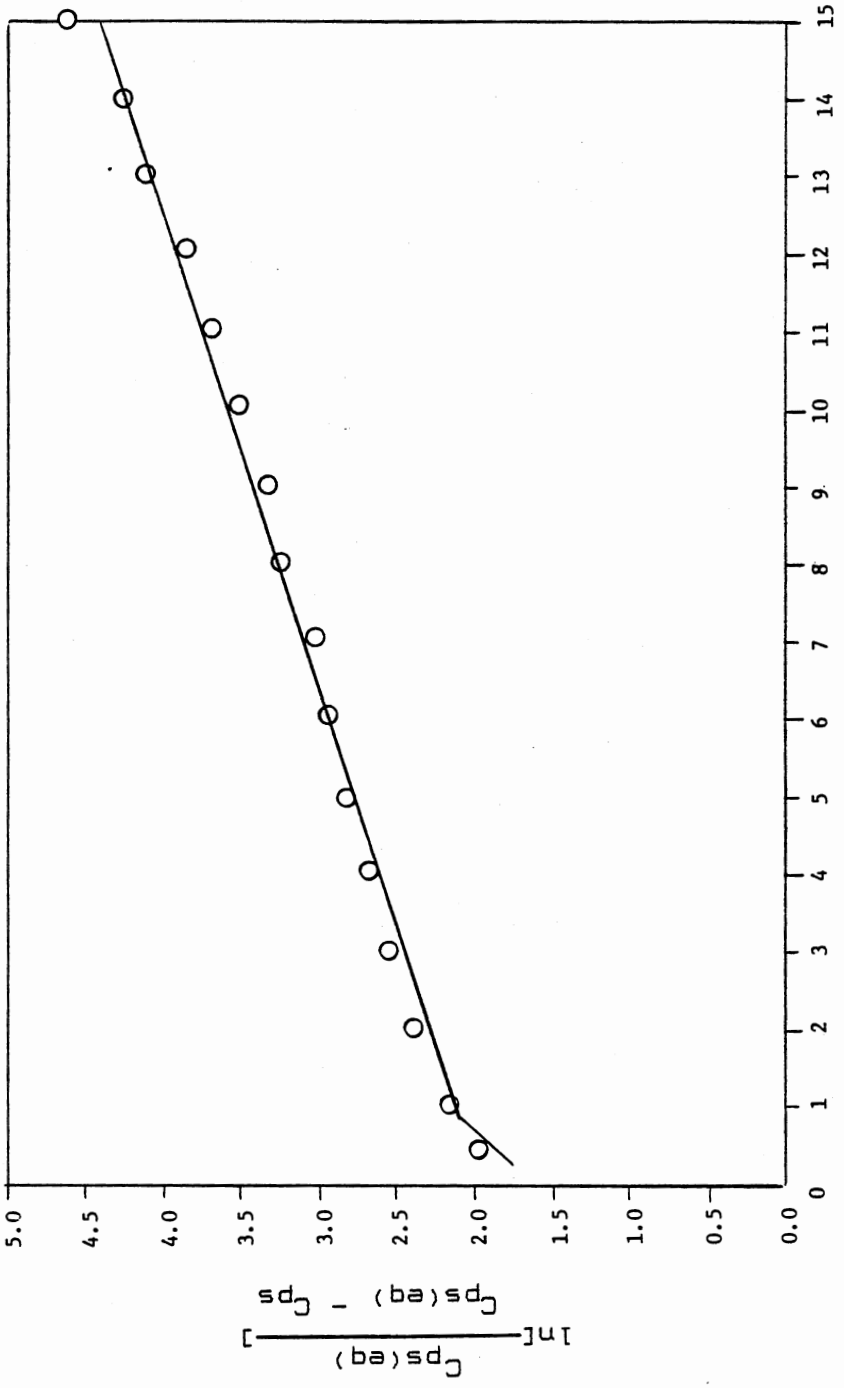

Figure 18. (Continued)

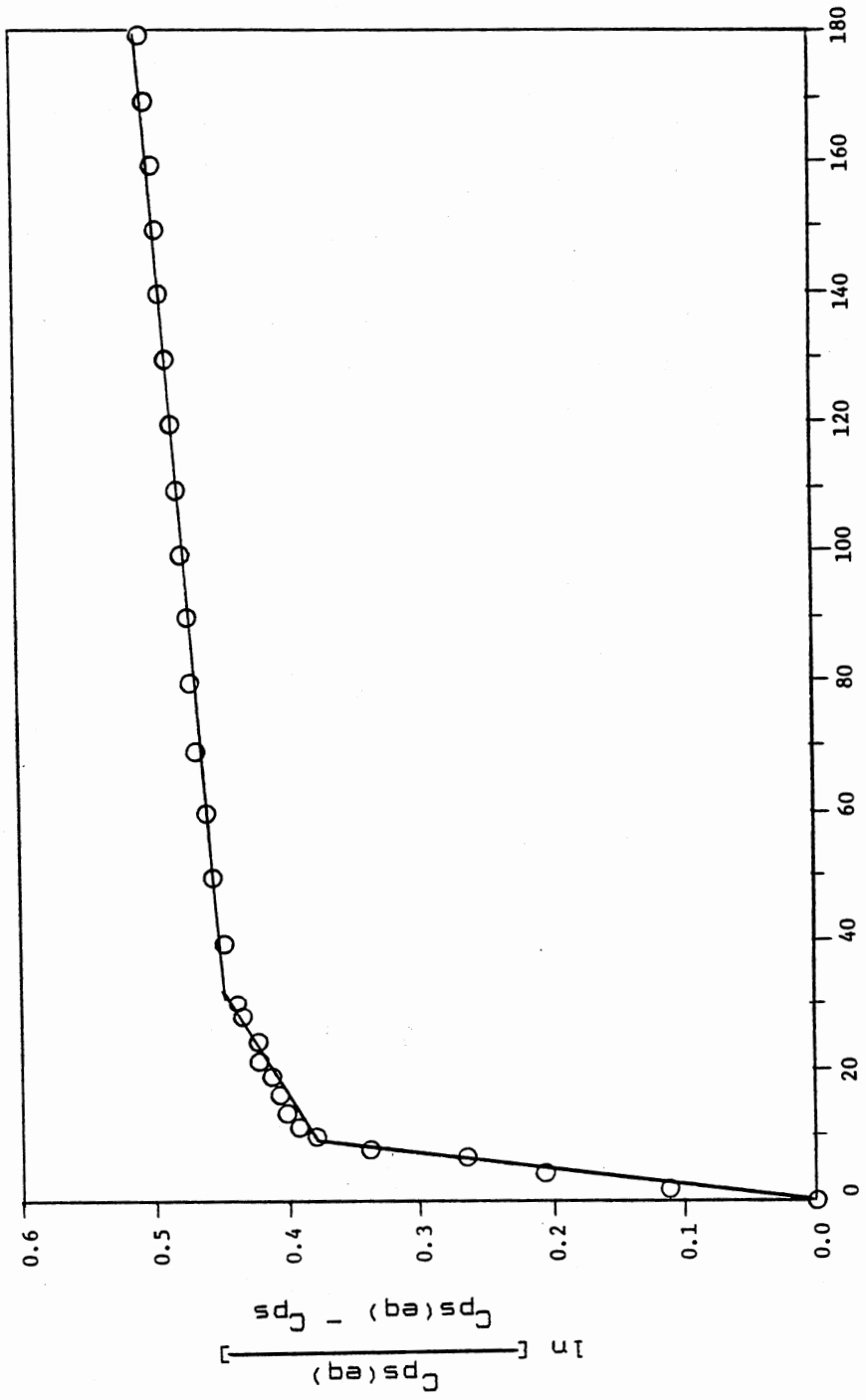

Figure 19. Reversible Adsorption Model Plot of Run 18, 300 C (Shell 324)

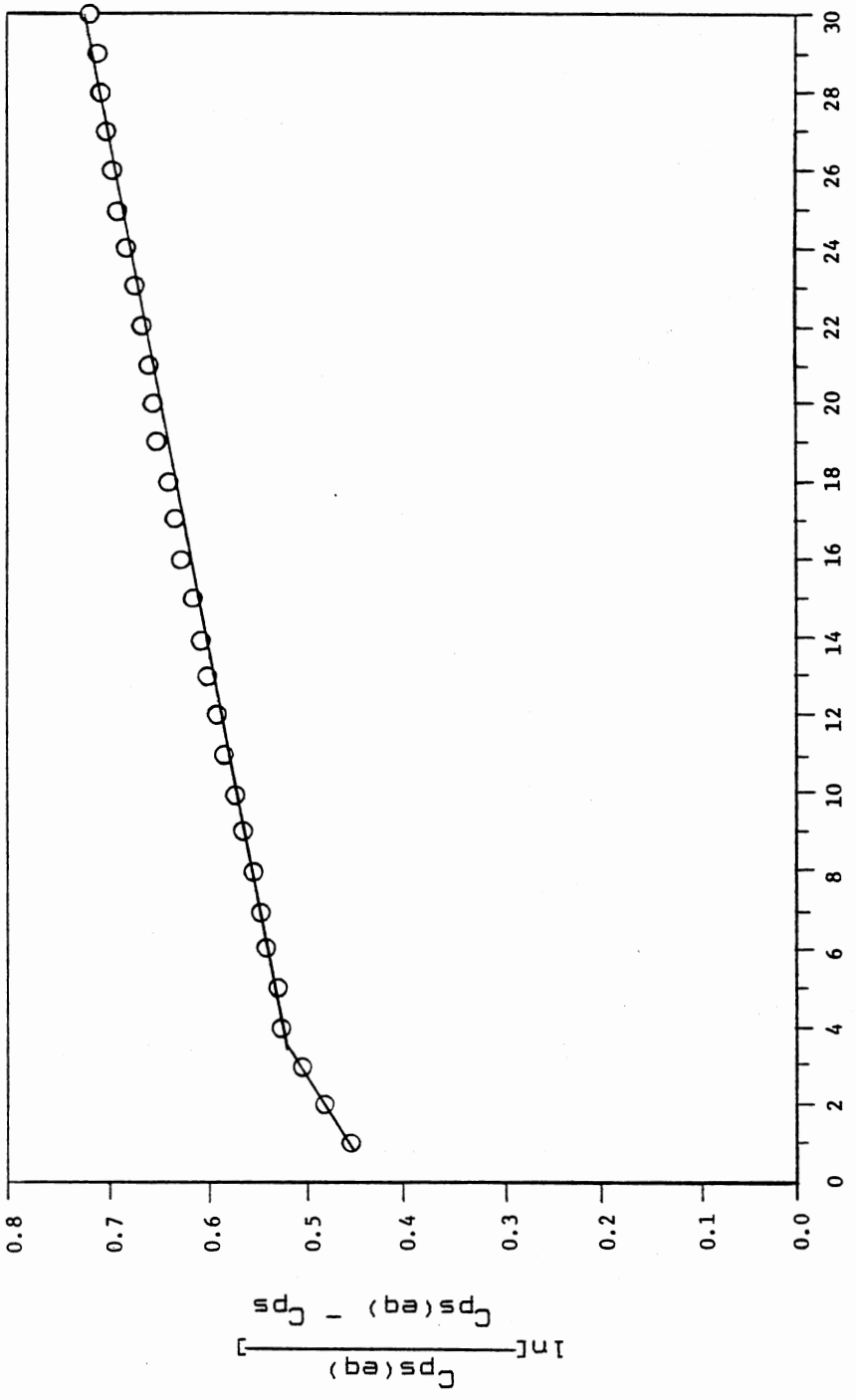

Figure 19. (Continued)

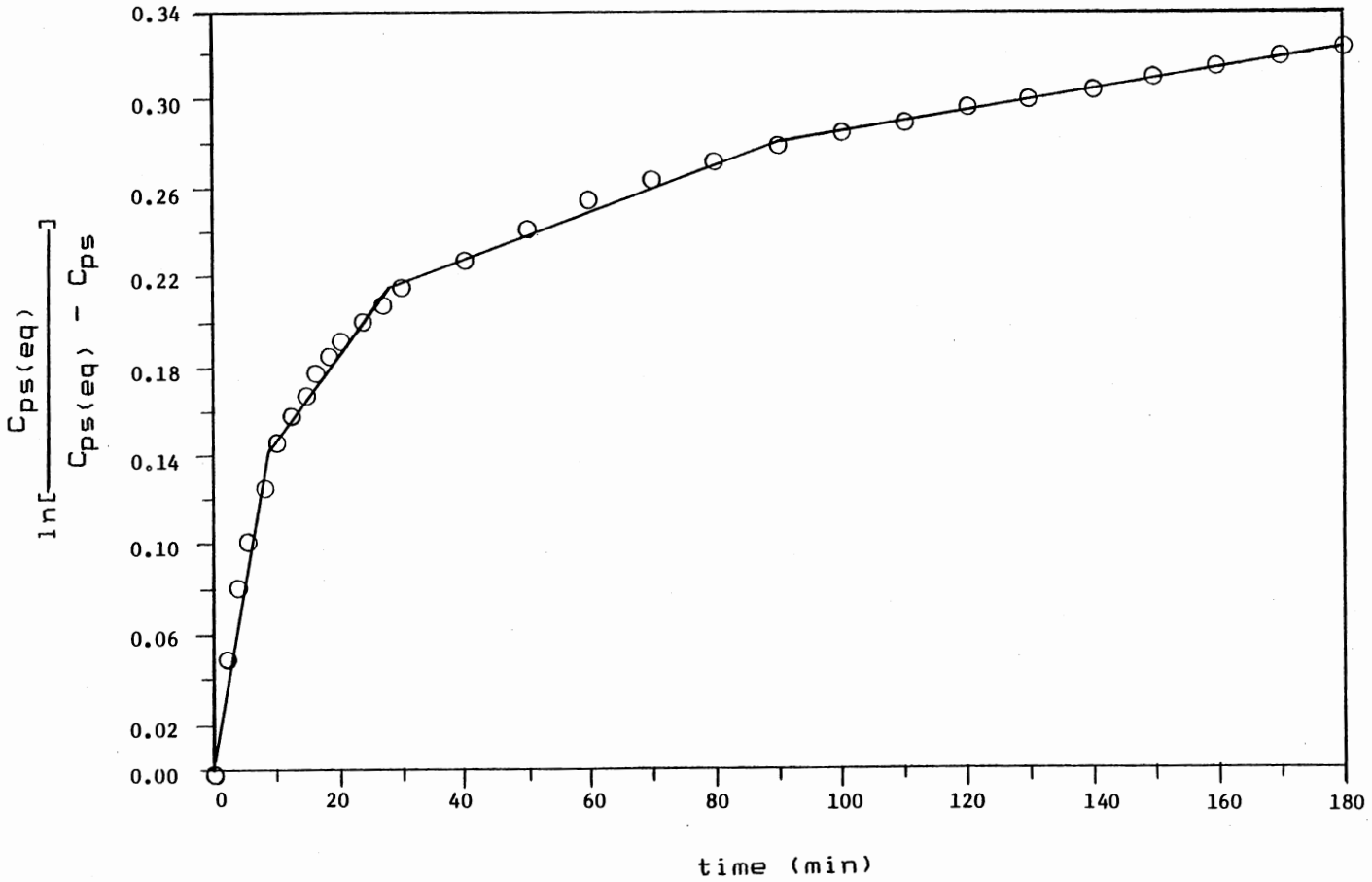

Figure 20. Reversible Adsorption Model Plot of Run 17, 400 C (Shell 324)

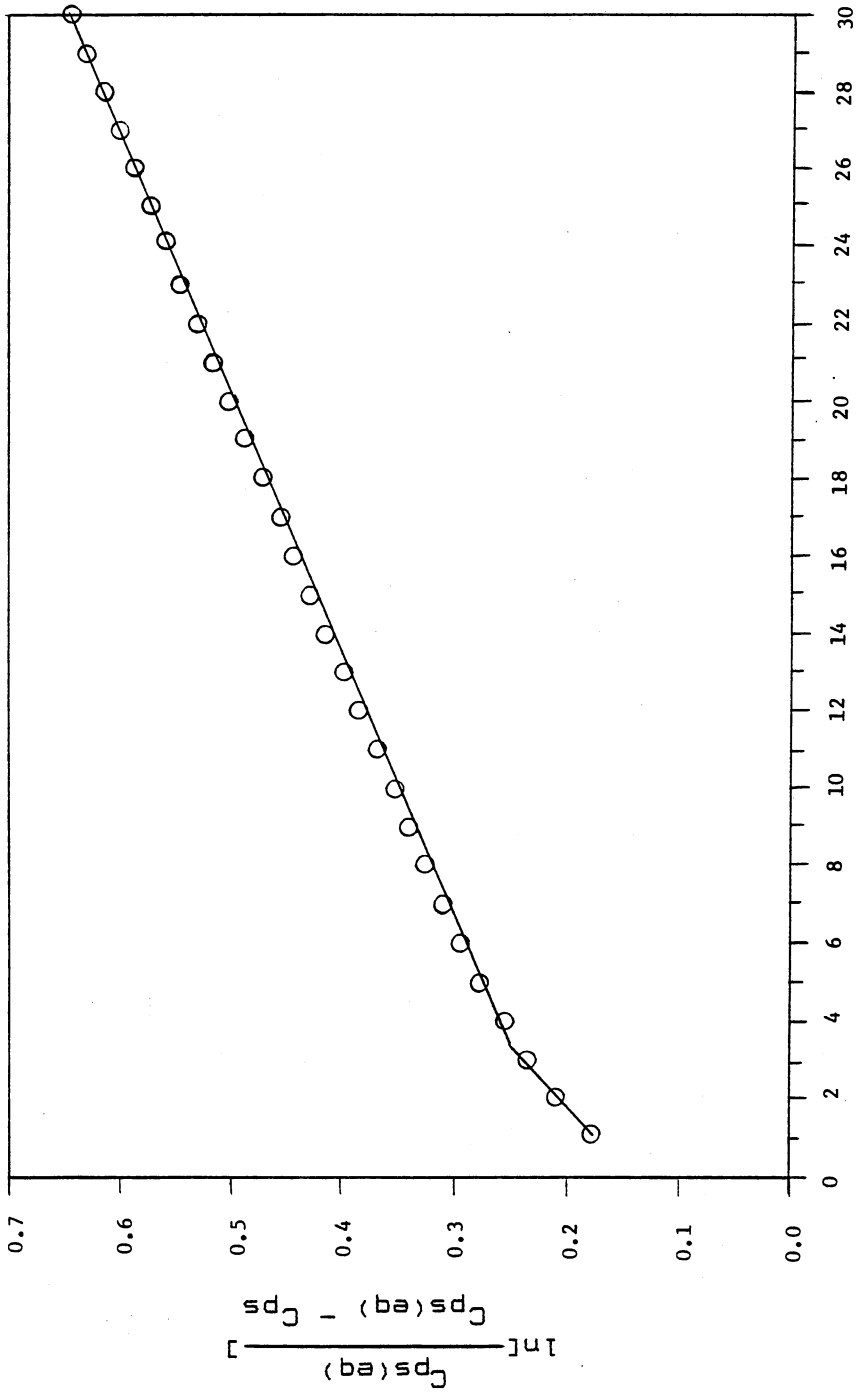

Figure 20. (Continued)

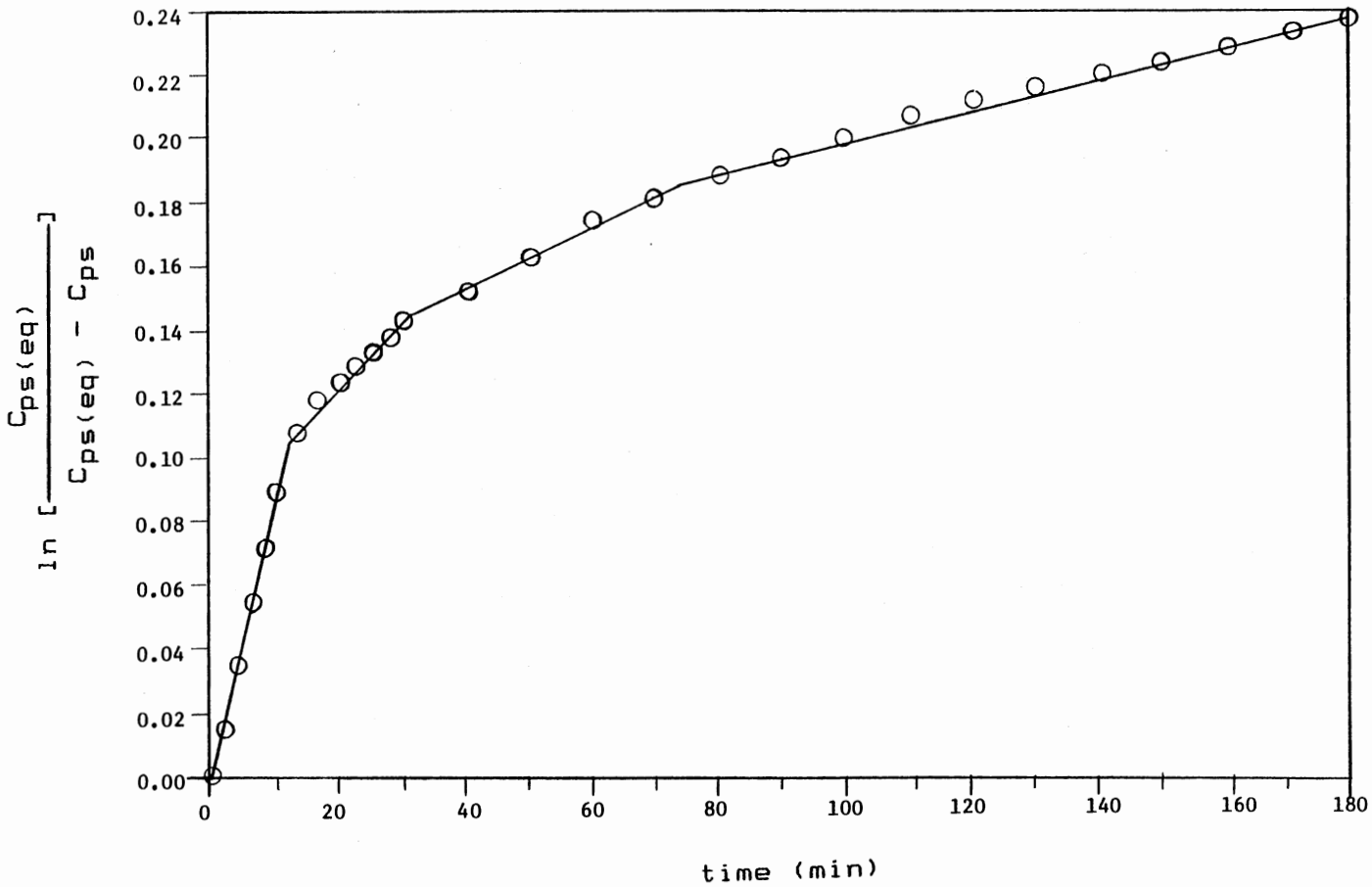

Figure 21. Reversible Adsorption Model Plot of Run 16, 450 C (Shell 324)

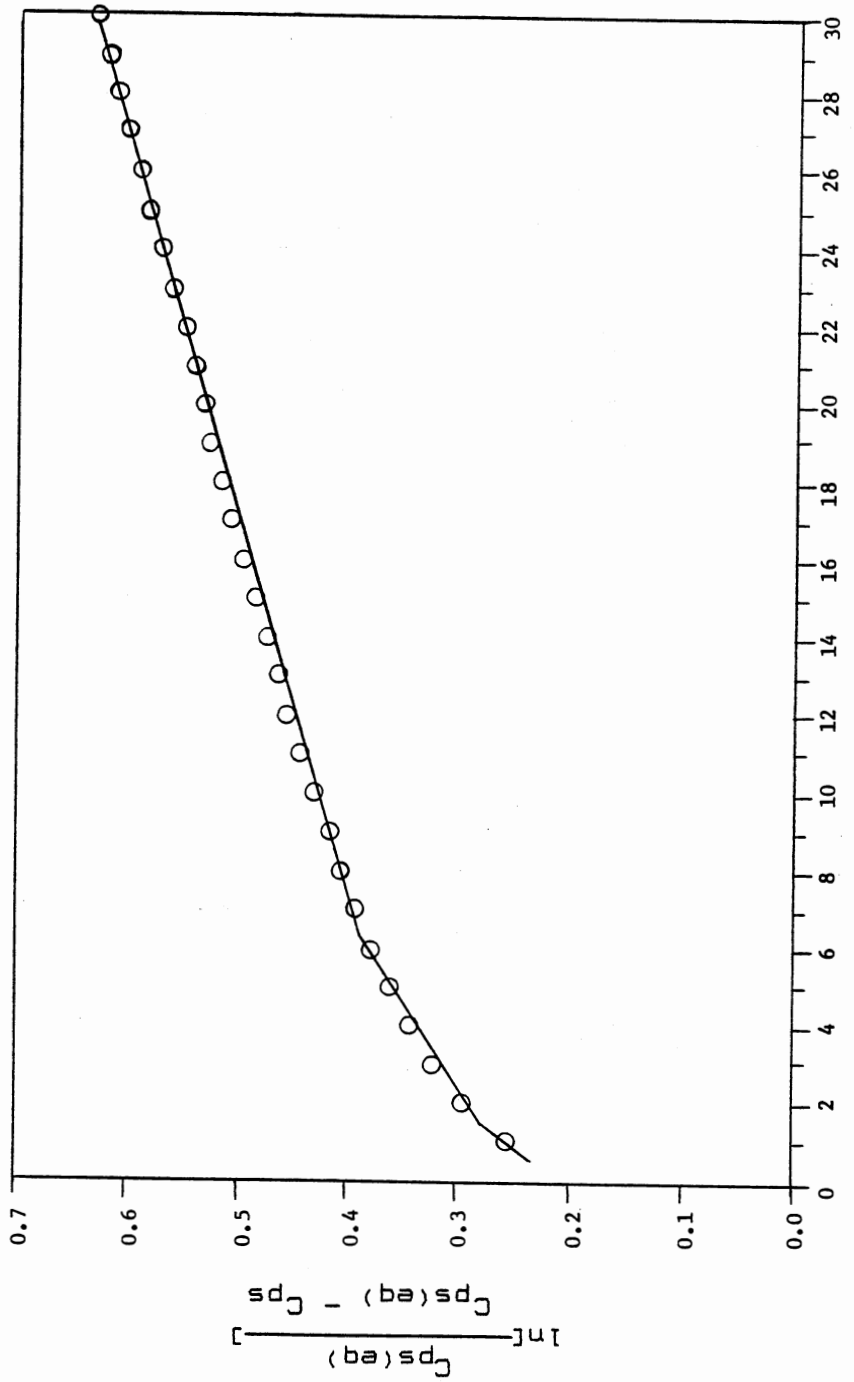

Figure 21. (Continued)

a slow chemisorption site, a physical and/or non-activated site, and a site which coke may be formed especially at high temperatures.

A similar phenomena is observed for HDN-60 catalyst, where three mechanisms are observed at 200 C and four mechanisms at 300 C. The reversible adsorption model for HDN-60 at 200 C is shown in Figures 22 and 23, and the model at 300 C is shown in Figure 24. The results of this analysis are listed in Table VI. It shows that the time required for the completion of the first and second mechanisms of adsorption are almost independent of the experimental conditions.

A plot of reversible adsorption model for HDN-60 catalyst at 300 C of Run 12 in Figure 25, shows that the rate of adsorption of the fourth mechanism is higher than that of the third one. This unusual behavior may be speculated to multilayer coke formation on the top of a monolayer surface coverage.

It should be pointed out that Deeba, et al., (1985) observed only one type of adsorption in their studies. A major difference between their experimental techniques and this work is the criterion to achieve equilibrium adsorption. They considered a weight gain of 0.1 mg/h as low enough to be accepted equilibrium. In this work, the criterion was 0.001 mg/h for 2 or 3 hours. It is possible that they could have observed other kinds of slow adsorption had they conducted their experiments for longer

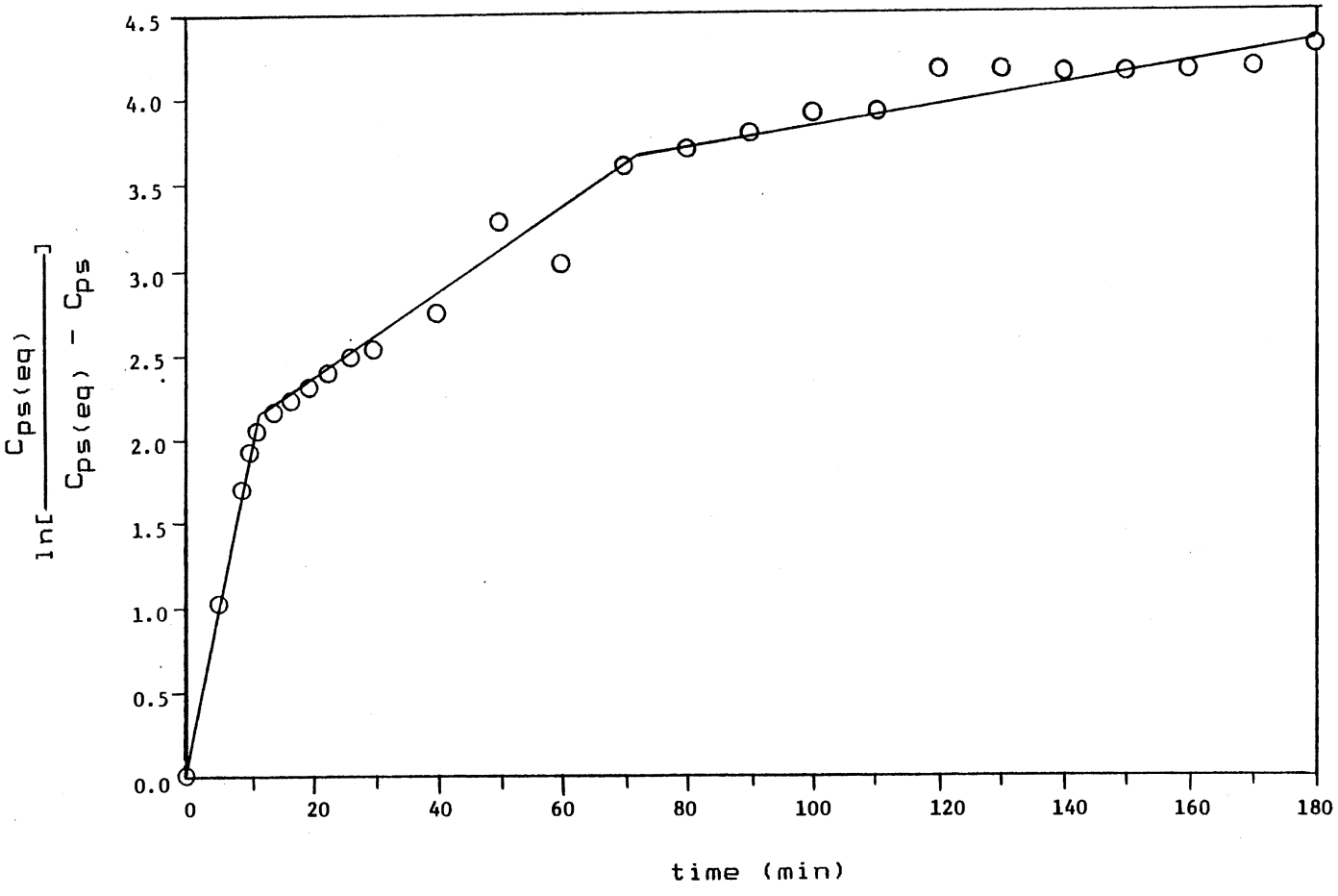

Figure 22. Reversible Adsorption Model Plot of Run 10, 200 C (HDN-60)

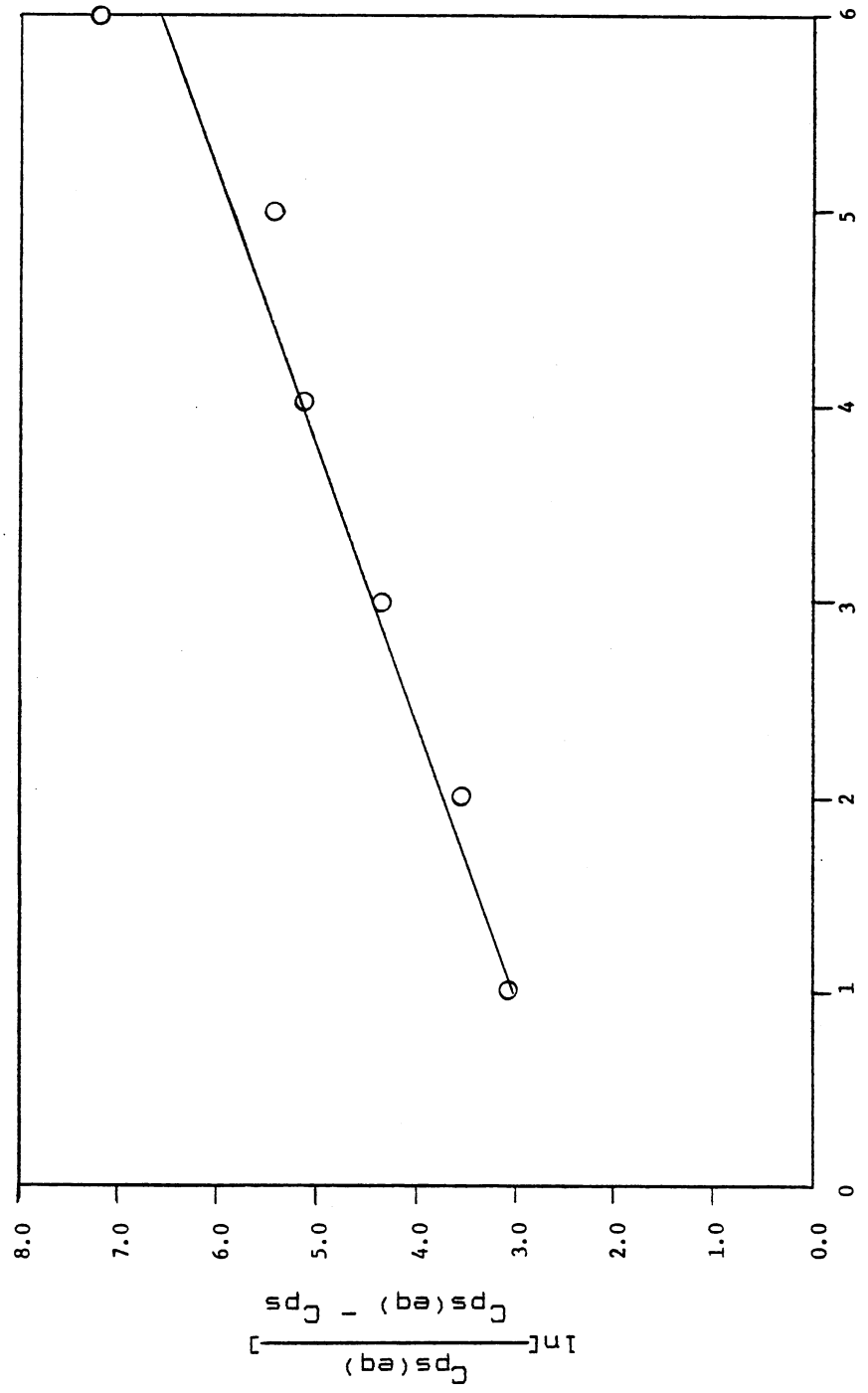

Figure 22. (continued)

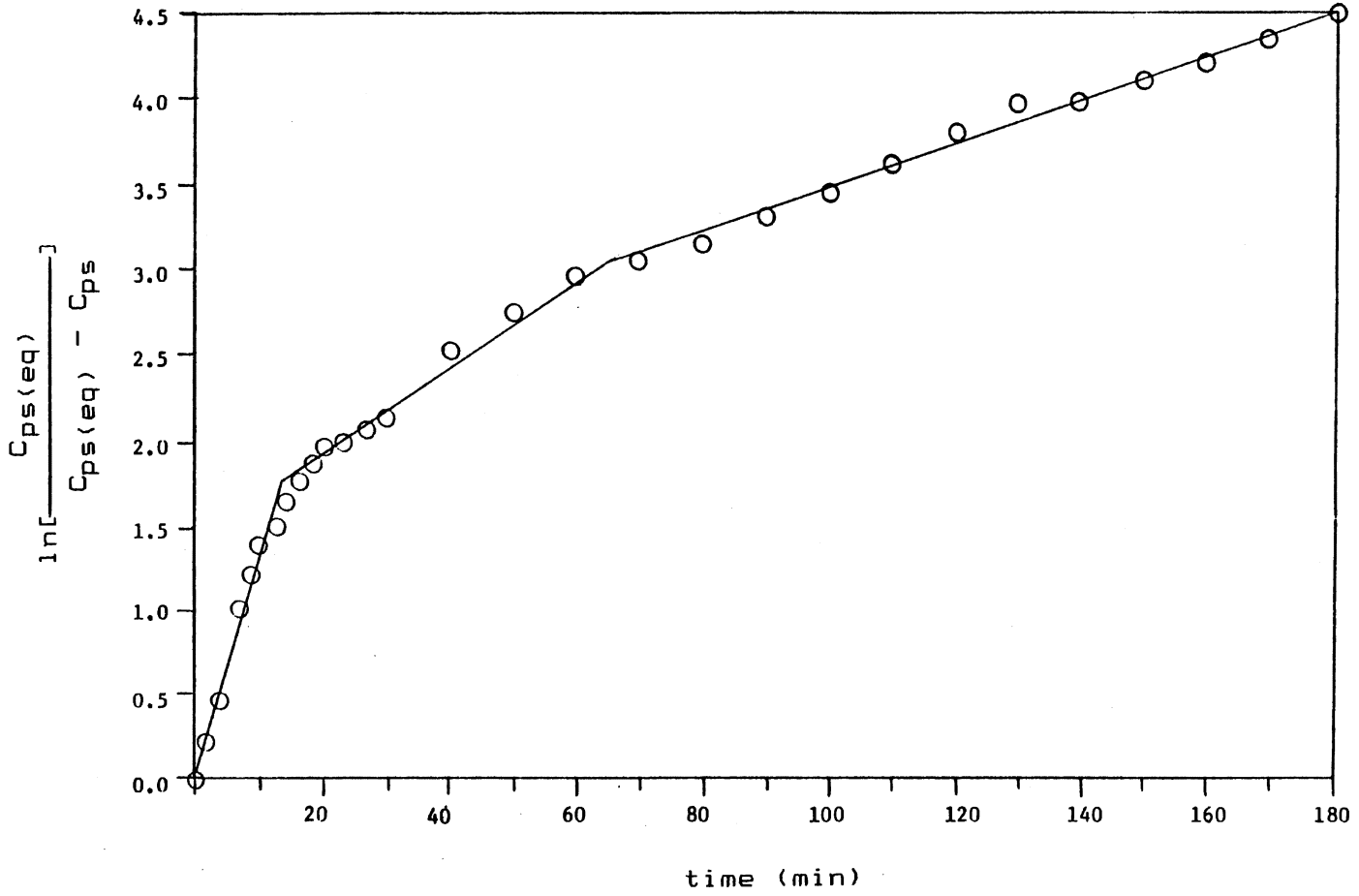

Figure 23. Reversible Adsorption Model Plot of Run 13, 200 C (HDN-60)

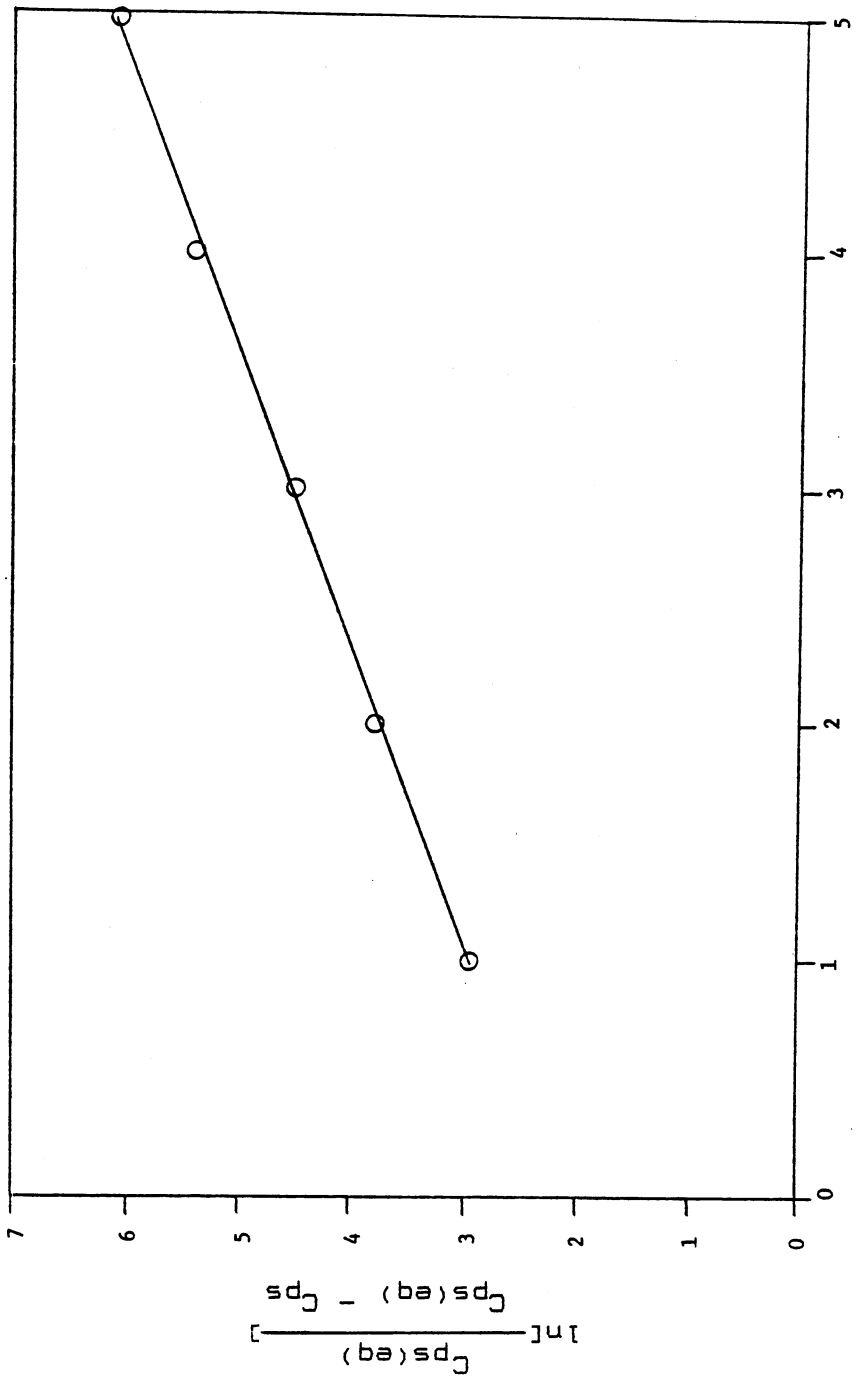

Figure 23. (continued)

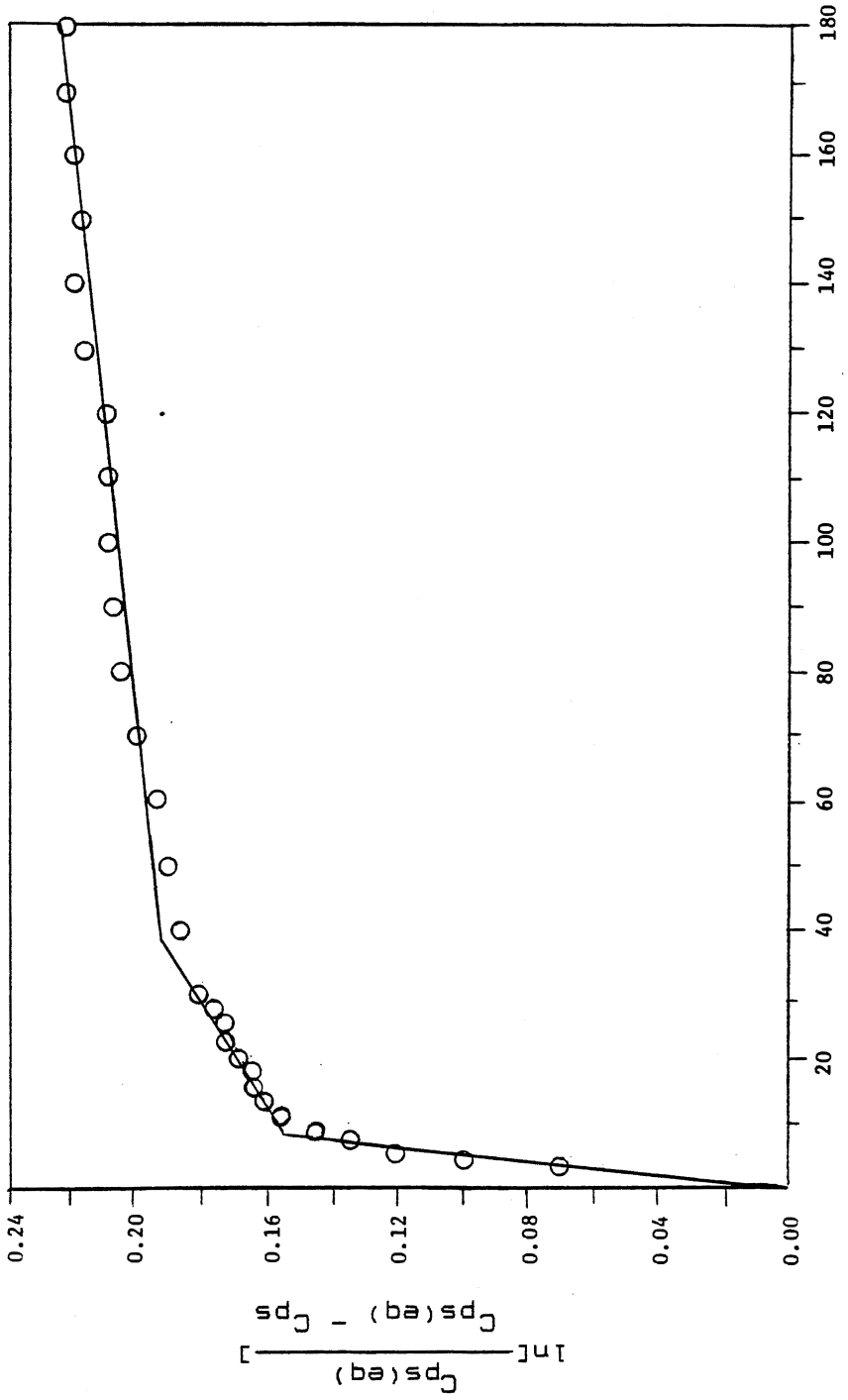

Figure 24. Reversible Adsorption Model Plot of Run 12, 300 C (HDN-60)

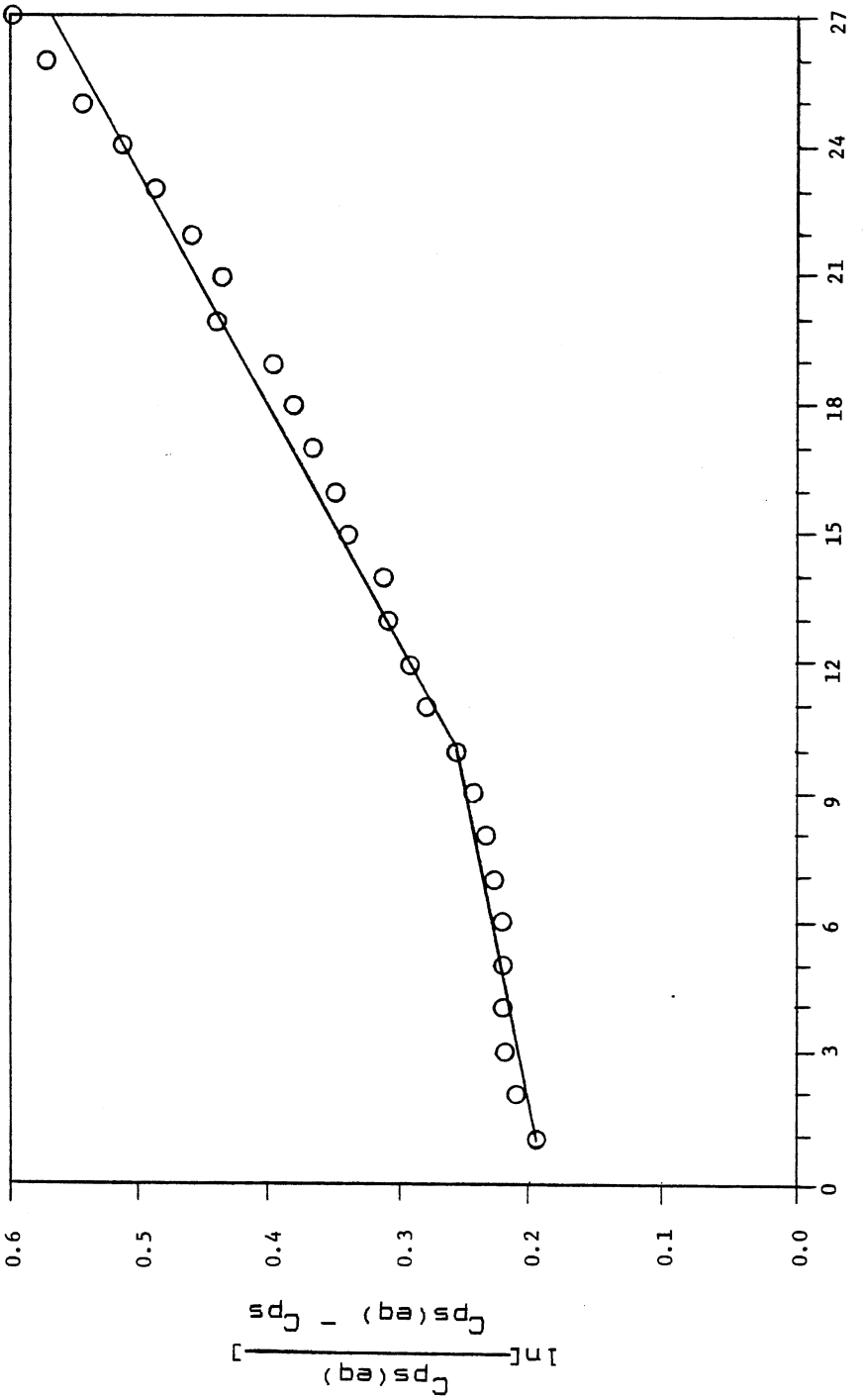

Figure 24. (Continued)

TABLE V

TIME AND WEIGHT CONTENT AT BREAKING POINTS
FROM REVERSIBLE ADSORPTION MODEL

Temp (C)		100		200		250
Run	22*	25*	25#*	19*	21*	24*
t_1 (min.)	10	12	9	9	11	9
C_{ps1} (μ mol/g cat.)	354.2	319.6	360.9	258.6	180.9	173.2
t_2 (min.)	35	32	35	40	30	40
C_{ps2} (μ mol/g cat.)	319.6	349.4	387.8	325.7	179.9	202.1
t_3 (min.)	–	–	–	–	–	–
C_{ps3} (μ mol/g cat.)	–	–	–	–	–	–
t_4 (min.)	–	–	–	–	–	–
C_{ps4} (μ mol/g cat.)	–	–	–	–	–	–
t_{eq} (hr.)	10	28	17	58	27	20
C_{pseq} (μ mol/g cat.)	465.4	410.2	418.3	399.7	229.2	232.9

TABLE V (Continued)

Temp (C)	300	400	450	200		300
Run	18*	17*	16*	10**	13**	12**
t_1 (min.)	9	9	11	12	14	10
C_{ps1} (μ mol/g cat.)	153.9	97.9	107.1	175.4	202.2	77.4
t_2 (min.)	31	30	30	72	68	46
C_{ps2} (μ mol/g cat.)	176.6	144.7	160.5	228.5	237.5	98.1
t_3 (min.)	210	85	75	-	-	620
C_{ps3} (μ mol/g cat.)	239.9	179.4	204.8	-	-	132.1
t_4 (min.)	-	380	370	-	-	-
C_{ps4} (μ mol/g cat.)	-	226.6	312.9	-	-	-
t_{eq} (hr.)	300	210	220	7	7	92
C_{pseq} (μ mol/ g cat.)	499.9	749.5	1212	232.2	244.9	569.2

* Shell 324
** HDN-60
\# Readsorption after desorption experiments

periods.

Kittrell (1986) who conducted the earlier experiments similar to this work observed two straight lines. Based on equation (24), he developed two exponential models to explain the two different types of adsorption by using time and weight gain at the break point in the slope of plot (24). One model accounted for the initial simultaneous coke formation and poisoning. The other model accounted for reversible poisoning after a steady-state coke level had been attained. In examining his derivations, it was realized that his assumption of equation (11), page 56, in his thesis is not valid. Therefore, his proposed technique to calculate rate constant could not be justified. Several attempts were made in this work to develop a better model, however, none of the attempts could give a satisfactory answer.

An interesting point was observed in the study of irreversibility in Run 25. After the equilibrium was achieved at 100 C, the reversibly adsorbed pyridine was desorbed in helium atmosphere. The adsorption/desorption was then repeated. Table IV shows that the equilibrium pyridine adsorptions were nearly equal in both cases (418.2 compared with 410.05 μ mol/g cat or 33.04 compared with 32.392 mg/g cat). Moreover, the irreversibly adsorbed pyridine, represented by the weight which was left on the catalyst surface after desorption, was almost identical in both cases (231.9 versus 170.6 μ mol/g cat or 18.326 versus

13.477 mg/g cat). This phenomena clearly shows the reproducibility of experiments and indicates that the adsorption sites for reversible and irreversible adsorption are distinctly different. Figure 25 shows the schematic transient adsorption/desorption data in Run 25. Figure 15 also shows three mechanisms of pyridine readsorption in Run 25.

One unexpected result was from the temperature programmed adsorption experiments in the presence of pyridine. In Run 21, after equilibrium was achieved at 250 C (229.28 μ mol/g cat), the temperature was increased from 250 C to 450 C at a rate of 1.67 C/min. As the temperature increased, the adsorbed amount on the catalyst decreased until 420 C. At this point, pyridine started to readsorb on the catalyst surface. This high temperature adsorption mechanism may be attributed to coke formation on the catalyst. One possible explanation is that coke formation may occur at high temperatures by the reaction between the benzene ring of pyridine molecule and the catalyst active sites.

Equilibrium adsorption at 450 C showed the largest amounts in all the temperatures studied. The principal mechanism that causes this major adsorption starts at a temperature of approximately 420 C. There is strong evidence to believe that this high temperature adsorption is due to coke formation. The equilibrium adsorption level at 450 C is between 100-125 mg/g cat. This corresponds to a

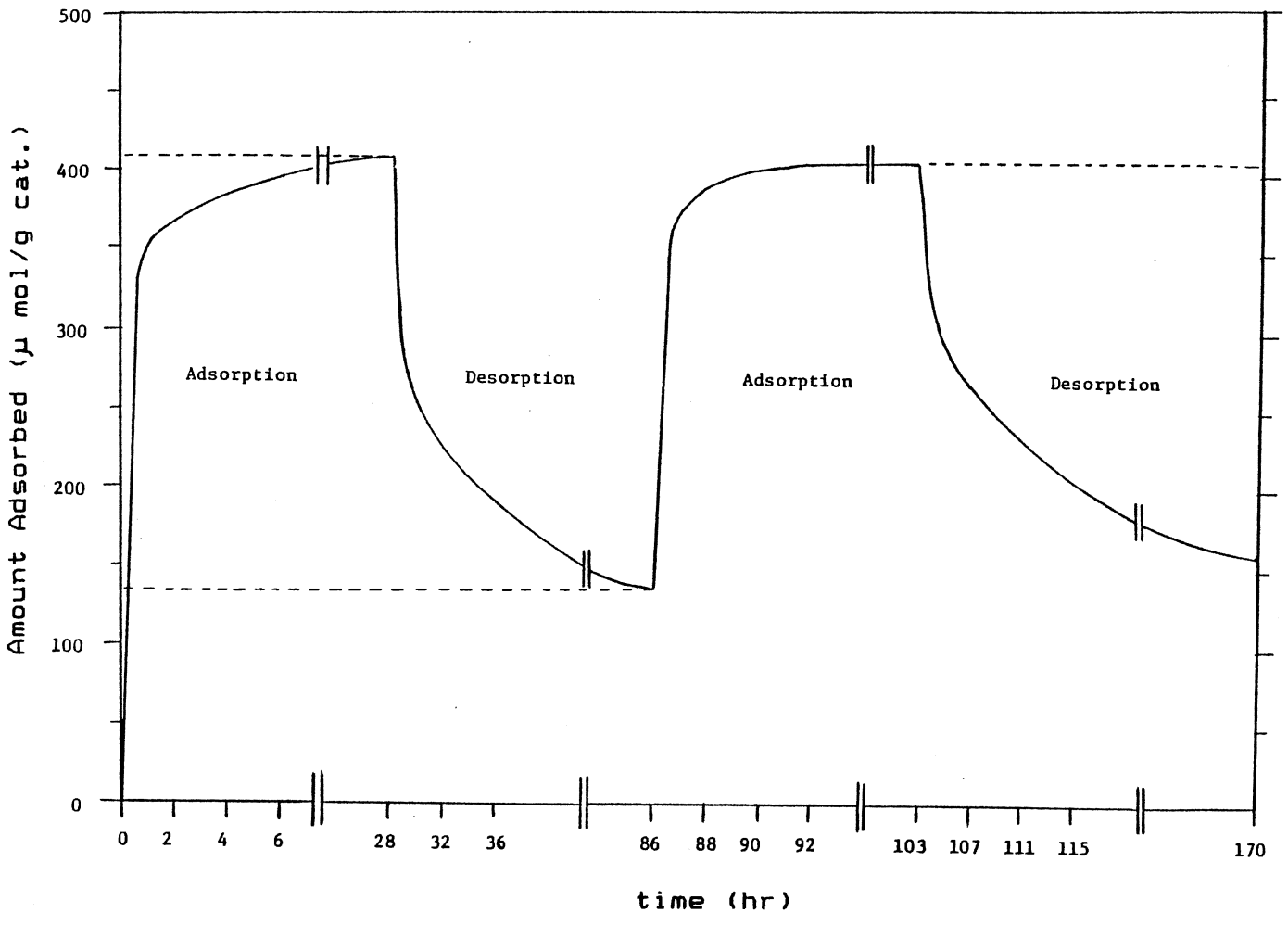

Figure 25. Schematic Transient Adsorption/Desorption Diagram-Run 25 (100 C)

lay down of 12.5 g coke/100 g of catalyst which closely matches the industrial coke level when these types of catalysts are exposed to light hydrocarbon fuels. As shown in Appendix C, this level of coke corresponds to only a monolayer coverage of the surface. A study of Laser Raman Spectroscopy (LRS) of the catalyst sample which was prepared by pyridine adsorption at temperature higher than 400 C showed numerous adsorption bands, indicating that pyridine formed complex polymerized bonds. The LRS results are shown in Figure 33 in Appendix E. The black color of catlaysts exposed to pyridine, especially at high temperatures is another indication of the presence of coked material on the surface of catalyst.

The adsorption experiment at 250 C was reproduced for Shell 324 catalyst in Runs 21 and 24, and at 100 C in Runs 22 and 25. Moreover, the reproducibility of adsorption for HDN-60 at 200 C was tested in Runs 11 and 13. The data show the similarity of adsorption dynamics and that the amounts adsorbed at equilibrium were nearly equal. Figure 26 shows the transient adsorption behavior at 250 C of Runs 21 and 24 and the behavior at 100 C of Runs 22 and 25. Because of the different suppression weight in Run 22 (only three digit recording), the deviation of equilibrium value is $\pm$ 1.58 mg/g cat.

HDN-60 catalyst demonstrates similar equilibrium behavior as Shell 324 catalyst. Although, equilibrium of pyridine adsorption at 450 C on HDN-60 catalyst in Runs 11

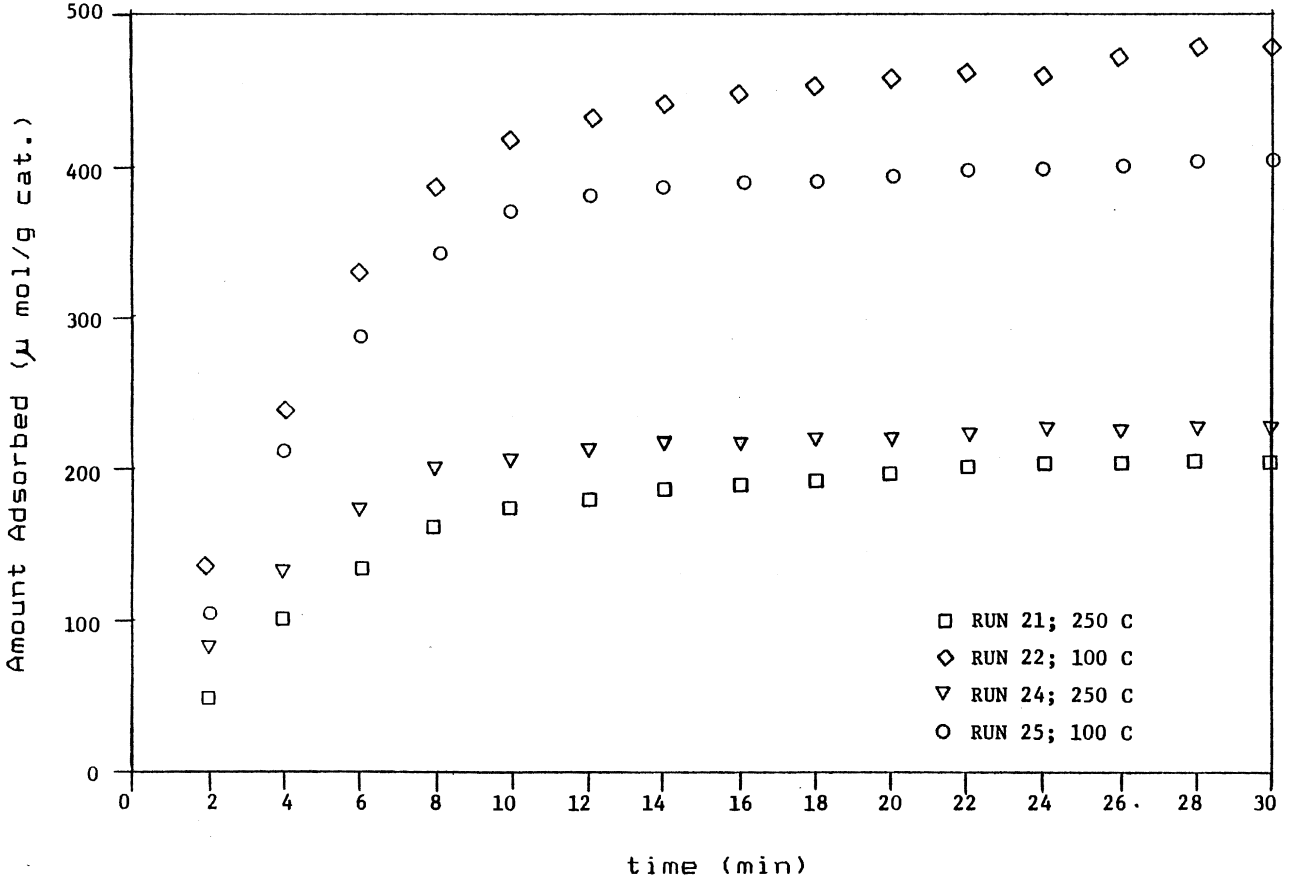

Figure 26. Transient Adsorption Reproducibility at 100 and 250 C (Shell 324)

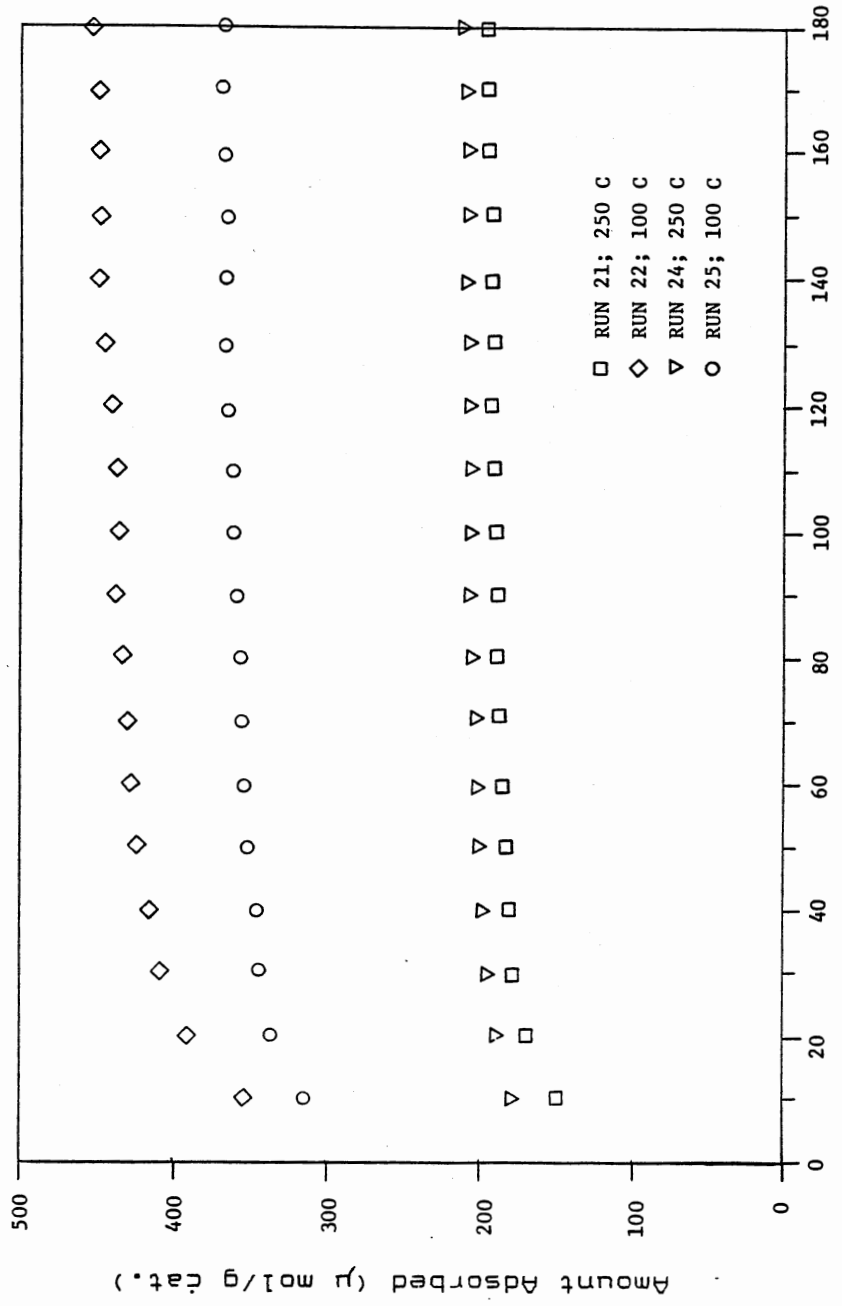

Figure 26. (Continued)

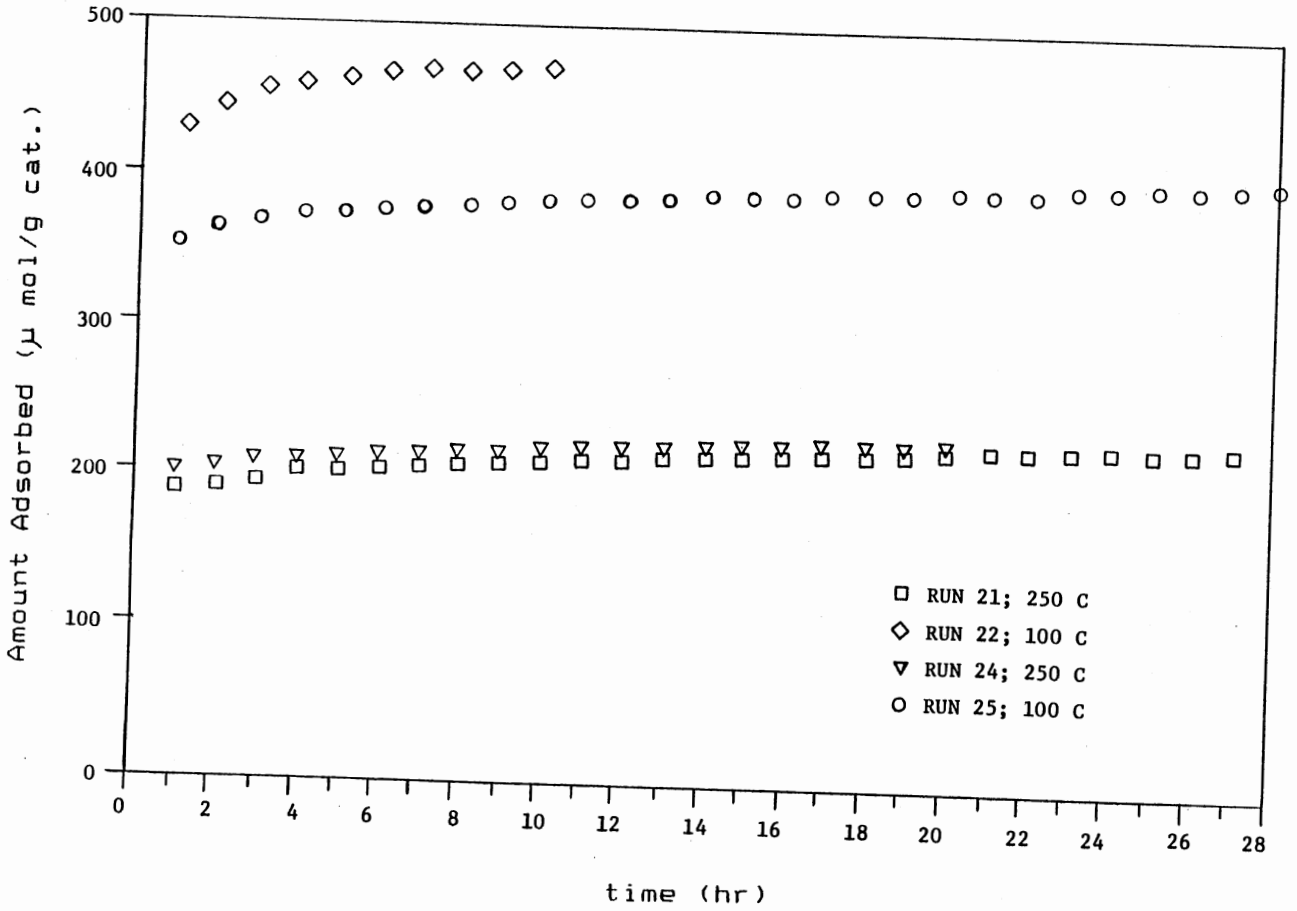

Figure 26. (Continued)

and 15 were not complete, the weight gain on catalyst is still higher than that at lower temperatures. Hence, none of the experimental results show any unusual behavior which would refer to equipment sensitivity or disturbance problems. However, the small deviation of adsorption measurement may be attributed to catalyst pellet whose properties may have been slightly different from the other pellets.

CHAPTER VI

CONCLUSIONS AND RECOMMENDATIONS

Several conclusions can be drawn from the results of pyridine adsorption in this work.

1. At temperatures below 250 C, the equilibrium adsorption decreased with temperature, whereas, at temperatures above 250 C, the equilibrium adsorption increased with temperature.

2. The initial rate of adsorption at low temperatures was higher than that at high temperatures and the time to reach equilibrium at low temperatures was shorter than that at high temperatures.

3. Pyridine adsorption at 200 and 300 C for HDN-60 catalyst and that at 100 and 250 C for Shell 324 catalyst demonstrated a 30-60 % irreversibility which was attributed to chemisorption.

4. A reversible adsorption model indicated different types of pyridine adsorption on catalyst surface at different experimental temperatures.

5. The temperature programmed adsorption in the presence of pyridine partial pressure indicated that the amount of adsorption decreased as the temperature increased until the temperature reached 420 C. At this point,

pyridine started to readsorb on the catalyst surface. This high temperature adsorption may be attributed to coke formation.

6. There are major similarities between the behavior of both Shell 324 and HDN-60 catalysts

Some recommendations for future investigation are made as follows:

1. Collect adsorption data at various pyridine partial pressures and temperatures; and observe the irreversibility adsorption at high temperatures.

2. Investigate the competitive adsorption effects of various nitrogen compound bases and products which may form by the reactions.

3. Study the temperature programmed adsorption as increasing temperature different from 1.67 C/min.

4. Study the temperature programmed desorption with a different rate of temperature increase.

5. Develop a model to fit the transient adsorption data.

BIBLIOGRAPHY

Deeba, M., and Hall, W. K. (1985). The Measurement of Catalyst Acidity II: Chemisorption Studies, Z. Phys. Chem. (Munich) 144, 85-103.

Entz, R. W. (1984). The Poisoning of a Hydrotreating Catalyst by Pyridine and Its Hydrogenation Derivatives, M. S. Thesis, Oklahoma State University, Stillwater, Oklahoma.

Fransen, T., Meer, O. van der, and Mars, P. (1976). Surface Structure and Catalytic Activity of a Reduced Molybdenum-Oxide Alumina Catalyst I: The Adsorption Pyridine in Relation with the Molybdenum Valence, J. Phys. Chem. 80(19), 2103-2107.

Hall, W. K., Schneider, R. L., and Valyon, J. (1984). Site Selective Chemisorption on Sulfided Molybdenum-Alumina Catalyst, J. Catal. 85, 277-283.

Hayward, D. O., and Trapnell, B. M. W. (1964). Chemisorption. Washington: Butterworhs.

Kittrell, A. J. (1986). Equilibrium and Transient Pyridine Poisoning of A Hydrotreating Catalyst, M. S. Thesis, Oklahoma State University, Stillwater, Oklahoma.

Mapes, J. E., and Eichens, R. P. (1954). The Infrared Spectra of Amonia Chemisorbed on Cracking Catalysts, J. Phys. Chem. 58, 1059-1062.

Mills, G. A., Boedeker, E. R., and Oblad, A. G. (1950). Chemical Characterization of Catalysts I: Poisoning of Cracking Catalysts by Nitrogen Compounds and Potassium Ion, J. Amer. Chem. Soc. 72, 1554-1560.

Morrow, B. A., Cody I. A., Moran I. E., and Palepu, R. (1976). An Infrared study of the Adsorption on Platinum and Nickel, J. Catal. 44, 467-476.

Morterra, C., Chiorino, A., Chiotti, G., and Garrone, E. (1979). Surface Acidity of n-Alumina, J. of Chem. Soc. Faraday Trans. I. 75(2), 271-288.

Parry, E. P. (1963). An Infrared Study of Pyridine Adsorbed on Acidic Solids: Characterization of Surface Acidity, J. Catal. 2, 371-379.

Pines, H., and Haag, W. O. (1960). Catalyst and Support I: Alumina, its Intrinsic Acidity and Catalytic Acidity, J. Amer. Chem. Soc. 82, 2471-2483.

Reid, R. C., Prausnitz J. M., and Sherwood, T. K. (1977). The Properties of Gases and Liquids. New York: McGraw-Hill Book Company.

Richardson, R. L., and Benson, B. W. (1957). A Study of the Surface Acidity of Cracking Catalyst, J. Phys. Chem. 61, 405-411.

Schwarz, J. A., Russell, B. G., and Harnsberger, H. F. (1978). A Study of Pyridine Adsorbed on Silica-Alumina Catalyst by Combined Infrared Spectroscopy and Temperature Programmed Desorption, J. Catal. 54, 303-317.

Segawa, K., and Hall, W. K. (1982). Catalysis and Surface Chemistry III: The Adsorption of Pyridine on Molybdenum-Alumina Catalysts, J. Catal. 76(1), 133-143.

Sheets, R. W., and Hansen, R. S. (1972). Promoted Adsorption of Pyridine on Nickel, J. Phys. Chem. 76(7), 972-976.

Smith, J. M. (1981). Chemical Engineering Kinetics. New York: McGraw-Hill Book Company.

Suarez, W., Dumesic, J. A., and Hill, C. G. (1985). Acidic Properties of Molybdenum-Alumina for Different Extents of Reduction: Infrared and Gravimetric Studies of Adsorbed Pyridine, J. Catal. 94,:408-421.

Tanabe, K. (1970). Solid Acids and Bases. New York: Academic Press.

Takahashi M., Iwasawa, Y., and Ogasawara, S. (1976). The Nature of Adsorbed Sites on Catalysts II: Behavior of Basic Compounds on Silica-Alumina Catalyst at Elevated Temperatures", J. Catal. 45, 15-24.

APPENDIX A

RAW TRANSIENT ADSORPTION AND DATA DESORPTION DATA

TABLE A-I

TRANSIENT ADSORPTION AND DESORPTION
DATA ON SHELL 324

Run	Temp. (C)	Time (min)	Cat. Wt. (mg)	Amount Adsorbed (mg/g cat.)	Amount Adsorbed (μ mol/g cat.)
9	300	0	15.5962	0.000	0.000
		2	15.6676	4.581	65.58
		4	15.7137	7.534	93.09
		6	15.7730	11.336	143.49
		8	15.7921	12.561	158.99
		10	15.8019	13.189	166.95
		12	15.8038	13.311	168.49
		14	15.8064	13.478	170.59
		16	15.8082	13.593	172.06
		18	15.8103	13.728	173.77
		20	15.8129	13.894	175.88
		22	15.8140	13.965	176.77
		24	15.8151	14.036	177.66
		26	15.8161	14.093	178.39
		28	15.8172	14.170	179.37
		30	15.8184	14.247	180.34
		40	15.8216	14.452	182.94
		50	15.8250	14.670	185.69
		60	15.8275	14.830	187.73
		70	15.8292	14.940	189.11
		80	15.8309	15.048	190.49
		90	15.8321	15.126	191.46
		100	15.8340	15.183	192.19
		110	15.8340	15.247	192.99
		120	15.8361	15.382	194.71
		130	15.8369	15.433	195.36
		140	15.8383	15.523	196.49
		150	15.8401	15.638	197.95
		160	15.8405	15.664	198.28
		170	15.8414	15.722	199.01
		180	15.8422	15.773	199.66
16	450	0	13.1500	0.000	0.000
		2	13.1701	1.548	19.59
		4	13.1908	3.103	39.28
		6	13.2150	4.943	62.57
		8	13.2339	6.380	80.76
		10	13.2572	8.152	103.2
		12	13.2674	8.928	113.0
		14	13.2816	10.008	126.68
		16	13.2904	10.677	135.15
		18	13.2925	10.836	137.17

TABLE A-I (continued)

Run	Temp. (C)	Time (min)	Cat. Wt. (mg)	Amount Adsorbed (mg/g cat.)	Amount Adsorbed (μ mol/g cat.)
16	450	20	13.2961	11.110	140.63
		22	13.3012	11.498	145.55
		24	13.3046	11.757	148.82
		26	13.3083	12.038	152.38
		28	13.3115	12.281	155.46
		30	13.3168	12.684	160.56
		40	13.3272	13.457	170.57
		50	13.3371	14.228	180.09
		60	13.3515	15.323	193.96
		70	13.3581	15.825	200.32
		80	13.3650	16.350	206.96
		90	13.3707	16.783	212.45
		100	13.3773	17.285	218.79
		110	13.3842	17.810	225.44
		120	13.3894	18.205	230.45
		130	13.3945	18.595	235.36
		140	13.3979	18.852	238.63
		150	13.4022	19.179	242.77
		160	13.4064	19.498	246.81
		170	13.4108	19.833	251.05
		180	13.4143	20.099	254.42
		240	13.4342	21.612	273.47
		300	13.4560	23.270	294.46
		360	13.4725	24.525	310.34
		420	13.4875	25.665	324.78
		480	13.5015	26.730	338.26
		540	13.5140	27.681	350.29
		600	13.5279	28.738	363.67
		660	13.5400	29.658	375.32
		720	13.5539	30.715	388.69
		780	13.5650	31.559	399.38
		840	13.5788	32.608	412.66
		900	13.5908	33.521	424.22
		960	13.6023	34.395	435.29
		1020	13.6131	35.217	445.68
		1080	13.6250	36.122	457.14
		1140	13.6369	37.027	468.59
		1200	13.6474	37.825	478.69
		1260	13.6594	38.737	490.25
		1320	13.6689	39.460	499.39
		1380	13.6805	40.342	510.56
		1440	13.6891	40.996	518.84
		1500	13.6983	41.696	527.96
		1560	13.7083	42.456	537.32
		1620	13.7185	43.232	547.14

TABLE A-I (Continued)

Run	Temp. (C)	Time (min)	Cat. Wt. (mg)	Amount Adsorbed (mg/g cat.)	Amount Adsorbed (μ mol/g cat.)
16	450	1680	13.7295	44.068	557.73
		1740	13.7371	44.646	565.04
		1800	13.7470	45.399	574.57
17	400	0	14.4375	0.000	0.000
		2	14.4788	2.861	36.21
		4	14.5032	4.551	57.59
		6	14.5190	5.645	71.45
		8	14.5376	6.933	87.76
		10	14.5538	8.055	101.9
		12	14.5645	8.796	111.3
		14	14.5704	9.205	116.5
		16	14.5765	9.628	121.9
		18	14.5812	9.953	125.9
		20	14.5870	10.355	131.08
		22	14.5892	10.507	133.01
		24	14.5925	10.736	135.89
		26	14.5970	11.048	139.43
		28	14.5999	11.248	142.39
		30	14.6025	11.429	144.67
		40	14.6105	11.983	151.68
		50	14.6216	12.752	161.41
		60	14.6298	13.320	168.59
		70	14.6351	13.687	173.25
		80	14.6405	14.607	177.98
		90	14.6446	14.345	181.58
		100	14.6489	14.642	185.35
		110	14.6518	14.843	187.89
		120	14.6569	15.196	192.36
		130	14.6593	15.363	194.47
		140	14.6622	15.564	197.01
		150	14.6654	15.785	199.81
		160	14.6680	15.965	202.09
		170	14.6709	16.166	204.64
		180	14.6734	16.339	206.83
		240	14.6862	17.226	218.05
		300	14.6969	17.967	227.43
		360	14.7066	18.638	235.92
		420	14.7158	19.267	243.99
		480	14.7238	19.830	251.02
		540	14.7286	20.163	255.23
		600	14.7369	20.738	262.49
		660	14.7440	21.226	268.73
		720	14.7506	21.687	274.51
		780	14.7552	22.008	278.59

TABLE A-I (Continued)

Run	Temp. (C)	Time (min)	Cat. Wt. (mg)	Amount Adsorbed (mg/g cat.)	Amount Adsorbed (μ mol/g cat.)
17	400	840	14.7613	22.428	282.99
		900	14.7661	22.760	288.09
		960	14.7720	23.169	293.28
		1020	14.7774	23.543	298.01
		1080	14.7825	23.896	302.48
		1140	14.7879	24.270	307.22
		1200	14.7911	24.492	310.02
		1260	14.7954	24.788	313.79
		1320	14.7995	25.074	317.39
		1380	14.8042	25.399	321.51
		1440	14.8092	25.745	325.89
		1500	14.8150	26.147	330.98
		1560	14.8195	26.459	334.92
		1620	14.8248	26.826	339.57
		1680	14.8289	27.110	343.16
		1740	14.8329	27.837	346.67
		1800	14.8374	27.699	350.62
18	300	0	17.3844	0.000	0.000
		2	17.4535	3.975	50.31
		4	17.5908	7.213	91.31
		6	17.5500	9.526	120.6
		8	17.5685	10.590	134.05
		10	17.6018	12.506	158.29
		12	17.6095	12.948	163.89
		14	17.6132	13.161	166.59
		16	17.6165	13.351	169.01
		18	17.6188	13.483	170.68
		20	17.6204	13.575	171.84
		22	17.6222	13.679	173.15
		24	17.6236	13.760	174.17
		26	17.6254	13.863	175.48
		28	17.6265	13.926	176.28
		30	17.6275	13.984	177.01
		40	17.6322	14.254	180.43
		50	17.6350	14.415	182.47
		60	17.6375	14.559	184.29
		70	17.6399	14.697	186.04
		80	17.6418	14.806	187.42
		90	17.6439	14.927	188.95
		100	17.6456	15.025	190.19
		110	17.6471	15.111	191.28
		120	17.6485	15.182	192.29
		130	17.6499	15.272	193.32
		140	17.6510	15.336	194.12

TABLE A-I (Continued)

Run	Temp. (C)	Time (min)	Cat. Wt. (mg)	Amount Adsorbed (mg/g cat.)	Amount Adsorbed (μ mol/g cat.)
18	300	150	17.6528	15.439	195.43
		160	17.6540	15.508	196.31
		170	17.6552	15.577	197.18
		180	17.6569	15.675	198.42
		240	17.6636	16.060	203.29
		300	17.6671	16.262	205.84
		360	17.6709	16.480	208.61
		420	17.6734	16.624	210.43
		480	17.6770	16.381	213.05
		540	17.6805	17.032	216.59
		600	17.6841	17.240	218.22
		660	17.6874	17.429	220.63
		720	17.6909	17.631	223.17
		780	17.6939	17.803	225.36
		840	17.6965	17.953	227.25
		900	17.7000	18.154	229.79
		960	17.7031	18.332	232.06
		1020	17.7058	18.488	234.02
		1080	17.7080	18.614	235.63
		1140	17.7126	18.878	238.96
		1200	17.7140	18.960	239.99
		1260	17.7152	19.028	240.86
		1320	17.7183	19.207	243.13
		1380	17.7208	19.351	244.95
		1440	17.7229	19.472	246.47
		1500	17.7266	19.684	249.17
		1560	17.7279	19.759	250.12
		1620	17.7299	19.874	251.57
		1680	17.7320	19.995	253.09
		1740	17.7341	20.116	254.63
		1800	17.7362	20.236	256.16
19	200	0	11.6205	0.000	0.000
		2	11.6995	6.798	86.06
		4	11.7546	11.540	146.08
		6	11.8100	16.307	206.42
		8	11.8474	19.526	247.16
		10	11.8810	22.417	283.76
		12	11.8972	23.811	301.41
		14	11.9015	24.181	306.09
		16	11.9039	24.388	308.71
		18	11.9061	24.577	311.11
		20	11.9086	24.792	313.83
		22	11.9102	24.930	315.57
		24	11.9119	25.076	317.42

TABLE A-I (Continued)

Run	Temp. (C)	Time (min)	Cat. Wt. (mg)	Amount Adsorbed (mg/g cat.)	Amount Adsorbed (μ mol/g cat.)
19	200	26	11.9134	25.206	319.06
		28	11.9142	25.274	319.93
		30	11.9156	25.395	321.45
		40	11.9195	25.730	325.69
		50	11.9223	25.971	328.75
		60	11.9239	26.109	330.49
		70	11.9258	26.274	332.56
		80	11.9269	26.367	333.76
		90	11.9280	26.462	334.96
		100	11.9290	26.548	336.05
		110	11.9269	26.600	336.69
		120	11.9306	26.686	337.79
		130	11.9315	26.763	338.77
		140	11.9324	26.840	339.75
		150	11.9335	26.935	340.95
		160	11.9340	26.978	341.49
		170	11.9349	27.056	342.48
		180	11.9359	27.142	343.57
		240	11.9384	27.357	346.29
		300	11.9415	27.624	349.67
		360	11.9440	27.839	352.39
		420	11.9456	27.976	354.13
		480	11.9468	28.080	355.44
		540	11.9485	28.226	357.29
		600	11.9502	28.372	359.14
		660	11.9512	28.458	360.23
		720	11.9524	28.562	361.54
		780	11.9542	28.716	363.49
		840	11.9545	28.742	363.83
		900	11.9555	28.828	364.92
		960	11.9565	28.914	366.01
		1020	11.9576	29.009	367.19
		1080	11.9583	29.069	367.97
		1140	11.9592	29.147	368.95
		1200	11.9608	29.284	370.69
		1260	11.9618	29.371	371.78
		1320	11.9620	29.388	372.01
		1380	11.9625	29.431	372.54
		1440	11.9632	29.491	373.29
		1500	11.9641	29.568	374.28
		1560	11.9645	29.603	374.72
		1620	11.9652	29.663	375.48
		1680	11.9664	29.766	376.79
		1740	11.9671	29.827	377.55
		1800	11.9676	29.870	378.09

TABLE A-I (Continued)

Run	Temp. (C)	Time (min)	Cat. Wt. (mg)	Amount Adsorbed (mg/g cat.)	Amount Adsorbed (μ mol/g cat.)
20	450	0	14.6745	0.000	0.000
		2	14.7026	1.915	24.24
		4	14.7312	3.864	49.91
		6	14.7502	5.159	65.29
		8	14.7700	6.508	82.38
		10	14.7846	7.503	94.97
		12	14.7975	8.382	106.1
		14	14.8066	9.002	113.9
		16	14.8155	9.608	121.6
		18	14.8224	10.079	127.58
		20	14.8280	10.460	132.41
		22	14.8342	10.883	137.75
		24	14.8400	11.278	142.76
		26	14.8459	11.680	147.85
		28	14.8510	12.028	152.25
		30	14.8515	12.062	152.68
		40	14.8776	13.840	175.19
		50	14.8934	14.917	188.82
		60	14.9050	15.708	198.83
		70	14.9145	16.355	207.02
		80	14.9221	16.873	213.58
		90	14.9286	17.316	219.19
		100	14.9359	17.813	225.48
		110	14.9425	18.263	231.18
		120	14.9492	18.720	236.96
		130	14.9550	19.115	241.96
		140	14.9615	19.558	247.57
		150	14.9669	19.926	252.22
		160	14.9721	20.280	256.71
		170	14.9768	20.600	260.76
		180	14.9798	20.805	263.35
21	250	0	13.7278	0.000	0.000
		2	13.7893	4.482	44.08
		4	13.8232	6.946	87.97
		6	13.5874	9.442	119.5
		8	13.8806	11.131	140.89
		10	13.8926	12.005	151.96
		12	13.8985	12.435	157.39
		14	13.9029	12.755	161.46
		16	13.9060	12.981	164.32
		18	13.9098	13.258	167.82
		20	13.9135	13.527	171.23
		22	13.9165	13.746	173.99
		24	13.9192	13.942	176.49

TABLE A-I (Continued)

Run	Temp. (C)	Time (min)	Cat. Wt. (mg)	Amount Adsorbed (mg/g cat.)	Amount Adsorbed (μ mol/g cat.)
21	250	26	13.9204	14.030	177.59
		28	13.9218	14.132	178.89
		30	13.9230	14.219	179.99
		40	13.9254	14.394	182.19
		50	13.9282	14.598	184.79
		60	13.9306	14.773	186.99
		70	13.9320	14.875	188.29
		80	13.9336	14.992	189.77
		90	13.9348	15.079	190.87
		100	13.9362	15.181	192.16
		110	13.9373	15.261	193.18
		120	13.9382	15.327	194.01
		130	13.9389	15.378	194.65
		140	13.9400	15.458	195.67
		150	13.9408	15.516	196.39
		160	13.9419	15.596	197.42
		170	13.9425	15.640	197.97
		180	13.9434	15.705	198.79
		240	13.9508	16.281	206.09
		300	13.9537	16.493	208.77
		360	13.9650	16.660	210.89
		420	13.9574	16.762	212.18
		480	13.9593	16.901	213.93
		540	13.9604	16.981	214.95
		600	13.9625	17.134	216.88
		660	13.9634	17.199	217.71
		720	13.9650	17.316	219.19
		780	13.9665	17.425	220.57
		840	13.7678	17.520	221.77
		900	13.9695	17.644	223.34
		960	13.9711	17.760	224.81
		1020	13.9720	17.826	225.64
		1080	13.9731	17.906	226.66
		1140	13.9738	17.966	227.29
		1200	13.9749	18.037	228.32
		1260	13.9758	18.103	229.15
		1320	13.9764	18.146	229.69
		1380	13.9775	18.226	230.71
		1440	13.9781	18.270	231.27
		1500	13.9738	17.957	231.91
		1560	13.9790	18.336	232.09
		1620	13.9795	18.372	232.56
22	100	0	12.865	0.00	0.00
		2	12.985	9.33	119

TABLE A-I (Continued)

Run	Temp. (C)	Time (min)	Cat. Wt. (mg)	Amount Adsorbed (mg/g cat.)	Amount Adsorbed (μ mol/g cat.)
22	100	4	13.072	16.09	203.8
		6	13.151	22.23	281.4
		8	13.881	25.88	327.6
		10	13.225	27.98	354.2
		12	13.235	28.76	364.1
		14	13.246	29.61	374.8
		16	13.252	30.08	380.6
		18	13.256	30.39	384.7
		20	13.262	30.86	390.6
		22	13.265	31.09	393.5
		24	13.262	30.86	390.6
		26	13.272	31.64	400.5
		28	13.278	32.10	406.3
		30	13.279	32.18	407.3
		40	13.286	32.72	414.2
		50	13.294	33.35	422.2
		60	13.300	33.81	428.1
		70	13.301	33.89	439.1
		80	13.305	34.20	432.9
		90	13.309	34.51	436.8
		100	13.304	34.13	432.0
		110	13.311	34.67	438.9
		120	13.315	34.98	442.8
		130	13.319	35.29	446.7
		140	13.321	35.44	448.6
		150	13.321	35.44	448.6
		160	13.322	35.52	449.6
		170	13.323	35.60	450.6
		180	13.326	35.83	453.5
		240	13.330	36.14	457.5
		300	13.335	36.53	462.4
		360	13.337	36.69	464.4
		420	13.338	36.77	465.4
		480	13.341	36.99	468.2
		540	13.338	36.77	465.4
24	250	0	13.7180	0.000	0.000
		2	13.7967	5.737	72.62
		4	13.8465	9.367	118.6
		6	13.8826	11.999	151.88
		8	13.9074	13.807	174.77
		10	13.9148	14.346	181.59
		12	13.9180	14.579	184.55
		14	13.9221	14.873	188.33
		16	13.9242	15.031	190.27

TABLE A-I (Continued)

Run	Temp. (C)	Time (min)	Cat. Wt. (mg)	Amount Adsorbed (mg/g cat.)	Amount Adsorbed (μ mol/g cat.)
24	250	18	13.9260	15.162	191.93
		20	13.9275	15.272	193.31
		22	13.9289	15.374	194.61
		24	13.9302	15.469	195.81
		26	13.9315	15.563	197.01
		28	13.9325	15.636	197.93
		30	13.9330	15.673	198.39
		40	13.9362	15.960	201.34
		50	15.9384	16.066	203.37
		60	13.9400	16.183	204.85
		70	13.9416	16.300	206.33
		80	13.9432	16.416	207.79
		90	13.9441	16.482	208.63
		100	13.9445	16.511	209.09
		110	13.9456	16.591	210.02
		120	13.9462	16.635	210.57
		130	13.9469	16.686	211.22
		140	13.9475	16.730	211.77
		150	13.9484	16.795	212.59
		160	13.9480	16.825	212.23
		170	13.9493	16.861	213.43
		180	13.9500	16.912	214.08
		240	13.9523	17.080	216.19
		300	13.9543	17.226	218.04
		360	13.9562	17.346	219.81
		420	13.9570	17.422	220.54
		480	13.9595	17.605	222.84
		540	13.9604	17.670	223.67
		600	13.9618	17.772	224.97
		660	13.9631	17.567	226.17
		720	13.9640	17.933	227.01
		780	13.9652	18.020	228.09
		840	13.9658	18.064	228.66
		900	13.9669	18.440	229.67
		960	13.9675	18.188	230.23
		1020	13.9681	18.232	230.78
		1080	13.9689	18.290	231.52
		1140	13.9692	18.312	231.79
		1200	13.9694	18.326	231.98
25	100	0	12.7255	0.000	0.000
		2	12.8176	7.237	91.61
		4	12.9098	14.483	183.32
		6	12.9749	19.598	248.08
		8	13.0217	23.276	294.63

TABLE A-I (Continued)

Run	Temp. (C)	Time (min)	Cat. Wt. (mg)	Amount Adsorbed (mg/g cat.)	Amount Adsorbed (μ mol/g cat.)
25	100	10	13.0468	25.248	319.59
		12	13.0542	25.830	326.96
		14	13.0594	26.239	332.13
		16	13.0621	26.451	334.82
		18	13.0645	26.639	337.21
		20	13.0682	26.930	340.89
		22	13.0694	27.024	342.08
		24	13.0711	27.158	343.77
		26	13.0732	27.323	345.86
		28	13.0744	27.417	347.06
		30	13.0759	27.535	348.55
		40	13.0808	27.920	353.42
		50	13.0850	28.250	357.59
		60	13.0863	28.353	358.89
		70	13.0894	28.596	361.98
		80	13.0908	28.706	363.37
		90	13.0919	28.793	364.46
		100	13.0940	28.958	366.55
		110	13.0952	29.052	367.75
		120	13.0978	29.256	370.33
		130	13.0983	29.296	370.83
		140	13.0995	29.390	372.02
		150	13.1008	29.492	373.32
		160	13.1015	29.547	374.01
		170	13.1025	29.626	375.01
		180	13.1029	29.657	375.39
		240	13.1079	30.050	380.38
		300	13.1101	30.223	382.57
		360	13.1114	30.325	383.86
		420	13.1135	30.490	385.95
		480	13.1154	30.639	387.84
		540	13.1165	30.726	388.93
		600	13.1180	30.844	390.43
		660	13.1191	30.930	391.52
		720	13.1201	31.009	392.51
		780	13.1220	31.157	394.39
		840	13.1236	31.284	395.99
		900	13.1245	31.354	396.89
		960	13.1255	31.433	397.89
		1020	13.1269	31.543	399.28
		1080	13.1275	31.590	399.87
		1140	13.1281	31.637	400.47
		1200	13.1294	31.739	401.76
		1260	13.1303	31.810	402.66
		1320	13.1314	31.897	403.75

TABLE A-I (Continued)

Run	Temp. (C)	Time (min)	Cat. Wt. (mg)	Amount Adsorbed (mg/g cat.)	Amount Adsorbed (μ mol/g cat.)
25	100	1380	13.1326	31.991	404.95
		1440	13.1346	31.148	406.94
		1500	13.1363	32.282	408.63
		1560	13.1369	32.329	409.23
		1620	13.1372	32.353	409.52
		1680	13.1377	32.392	410.02
25*	100	0	13.1377	32.392	410.02
		10	13.0529	25.728	325.67
		20	13.0249	23.528	297.82
		30	13.0127	22.569	285.68
		40	13.0049	21.964	278.02
		50	12.9978	21.398	270.86
		60	12.9919	20.934	264.99
		70	12.9874	20.581	260.52
		80	12.9849	20.384	258.03
		90	12.9808	20.062	253.95
		100	12.9777	19.818	250.87
		110	12.9574	19.638	248.58
		120	12.9724	19.402	245.59
		180	12.9606	18.475	233.86
		240	12.9499	17.634	223.21
		300	12.9406	16.903	213.96
		360	12.9344	16.416	207.79
		420	12.928	15.91	201.4
		600	12.916	14.97	189.5
		900	12.928	14.73	186.5
		1200	12.911	14.58	184.5
		1500	12.8834	12.408	157.07
		1800	12.8876	12.738	161.24
		2400	12.8622	10.742	135.98
		3480	12.8578	10.396	131.61
25**	100	0	12.8578	10.396	131.61
		2	12.9461	17.335	219.43
		4	13.0220	23.300	294.93
		6	13.0643	26.624	337.01
		8	13.0839	28.164	356.51
		10	13.0931	28.887	365.66
		12	13.0968	29.178	369.34
		14	13.0995	29.390	372.02
		16	13.1206	29.633	375.11
		18	13.1048	29.806	377.29
		20	13.1074	30.011	379.88
		22	13.1090	30.163	381.47

TABLE A-I (Continued)

Run	Temp. (C)	Time (min)	Cat. Wt. (mg)	Amount Adsorbed (mg/g cat.)	Amount Adsorbed (μ mol/g cat.)
25**	100	24	13.1110	30.293	383.46
		26	13.1115	30.333	383.96
		28	13.1126	30.419	385.05
		30	13.1140	30.514	386.25
		40	13.1175	30.804	389.93
		50	13.1201	31.009	392.51
		60	13.1219	31.150	394.29
		70	13.1234	31.268	395.80
		80	13.1246	31.362	396.99
		90	13.1258	31.457	398.18
		100	13.1262	31.488	398.58
		110	13.1275	31.590	399.87
		120	13.1280	31.629	400.37
		180	13.129	31.71	401.4
		240	13.131	31.86	403.4
		300	13.133	32.02	405.3
		360	13.135	32.18	407.3
		420	13.137	32.34	409.3
		480	13.137	32.34	409.3
		540	13.138	32.41	410.3
		600	13.140	32.57	412.3
		660	13.141	32.65	413.3
		720	13.142	32.73	414.3
		780	13.143	32.89	416.3
		840	13.145	32.97	417.3
		900	13.146	33.04	417.3
		960	13.146	33.04	418.3
		1020	13.146	33.04	418.3
25#	100	0	13.146	33.04	418.3
		10	13.9305	28.863	363.07
		20	13.0641	26.608	336.81
		30	13.0514	25.610	324.18
		40	13.0446	25.076	317.41
		50	13.0382	24.573	311.05
		60	13.0332	24.179	306.07
		70	13.0285	23.809	301.39
		80	13.0249	23.535	297.92
		90	13.0218	23.284	294.73
		100	13.0191	23.072	292.05
		110	13.0164	22.859	289.36
		120	13.0145	22.711	287.47
		180	12.998	21.41	271.1
		240	12.989	20.71	262.1
		300	12.982	20.16	255.1

TABLE A-I (Continued)

Run	Temp. (C)	Time (min)	Cat. Wt. (mg)	Amount Adsorbed (mg/g cat.)	Amount Adsorbed (μ mol/g cat.)
25#	100	360	12.979	19.92	252.2
		420	12.975	19.61	248.2
		600	12.964	18.74	237.2
		900	12.949	17.56	222.3
		1200	12.938	16.70	211.4
		1500	12.931	16.16	204.4
		1800	12.926	15.76	199.4
		2400	12.917	15.05	190.5
		3600	12.904	14.03	177.6
		4500	12.897	13.48	170.5

* Pyridine desorption after equilibrium was achieved.
** Pyridine readsorption after desorption experiment.
\# Pyridine redesorption after the second equilibrium was achieved.

TABLE A-II

TRANSIENT ADSORPTION DATA ON HDN-60

Run	Temp. (C)	Time (min)	Cat. Wt. (mg)	Amount Adsorbed (mg/g cat.)	Amount Adsorbed (μ mol/g cat.)
10	200	0	7.4765	0.000	0.000
		2	*	*	*
		4	*	*	*
		6	7.5570	10.767	136.29
		8	7.5885	14.980	190.62
		10	7.5936	15.662	198.26
		12	7.5951	13.863	201.79
		14	7.5963	16.024	203.83
		16	7.5978	16.224	205.37
		18	7.5990	16.385	207.41
		20	7.5999	16.505	209.92
		22	7.6005	16.585	210.94
		24	7.6014	16.706	211.46
		26	7.6018	16.759	212.14
		28	7.6023	16.826	213.99
		30	7.6029	16.906	214.00
		40	7.6048	17.160	217.22
		50	7.6085	17.655	223.49
		60	7.6071	17.468	221.11
		70	7.6099	17.843	226.86
		80	7.6102	18.883	226.36
		90	7.6105	17.923	226.87
		100	7.6109	17.976	227.55
		110	7.6109	17.976	227.55
		120	7.6115	18.057	228.56
		130	7.6115	18.057	228.56
		140	7.6116	18.070	228.56
		150	7.6117	18.083	228.56
		160	7.6118	18.097	228.56
		170	7.6118	18.097	228.56
		180	7.6119	18.110	229.07
		240	7.6128	18.230	230.77
		300	7.6130	18.257	231.10
		360	7.6135	18.324	231.95
		420	7.6136	18.338	232.12
11	450	0	6.8756	0.000	0.000
		2	*	*	*
		4	*	*	*
		6	*	*	*
		8	*	*	*
		10	6.9226	6.854	86.529
		12	6.9255	7.258	91.873

TABLE A-II (Continued)

Run	Temp. (C)	Time (min)	Cat. Wt. (mg)	Amount Adsorbed (mg/g cat.)	Amount Adsorbed (μ mol/g cat.)
11	450	14	6.9299	7.898	99.975
		16	6.9334	8.407	106.41
		18	6.9365	8.857	112.12
		20	6.9400	9.367	118.56
		22	6.9424	9.716	122.98
		24	6.9410	9.512	120.40
		26	6.9465	10.312	130.53
		28	6.9476	10.472	132.55
		30	6.9512	10.995	139.18
		40	6.9579	11.970	151.52
		50	6.9632	12.741	161.27
		60	6.9674	13.352	169.01
		70	6.9705	13.802	174.71
		80	6.9751	14.472	183.18
		90	6.9785	14.966	189.44
		100	6.9821	15.490	196.07
		110	6.9848	15.882	201.04
		120	6.9872	16.231	205.46
		130	6.9896	16.580	209.88
		140	6.9920	16.926	214.30
		150	6.9959	17.497	221.48
		160	6.9985	17.875	226.26
		170	7.0020	18.384	232.71
		180	7.0066	19.053	241.18
		240	7.0240	21.584	273.21
		300	7.0335	22.965	290.70
		360	7.0443	24.536	310.58
		420	7.0510	25.511	322.92
		480	7.0589	26.660	337.46
		540	7.0662	27.721	350.90
		600	7.0750	29.001	367.10
		660	7.0788	29.554	374.10
		720	7.0920	31.474	398.40
		780	7.1010	32.783	414.97
		840	7.1129	34.513	436.88
		900	7.1244	36.186	458.05
		960	7.1343	37.626	476.28
		1020	7.1440	39.037	494.13
		1080	7.1518	40.171	508.49
		1140	7.1602	41.393	523.96
		1200	7.1606	41.451	524.70
		1260	7.1705	42.891	542.92
		1320	7.1772	43.865	555.26
		1380	7.1838	44.825	567.41
		1440	7.1881	45.451	575.32

TABLE A-II (Continued)

Run	Temp. (C)	Time (min)	Cat. Wt. (mg)	Amount Adsorbed (mg/g cat.)	Amount Adsorbed (μ mol/g cat.)
11	450	1500	7.1945	46.381	587.11
		1560	7.2034	47.676	603.49
		1620	7.2134	49.130	621.90
		1680	7.2205	50.163	634.97
		1740	7.2275	51.181	647.86
		1800	7.2345	52.199	660.75
		3000	7.3605	70.525	892.72
12	300	0	7.6050	0.000	0.000
		2	7.6279	3.011	38.12
		4	7.6378	4.313	54.59
		6	7.6435	5.602	64.08
		8	7.6485	5.720	72.40
		10	7.6515	6.114	77.39
		12	6.6525	6.246	79.06
		14	7.6542	6.469	81.89
		16	7.6561	6.719	85.05
		18	7.6574	6.890	87.22
		20	7.6581	6.982	88.38
		22	7.6589	7.087	89.71
		24	7.6595	7.166	90.71
		26	7.6604	7.285	92.21
		28	7.6611	7.377	93.38
		30	7.6615	7.429	94.04
		40	7.6632	7.653	96.87
		50	7.6643	7.798	98.70
		60	7.6653	7.929	100.4
		70	7.6669	8.139	103.0
		80	7.6682	8.310	105.2
		90	7.6689	8.402	106.4
		100	7.6694	8.468	107.2
		110	7.6695	8.481	107.4
		120	7.6696	8.494	107.5
		130	7.6715	8.744	110.7
		140	7.6721	8.823	111.7
		150	7.6716	8.757	110.9
		160	7.6725	8.876	112.3
		170	7.6730	8.942	113.2
		180	7.6728	8.915	112.8
		240	7.6728	8.915	112.8
		300	7.6725	8.876	112.3
		360	7.6731	8.955	113.3
		420	7.6748	9.178	116.2
		480	7.6765	9.402	119.1
		540	7.6791	9.744	123.3

TABLE A-II (Continued)

Run	Temp. (C)	Time (min)	Cat. Wt. (mg)	Amount Adsorbed (mg/g cat.)	Amount Adsorbed (μ mol/g cat.)
12	300	600	7.6825	10.191	129.01
		660	7.6885	10.980	138.98
		720	7.6919	11.427	144.64
		780	7.6964	12.018	152.13
		840	7.6970	12.097	153.13
		900	7.7032	12.913	163.45
		960	7.7064	13.333	168.78
		1020	7.7102	13.833	175.10
		1080	7.7135	14.267	180.59
		1140	7.7171	14.740	186.59
		1200	7.7215	15.319	193.91
		1260	7.7260	15.911	201.40
		1320	7.7305	16.502	208.89
		1380	7.7368	17.331	219.38
		1440	7.7424	18.067	228.69
		1500	7.7485	18.869	238.85
		1560	7.7544	19.645	248.67
		1620	7.7592	20.276	256.66
		1680	7.7639	20.894	264.48
		1740	7.7690	21.565	272.97
		1800	7.7734	22.143	280.29
13	200	0	6.7402	0.000	0.000
		2	6.7659	3.813	48.26
		4	6.7940	7.982	100.9
		6	6.8319	13.605	172.21
		8	6.8361	14.228	180.09
		10	6.8405	14.881	188.37
		12	6.8438	15.370	194.56
		14	6.8468	15.816	200.19
		16	6.8515	16.513	209.02
		18	6.8540	16.884	213.72
		20	6.8550	17.032	215.60
		22	6.8559	17.166	217.29
		24	6.8562	17.210	217.85
		26	6.8568	17.299	218.98
		28	6.8572	17.359	219.73
		30	6.8574	17.388	220.10
		40	6.8625	18.145	229.68
		50	6.8650	18.516	234.38
		60	6.8665	18.738	237.19
		70	6.8672	18.842	238.51
		80	6.8678	18.931	239.64
		90	6.8686	19.050	241.14
		100	6.8693	19.154	242.45

TABLE A-II (Continued)

Run	Temp. (C)	Time (min)	Cat. Wt. (mg)	Amount Adsorbed (mg/g cat.)	Amount Adsorbed (μ mol/g cat.)
13	200	110	6.8699	19.243	243.58
		120	6.8705	19.332	244.71
		130	6.8710	19.406	245.64
		140	6.8710	19.406	245.64
		150	6.8713	19.451	246.21
		160	6.8715	19.480	246.58
		170	6.8718	19.525	247.15
		180	6.8720	19.554	248.52
		240	6.8729	19.688	249.21
		300	6.8732	19.732	249.78
		360	6.8735	19.777	250.34
		420	6.8735	19.777	250.34
15	450	0	8.0955	0.000	0.000
		2	8.1139	2.273	28.77
		4	8.1215	3.212	40.65
		6	8.1281	4.027	50.97
		8	8.1352	4.904	62.07
		10	8.1390	5.373	68.02
		12	8.1415	5.682	71.92
		14	8.1481	6.497	82.25
		16	8.1535	7.164	90.69
		18	8.1574	7.646	96.79
		20	8.1619	8.202	103.8
		22	8.1654	8.634	109.3
		24	8.1678	8.931	113.1
		26	8.1709	9.314	117.9
		28	8.1734	9.623	121.8
		30	8.1780	10.191	128.99
		40	8.1852	11.080	140.26
		50	8.1938	12.142	153.69
		60	8.2018	13.131	166.21
		70	8.2072	13.798	174.66
		80	8.2124	14.440	182.79
		90	8.2165	14.947	189.19
		100	8.2210	15.502	196.23
		110	8.2245	15.935	201.71
		120	8.2291	16.503	208.90
		130	8.2320	16.831	213.43
		140	8.2349	17.219	217.97
		150	8.2375	17.541	222.03
		160	8.2404	17.899	226.57
		170	8.2430	18.220	230.63
		180	8.2452	18.492	234.07
		240	8.2650	20.938	265.03

TABLE A-II (Continued)

Run	Temp. (C)	Time (min)	Cat. Wt. (mg)	Amount Adsorbed (mg/g cat.)	Amount Adsorbed (μ mol/g cat.)
15	450	300	8.2784	22.593	285.98
		360	8.2911	24.162	305.84
		420	8.3050	25.879	327.58
		480	8.3118	26.719	338.21
		540	8.3208	27.830	352.28
		600	8.3274	28.646	362.59
		660	8.3321	29.226	369.95
		720	8.3385	30.017	379.96
		780	8.3475	31.128	394.03
		840	8.3534	31.857	403.26
		900	8.3579	32.413	410.29
		960	8.3465	33.238	420.61
		1020	8.3724	34.204	432.96
		1080	8.3792	35.044	443.60
		1140	8.3859	35.872	454.07
		1200	8.3919	36.613	463.45
		1260	8.3980	37.366	472.99
		1320	8.4038	38.083	482.06
		1380	8.4101	38.861	491.91
		1440	8.4160	39.590	501.14
		1500	8.4209	40.195	508.79
		1560	8.4255	40.763	515.99
		1620	8.4286	41.146	520.84
		1680	8.4316	41.517	525.53
		1740	8.4365	42.122	533.19
		1800	8.4415	42.740	541.01
		4800	8.6632	70.125	887.66

* No interpretation of data available.

TABLE A-III

TEMPERATURE PROGRAMMED ADSORPTION
UNDER PYRIDINE PARTIAL PRESSURE

Run no.	Time (min)	Temp. (C)	Cat. Wt. (mg)	Amount Adsorbed (mg/g cat.)	Amount Adsorbed (μ mol/g cat.)
21	0.0	250	13.9795	18.335	232.09
	16.7	260	13.9696	17.614	222.96
	33.4	270	13.9583	16.791	212.54
	50.1	280	13.9453	15.844	200.55
	66.8	290	13.9326	14.919	188.84
	83.5	300	13.9190	13.928	176.29
	100.2	310	13.9039	12.828	162.38
	116.9	320	13.8893	11.764	148.92
	133.6	330	13.8742	10.664	134.99
	150.3	340	13.8612	9.718	122.9
	167.0	350	13.8468	8.669	109.7
	183.7	360	13.8346	7.779	99.48
	200.4	370	13.8240	7.008	88.71
	217.1	380	13.8155	6.388	80.87
	233.8	390	13.8064	5.726	72.48
	250.5	400	13.8022	5.421	68.29
	267.2	410	13.7982	5.128	64.92
	283.9	420	13.7961	4.975	62.98
	300.6	430	13.7972	5.055	63.99
	317.3	440	13.7994	5.216	66.02
	334.0	450	13.8034	5.507	69.71

TABLE A-IV

TRANSIENT ADSORPTION DATA AFTER TEMPERATURE PROGRAMMED ADSORPTION OF RUN 21 (450 C)

Run	Temp.	Time (hr)	Cat. Wt.	Adsorbed Amount (mg/g cat)	Adsorbed Amount (μ mol/g cat)
21	450	0	13.8034	5.507	69.71
		2	13.8718	10.489	132.78
		4	13.8964	12.282	155.46
		6	13.9179	13.848	175.29
		8	13.9372	15.254	193.09
		10	13.9543	16.499	208.85
		12	13.9708	17.701	224.07
		14	13.9849	18.728	237.07
		16	13.9995	19.792	250.53
		18	14.0135	20.812	263.44
		20	14.0261	21.729	275.06
		22	14.0374	22.553	285.48
		24	14.0492	23.412	296.36
		26	14.0618	24.331	307.98
		28	14.0738	25.204	319.04
		30	14.0851	26.027	329.46
		90	14.335	44.23	559.9
		100	14.397	48.75	617.1
		110	14.434	51.44	651.2
		120	14.472	54.21	686.2
		130	14.525	58.07	735.1
		140	14.584	62.37	789.5
		150	14.624	65.28	826.4
		160	14.672	68.78	870.6
		170	14.718	72.13	913.1
		180	14.763	75.41	954.5
		190	14.802	78.25	990.5
		200	14.838	80.87	1023
		210	14.851	81.82	1035
		220	14.872	83.35	1055
		230	14.881	84.01	1063
		240	14.893	84.88	1074
		247	14.089	85.39	1081

TABLE A-V

WEIGHT CHANGE DURING THE ADSORPTION OF PYRIDINE ON NICKEL-ALLOY BASKET

Temperature (C)	Pyridine Partial Pressure (N/m^2)	Time (h)	Weight (mg)
450	772	0	0.00000
		1	0.00018
		2	0.00030
		3	0.00035
		4	0.00035
		5	0.00040
250	772	0	0.00000
		1	0.00010
		2	0.00015
		3	0.00020
		4	0.00025
		5	0.00028
		6	0.00032
		7	0.00038

APPENDIX B

SURFACE MONOLAYER CALCULATION

Entz (1984) calculated the molecular size of pyridine from Leonnard-Jones collision diameter parameter for benzene. Based on his calculation, surface coverage of a pyridine molecule is 2.18×10^{-19} m^2/molecule.

A monolayer adsorption coverage of catalyst surface, n_o, is calculated below:

Surface area of Shell 324 = 202 m^2/g cat.

Molecular weight of pyridine = 79 g/g mol.

1 mole = 6.02×10^{23} molecule

$$n_o = \left[\frac{202\ m^2}{g\ cat.}\right]\left[\frac{molecule}{2.18\times10^{-19}\ m^2\ py}\right]\left[\frac{mole}{6.02\times10^{23}\ molecule}\right]\left[\frac{79\ g}{g\ mol}\right]$$

= 0.1216 g py/g cat = 121.6 mg/g cat

= 1540 μ equivalent mol/g cat

= 1.540 m equivalent mol/g cat

Similarly, for HDN-60 with surface area = 198 m^2/g cat, a monolayer adsorption coverage, n_o, is 119.2 mg/g cat (1509 μ equivalent mol/g cat).

Richardson and Benson (1957) estimated the surface coverage for pyridine molecule as 10 A^2 per pyridine molecule. Based on their estimate, a monolayer pyridine adsorption coverage of Shell 324 and HDN-60 catalysts would be 265.1 and 259.8 mg/g cat respectively. However, they did not state the criterion of their estimation for surface coverage of a pyridine molecule. Since the pyridine

molecular structure consists of one benzene ring, surface coverage of a pyridine molecule based on Entz's calculation is considered more reasonable and is used throughout this work.

APPENDIX C

ERROR ANALYSIS

Errors originating from pyridine adsorption on the nichrome wire basket, buoyancy effect, and the errors which came from reading the adsorbed weight are discussed and shown in this section.

One may expect pyridine to adsorb on the nichrome wire basket, causing an error in measurements. Therefore, two blank runs were conducted using the basket without catalyst at 250 C and 450 C. Table A-IV in Appendix A shows the weight of pyridine adsorbed on the basket which is about 0.0003 and 0.0004 mg (0.3 and 0.4 μg). Since the catalyst samples weighted between 6 to 18 mg with equilibrium adsorption of 20 to 100 mg/g cat, in the worst case, the adsorption on the basket could have introduced less than 0.1 % error in the data.

As the temperature and pyridine partial pressure in each experimental run are different, one may expect the gas buoyancy to have some effect on the measured weight results especially when the temperature and pyridine partial pressure are different. Buoyancy calculations were conducted as follows:

The volume of the solid matter is calculated by substracting the void volume (pore volume) from the volume of catalyst:

$$V_{solid} = V_{total} - V_{void}$$

The buoyancy force causes the catalyst weight to appear lower than true weight. The difference of weight due to

buoyancy is given by:

$$\text{Wt. change} = \rho_g \cdot V_{solid}$$

where,

ρ_g = density of the surrounding gas at system conditions, mass/volume.

Gas density is calculated from the ideal gas law as follows:

$$\rho_g = \frac{MP}{RT}$$

$$MW_{avg} = y_{He} \cdot MW_{He} + y_p \cdot MW_p$$

$$= \left(\frac{760 - P_p}{760}\right)(4) + \frac{P_p}{760}(79)$$

where,

y_{He}, y_p = mole fraction of He and pyridine in the gas phase, respectively.

MW_{He}, MW_p = molecular weight of He and pyridine, respcectively.

$$\rho_g = \frac{(MW_{avg})\ (1\ atm)}{\left(\frac{82.051\ l\ atm}{gmol\ K}\right)\ (T + 273)K}$$

The total catalyst volume is:

$$V_{total} = \frac{D^2}{4} L = \frac{(1/16\ in)^2}{4}\ (1/4\ in)\ \left(\frac{2.54\ cm}{in}\right)^3$$

$$= 0.0126\ cm^3/pellet$$

Assuming a value of void fraction of catalyst pellet, Σ_p, equal to 0.5 gives:

$$V_{void} = 0.50 \times V_{total}$$

$$V_{solid} = 0.5 \times V_{total} \quad cm^3/pellet$$

$$\text{Wt. change} = \rho_g \cdot V_{solid} \quad mg$$

$$= \rho_g \cdot V_{solid}/79 \quad m\ mol$$

Table C-I shows the errors in the measured weights due to a buoyancy effect which indicated that buoyancy could have produced less than 3 % error in the data. It should be emphasized that this buoyancy error is the absolute error compared to measurements in a vacuum. Since the gas concentration remains unchanged in each experiment, the relative errors due to change in gas density by thermal is much smaller than 3 %. Therefore, the effect of adsorption on the basket and the weight change due to buoyancy effect are negligible for the temperatures and partial pressures used in the system conditions.

Random errors in the reported weight gain (mg adsorbed/g cat.) come from the reading of the adsorbed weight and the initial weight of catalyst. The errors are calculated and shown as follow:

$$G = f(G_o, G_a)$$

where, G = mg of pyridine adsorbed/g cat.

TABLE C-I

BUOYANCY EFFECTS IN PYRIDINE ADSORPTION
DATA ON SHELL 324 CATALYST

Run no.	Temperature (C)	Pyridine Partial Pressure (N/m^2)	Catalyst Weight (mg)	Buoyancy Effect (mg/g cat.)
16	450	527	13.1501	0.48
17	400	568	14.4375	0.58
18	300	709	17.3844	0.83
19	200	653	11.6205	0.67
21	250	653	13.7278	0.72
22	100	732	12.865	0.95
24	250	571	13.7180	0.71
25	100	721	12.7255	1.03

G_o = initial catalyst weight, mg.

G_a = catalyst weight at any time, mg.

The equation relating G to these variables is

$$G = \left(\frac{G_a - G_o}{G_a}\right) \times 1000 = \left(1 - \frac{G_o}{G_a}\right) \times 1000 \qquad \text{(C-I)}$$

Differentiating this function gives

$$dG = \left(\frac{-1\ dG_o}{G_a} + \frac{G_o\ dG_o}{G_a^2}\right) \times 1000$$

If the differentials dG_o and dG_a are replaced by the small finite increments ΔG_o and ΔG_a, the results are approximately equal to ΔG (the deviation in reading catalyst weight).

$$G = \left(\frac{-1\ \Delta G_o}{G_a} + \frac{G_o\ \Delta G_a}{G_a^2}\right) \times 1000$$

where, ΔG_o = error in reading initial catalyst weight, $\pm$ 0.001 mg.

ΔG_a = error in reading catalyst weight at any time, $\pm$ 0.001 mg.

$$\Delta G = -1/G_a + G_o/G_a^2$$

The maximum error in reading catalyst weight is given by:

$$\Delta G = 1/G_a + G_o/G_a^2$$

Table C-II shows the values of ΔG. The results show only a small effect in weight measurement and are negligible in our calculations.

TABLE C-II

ERRORS IN READING CATALYST WEIGHT

Run	Initial Catalyst Weight (mg)	Catalyst Weight at Equilibrium Adsorption (mg)	Δ G (mg/g cat.)
16	13.1500	14.4099	0.16
17	14.4375	14.4375	0.15
18	17.3844	18.0709	0.12
19	11.6205	12.0312	0.18
21	13.7278	13.9795	0.12
22	12.865	13.338	1.58
24	13.7180	13.9694	0.15
25	12.7255	13.1377	0.16

APPENDIX D

SCANNING ELECTRON MICROSCOPY RESULTS

A Scanning Electron Microscope (SEM) was used to observe any differences in the surface texture of the fresh and used catalyst. After the adsorption equilibrium was reached at 400 C in Run 17, the catalyst sample was broken into two pieces. The first piece was analyzed by SEM while the second one was left in the TGA for desorption study. Figure 27 shows the micrograph of a fresh Shell 324 catalyst and Figures 28 and 29 show the micrograph of the first and second catalyst samples of Run 17. These figures do not show any different structure of catalyst surface.

Adsorption of pyridine on both HDN-60 (Runs 10, 12, and 13) and Shell 324 (Runs 18 and 19) catalysts at temperature range between 100-300 C showed a gray-black color ring on the outer edge of the catalyst pellets while a deep gray-green color was observed inside the catalyst pellet. Figure 30 shows the micrograph of such a pellet from Run 18 after equilibrium was reached at 300 C. However, the micrograph does not indicate any difference in the texture of the ring.

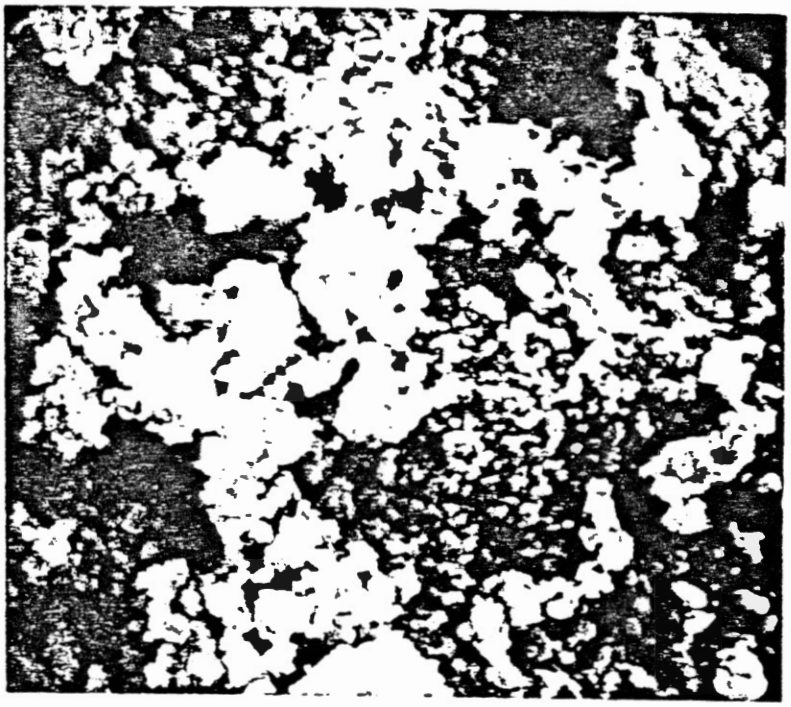

Figure 27. Electron Micrograph of a Shell 324 Catalyst after Calcination (6000x)

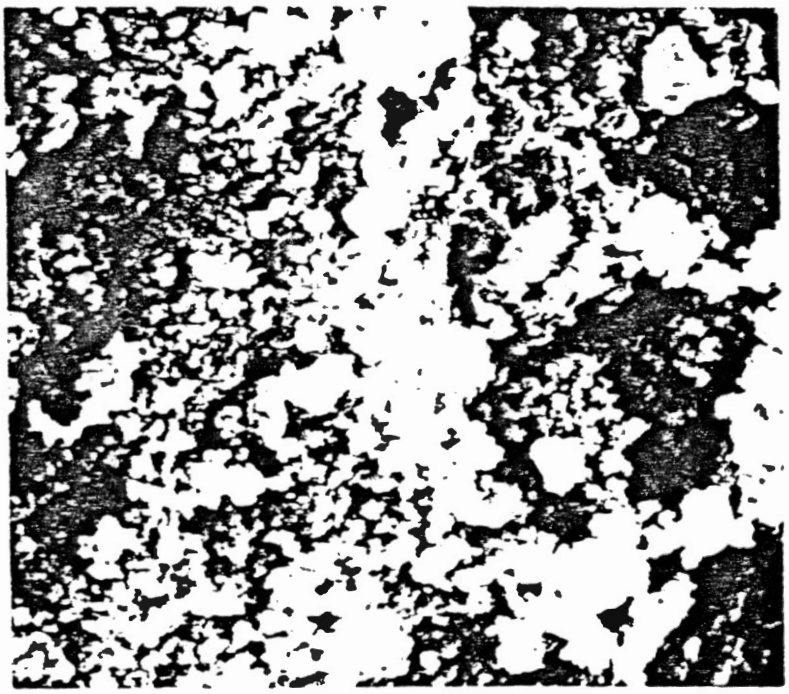

Figure 28. Electron Micrograph of a Shell 324 Catalyst after Pyridine Adsorption-Run 17 (6000x)

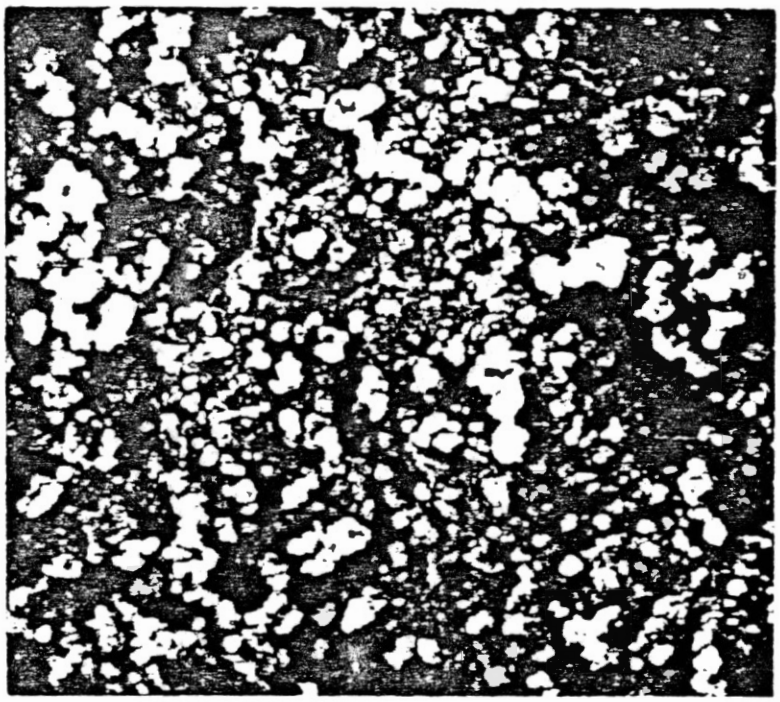

Figure 29. Electron Micrograph of a Shell 324 Catalyst after Desorption-Run 17 (6000x)

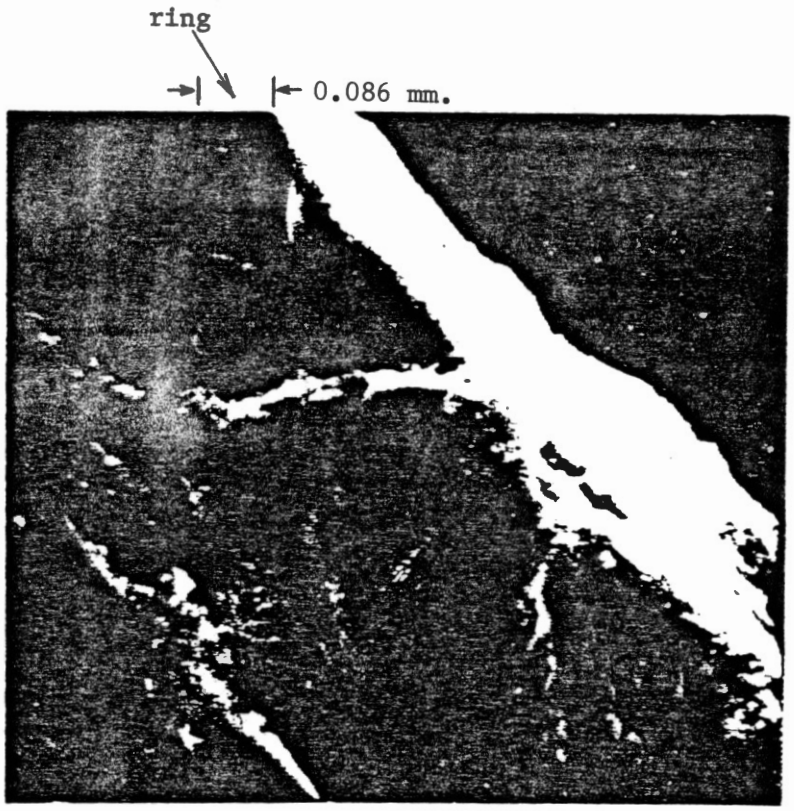

Figure 30. Electron Micrograph of a Shell 324 Catalyst after Pyridine Adsorption-Run 18 (6000x)

APPENDIX E

FTIR AND LASER RAMAN SPECTROSCOPY RESULTS

In one occasion, a micro-Fourier Transform Infrared Spectroscopy (FTIR) and a Laser Raman Spectroscopy (LRS) were used to study the adsorbed species on the catalyst samples. The first sample was a Shell 324 catalyst after calcination from Run 1. The FTIR results of this sample are shown in Figure 31. The second sample was the catalyst sample with pyridine adsorbed on it at 450 C from Run 4. The FTIR results for the second sample are shown in Figure 32 and the Laser Raman results are shown in Figure 33.

From FTIR results, Figures 31 and 32 indicate that no organic compounds exist on the catalyst surface. This is expected for the first sample which was only calcined. However, the second sample which contained pyridine should have shown the adsorption peaks. In addition, the catalyst sample was brown in color which indicated that some compounds were presented on the surface. Additional experiments, however, could not be conducted because of the unavailability of the equipment.

From the Laser Raman results, Figure 33 shows numerous adsorption bands, indicating that pyridine formed complex polymerized bonds on the catalyst at 450 C.

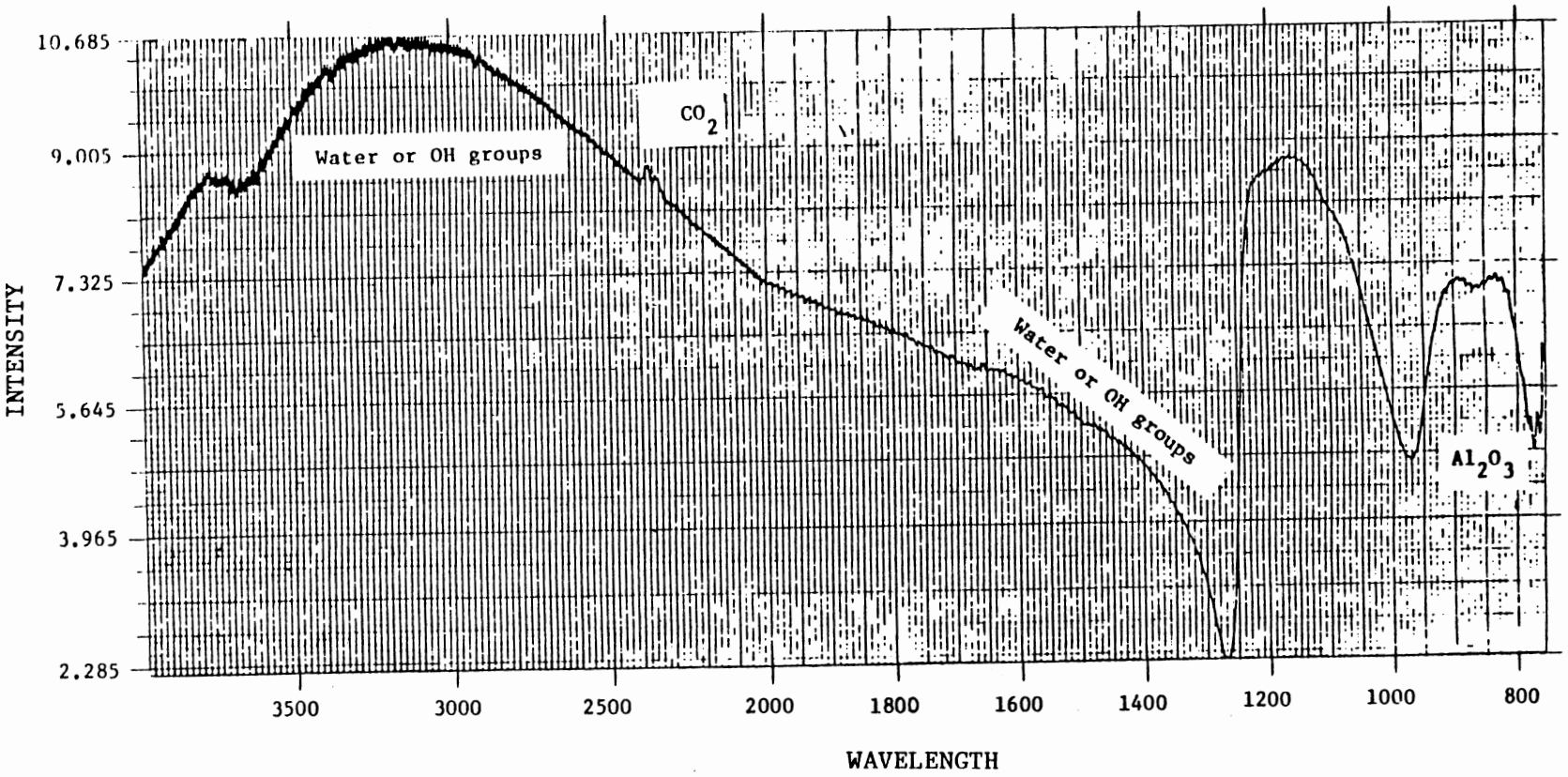

Figure 31. FTIR Results of a Shell 324 Catalyst after Calcination-Run 1

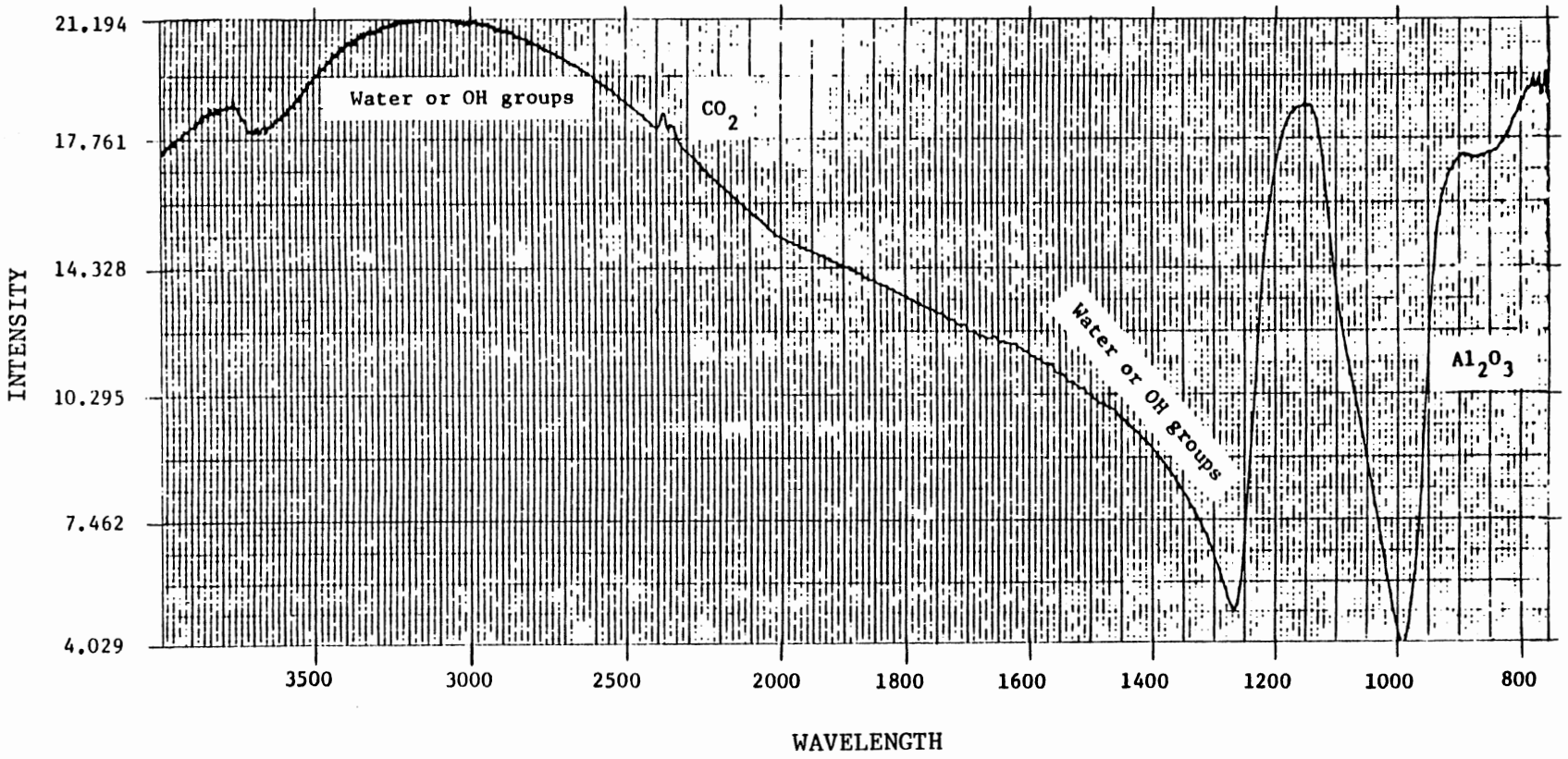

Figure 32. FTIR Results of Pyridine Adsorption on a Shell 324 Catalyst-Run 4

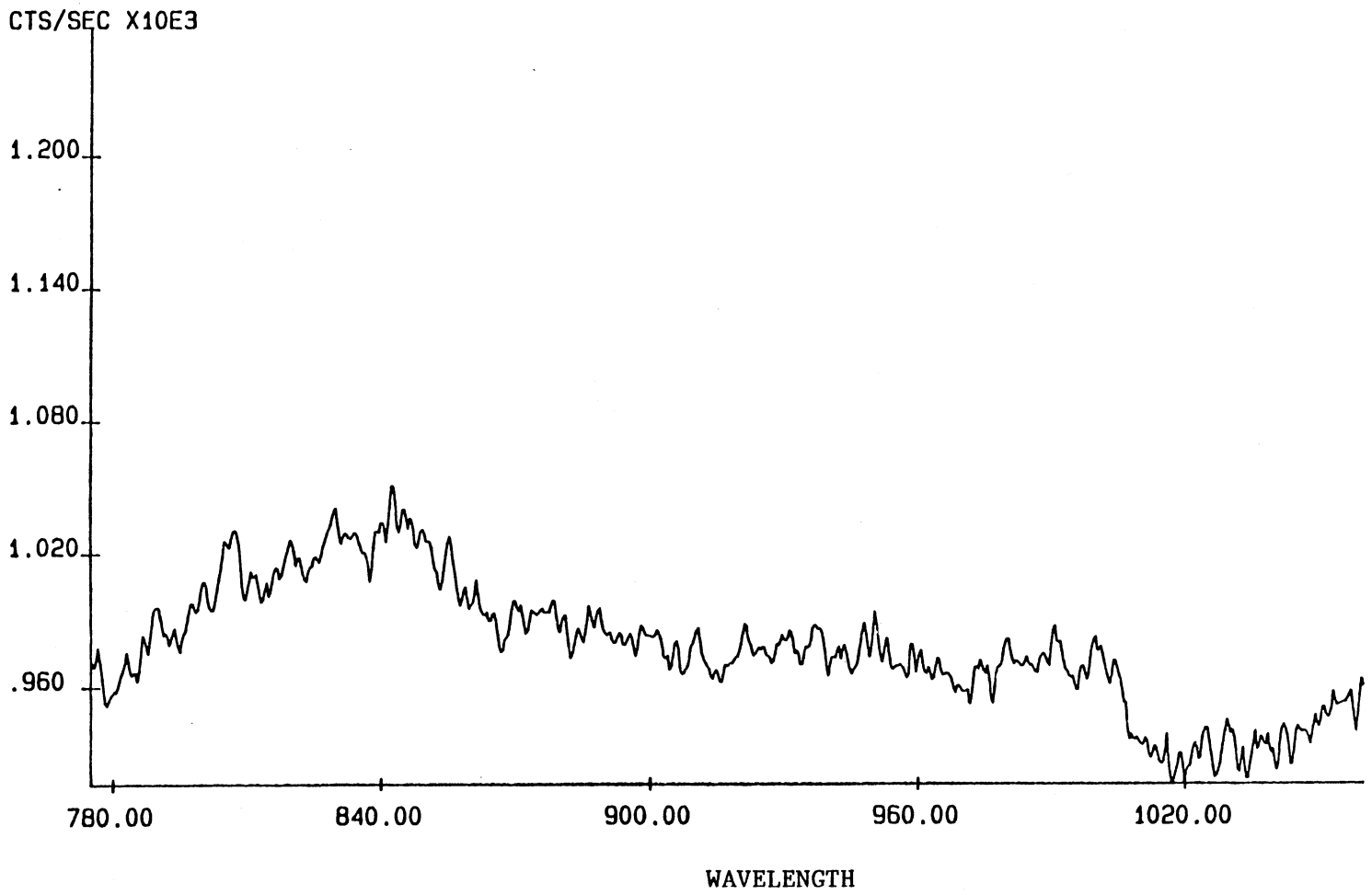

Figure 33. Laser Raman Spectroscopy Results of a Shell 324 Catalyst after Pyridine Adsorption-Run 4

VITA 2

Charoen Kongkatong

Candidate for the Degree of

Master of Science

Thesis: DYNAMICS OF PYRIDINE ADSORPTION ON HYDROTREATING CATALYSTS

Major Field: Chemical Engineering

Biographical:

Personal Data: Born in Bangkok, Thailand, June 18, 1963, the son of Chuchai and Kittima Kongkatong.

Education: Graduated from Assumption College, Bangkok, Thailand in March, 81; received a Bachelor of Science degree in Chemical Engineering from Chulalongkorn University, Banagkok, Thailand in April, 85; completed requirements for the Master of Science degree in Chemical Engineering at Oklahoma State University in July, 1988.

Professional Experience: Graduate Teaching/Research Assistant, School of Chemical Engineering, Oklahoma State University, Stillwater, Oklahoma, 6/86-6/88; Trainee, Boon Raud Brewery, Bangkok, Thailand, 3/84-5/84.